The Light Curves of W Ursae Majoris Systems

by

Ian Stuart Rudnick

A DISSERTATION PRESENTED TO THE GRADUATE COUNCIL OF
THE UNIVERSITY OF FLORIDA IN PARTIAL
FULFILLMENT OF THE REQUIREMENTS FOR THE DEGREE OF
DOCTOR OF PHILOSOPHY

UNIVERSITY OF FLORIDA

1972

To my wife, Andrea

ACKNOWLEDGMENTS

The author sincerely expresses his appreciation to his committee chairman and advisor, Dr. Frank Bradshaw Wood, for his comments and suggestions, which greatly aided the completion of this work. The author wishes to thank Dr. R. E. Wilson of the University of South Florida for providing one of the synthetic light curves and for serving on the author's committee. Thanks are also due to Drs. K-Y Chen and R. C. Isler for serving on the author's committee.

The author expresses his gratitude to Dr. S. M. Rucinski for providing the other synthetic light curve. The author wishes to thank Drs. J. E. Merrill and J. K. Gleim for their many helpful discussions. Thanks are also due to R. M. Williamon and T. F. Collins for their help in obtaining some of the data and for many enlightening conversations. W. W. Richardson deserves highest commendation for his untiring work on the drawings.

The author extends his thanks to the Department of Physics and Astronomy for providing financial support in the form of graduate assistantships, and to the Graduate School for support in the form of a Graduate School Fellowship.

The author is indeed grateful to his parents and to his wife's parents for their encouragement.

The author's wife deserves more than appreciation for her patience, encouragement, and hard work during five years of school life. Her devotion and understanding helped as nothing else could.

TABLE OF CONTENTS

LIST OF TABLES

LIST OF FIGURES

Abstract of Dissertation Presented to the
Graduate Council of the University of Florida in
Partial Fulfillment of the Requirements for
the Degree of Doctor of Philosophy

The Light Curves of W Ursae Majoris Systems

by

Ian Stuart Rudnick

June, 1972

Chairman: Frank Bradshaw Wood
Major Department: Astronomy

Two synthetic light curves computed from theoretical astrophysical models of W Ursae Majoris systems are discussed. Solutions of these light curves, based on the geometrical Russell model and the Russell-Merrill method of solution of the light curves of eclipsing binaries, are presented. The relatively shallow minima caused by the partial eclipses of the first synthetic light curve lead to a problem of indeterminacy in the solution. The "observed" points in the shoulders of both synthetic light curves fall below the theoretical light curves predicted by the solutions. The addition of third light in the solution of the two synthetic

light curves improves the fit of the solutions to the light curves; however, there is no sound basis for adding this third light. The orbital elements predicted by the Russell-Merrill solutions of the two synthetic light curves are not at all close to the orbital elements used to generate these light curves from the theoretical astrophysical models. In particular the Russell-Merrill solution underestimates the sizes of the components. It is concluded that the Russell model is not compatible with the theoretical astrophysical models used to generate the synthetic light curves.

Observations of the system of 44i Bootis, an example of a W Ursae Majoris system, are also discussed. The times of minimum light indicate that an increase in the period occurred in 1967.

CHAPTER I

INTRODUCTION

The W Ursae Majoris systems are eclipsing variable stars whose light curves have maxima which are strongly curved and minima which are nearly equal in depth. These systems have periods which average approximately one-half day. Orbital solutions in the literature indicate that W Ursae Majoris systems are close binaries whose separations are less than the dimensions of the components. Many complexities which are caused by the proximity of the components appear in the light curves (1). Most of the solutions of the light curves of W Ursae Majoris systems in the literature are based upon a geometrical model first proposed by Russell (2). Lucy has proposed that some or most of the W Ursae Majoris systems may be true contact systems, whose common boundary follows a single equipotential surface (3). It is the purpose of this thesis to apply the Russell-Merrill method of solution of the light curves of eclipsing binaries (2,4,5) to synthetic light curves from astrophysical models similar to Lucy's model in order to determine whether the geometrical Russell model is compati-

ble with the astrophysical models. Lucy (3), Rucinski (6), and Mochnacki and Doughty (7) have written computer programs for computing theoretical light curves of W Ursae Majoris system; Mochnacki and Doughty have published a trial and error fit to the system AW Ursae Majoris using their program. Wilson and Devinney (8) have published a general procedure for computing light curves of close binaries which includes the W Ursae Majoris systems as a special case. This procedure is now being applied to selected contact systems and the results will be published soon. Two synthetic light curves have been computed for this study, one by Rucinski (6) and one by Wilson (9). In addition, observations of the system of 44i Bootis, an example of a W Ursae Majoris system, are discussed.

The Russell Model

The Russell model and the Russell-Merrill method of solution of the light curves of eclipsing binaries are discussed in detail by Russell and Merrill (2). A brief discussion is given here in order to define the notation used. The Merrill tables and nomographs for solution of light curves of eclipsing binaries are based upon a spherical model (4,5). It is assumed that the orbit is circular, that the stars are spherical, and that they appear darkened at the limb by a linear cosine darkening law. This limb

darkening (x) may differ for the two components. The light of each star is constant for the spherical model; therefore the light of the system outside of eclipse is also constant. It is convenient to take the light of the system outside of eclipse as the unit of light and the radius of the spherical orbit as the unit of component dimensions. Then the components are defined by the following parameters:

Radius of the larger (greater) star	r_g
Radius of the smaller star	r_s
Inclination of the orbit	i
Light of the larger (greater) star	L_g
Light of the smaller star	L_s

with $L_g + L_s = 1$. If θ is the longitude in orbit (from conjunction), then the apparent distance between the centers of the disks is given by

$$\delta^2 = \cos^2 i + \sin^2 i \sin^2 \theta$$

Setting $p = (\delta - r_g)/r_s$, the eclipse will be absent, partial, or complete, for $p > 1$, $1 > p > -1$, or $p < -1$ respectively. Setting $k = r_s / r_g$ then $\delta = r_g(1 + kp)$. The quantities k and p are dimensionless, and their values completely define the geometrical circumstances of a given phase.

If f_g and f_s represent the fractions of the light of the two stars which are obscured at any phase of the eclipse of either, and ℓ is the normalized value of the light re-

ceived from the whole system:

$$\ell = L_g(1 - f_g) + L_s(1 - f_s) = 1 - L_g f_g - L_s f_s$$

For tabular purposes Russell and Merrill express these in terms of two other functions α and τ, where α is the ratio of light lost at any phase of an eclipse to the loss at internal tangency, and τ is that of the latter to the whole light of the star. Then for the light at any phase during an occultation (the larger star in front)

$$1 - \ell^{oc} = f^{oc} L_s = L_s \alpha^{oc}(x_s, k, p)$$

and during a transit (the smaller star in front)

$$1 - \ell^{tr} = f^{tr} L_g = L_g \, \tau(x_g, k) \alpha^{tr}(x_g, k, p)$$

It is convenient to use the χ-functions of Russell and Merrill to determine the solution of the light curve. Defining $n = \alpha/\alpha_o$ where the zero subscript refers to the value of the parameter at mid-eclipse, the χ-functions are given as

$$\chi(x,k,\alpha_o,n) = \frac{\sin^2\theta(n)}{\sin^2\theta(n=0.5)} = \frac{[1+kp(x,k,n\alpha_o)]^2}{[1+kp(x,k,0.5\alpha_o)]^2}$$

$$- \frac{[1+kp(x,k,\alpha_o)]^2}{[1+kp(x,k,\alpha_o)]^2}$$

These χ-functions have been tabulated by Merrill (4).

Russell and Merrill have shown that a system consisting of two similar triaxial ellipsoids with semi-axes a_g, b_g, c_g and $a_s = ka_g$, $b_s = kb_g$, $c_s = kc_g$ can be rectified to the spherical model making certain approximations which involve the gravity and reflection effects. The a-axis of each ellipsoid is along the line joining the centers of the components, the c-axis is parallel to the axis rotation of the system, and the b-axis is in the third mutually perpendicular direction. A mean radius $r = (a + b + c)/3$ may also be defined for these ellipsoids. The fundamental geometrical equations for this model (i.e. the Russell model) may be written as

$$\cos^2 i_r + \sin^2 i_r \sin^2 \theta = a_g^2 (1 + kp)^2$$

where i_r and θ are the rectified inclination and phase angle (orbital longitude) respectively. This equation is identical in form with the equation for spherical stars. Thus the observed intensity and phase angle can be rectified in such a way as to produce a rectified light curve which will be nearly that produced by the eclipse of a pair of spherical stars of radii a_g, $a_s = ka_g$, and inclination i_r.

CHAPTER II

FIRST SYNTHETIC LIGHT CURVE

A synthetic light curve for a W Ursae Majoris type eclipsing binary was generated by Dr. S. M. Rucinski from Lucy's model (6). The "observational" data for this light curve consisted of 37 values of the normalized light (or flux) as a function of phase angle, with the phases given in 5° intervals from 0° to 180°. The other half of the light curve (180° to 360°) was assumed to be symmetrical. An additional ten points were generated later to define better the centers of the eclipse regions of the light curve. This "observational" data is listed in Table I and plotted in Figure I. This synthetic light curve was to be treated as observational data and solved by the standard Russell-Merrill method of solution of light curves of eclipsing binaries. No additional information about the nature of the derivation of this light curve was to be used in the solution.

Rectification

The first step in the process of getting a solution

TABLE I

Observations of First Synthetic Light Curve

PHASE	INTENSITY	PHASE	INTENSITY
0.00	0.45242	95.00	0.99343
2.50	0.44826	100.00	0.98470
5.00	0.45216	105.00	0.96954
7.50	0.46429	110.00	0.94766
10.00	0.48257	115.00	0.92548
12.50	0.49728	120.00	0.90144
15.00	0.51875	125.00	0.86813
17.50	0.54518	130.00	0.83688
20.00	0.56516	135.00	0.80528
22.50	0.58812	140.00	0.77124
25.00	0.61087	145.00	0.73817
30.00	0.65572	150.00	0.70216
35.00	0.70708	155.00	0.66023
40.00	0.74969	157.50	0.64105
45.00	0.79267	160.00	0.62372
50.00	0.83087	162.50	0.60589
55.00	0.86916	165.00	0.58505
60.00	0.90446	167.50	0.56515
65.00	0.92940	170.00	0.55371
70.00	0.95640	172.50	0.54237
75.00	0.97754	175.00	0.53530
80.00	0.99117	177.50	0.53398
85.00	0.99632	180.00	0.53866
90.00	0.10000		

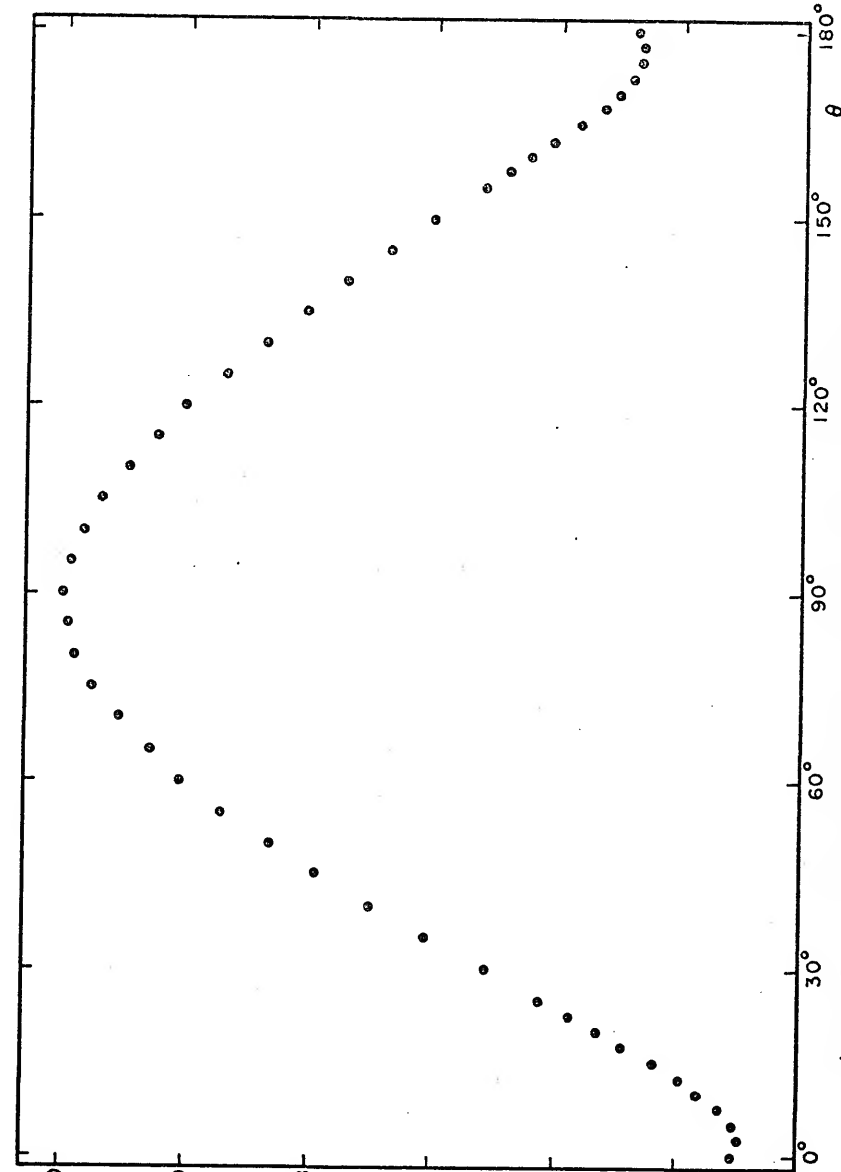

Figure 1. Observations of First Synthetic Light Curve.

for the light curve was an analysis of the light outside the eclipses in order to arrive at a rectification of the light curve to the spherical model. Two methods were used for this analysis: Merrill's graphical method (10) and a least squares Fourier analysis of the material outside of eclipse.

Let the light outside eclipse be represented by a truncated Fourier series of the form:

$$I = A_o + A_1 \cos \theta + A_2 \cos 2\theta + A_3 \cos 3\theta + A_4 \cos 4\theta.$$

(Since the light curve is symmetrical about $\theta = 180°$, it is not necessary to include sine terms in the above Fourier series.) Following Merrill's graphical method, a and b represent readings for θ and $180° - \theta$ on the light curve. (The given "observational" points were used rather than reading from a freehand curve since the scatter of the points was small.) It immediately follows that

$$\frac{1}{2}(a + b) = A_o + A_2 \cos 2\theta + A_4 \cos 4\theta$$

$$\frac{1}{2}(a - b) = A_1 \cos\theta + A_3 \cos 3\theta$$

Letting $C_1 = \frac{1}{2}(a - b)$ and $C_2 = \frac{1}{2}(a + b)$, by simple trigonometric substitution,

$$C_1 = (A_1 - 3A_3) \cos \theta + 4A_3 \cos 3\theta$$

$$C_2 = (A_o - A_4) + A_2 \cos 2\theta + 2A_4 \cos^2 2\theta$$

Therefore a plot of C_1 versus cosθ would have the form of a cubic and a plot of C_2 versus cos 2θ would have the form of a parabola. Such plots are given in Figure 2. The plot of C_1 versus cos θ shows the presence of a considerable A_3 (cos 3θ) term and indicates the possible presence of higher order odd cosine terms. The plot of C_2 versus cos 2θ is essentially linear, indicating that the A_4 term is negligible. The plotted points seem to fall below this straight line somewhere around 40°, thus locating θ_e (the value of θ at external tangency) to a first approximation. Values of the Fourier cosine coefficients were then derived from the plots and are listed in Table II.

Because of the similarity of the "colors" of the two "stars" and the small difference in the depths of the two minima, rectification coefficients for the reflection effect were obtained in the following manner (2):

$$C_1 = -A_1$$

$$C_o = 0.090 \sin^2 \theta_e$$

$$C_2 = 0.030 \sin^2 \theta_e$$

The eclipses were assumed to be partial and values were derived for $\theta_e = 39°$; these values are listed in Table II.

Figure 2. Graphical Rectification Plots for First Synthetic Light Curve.

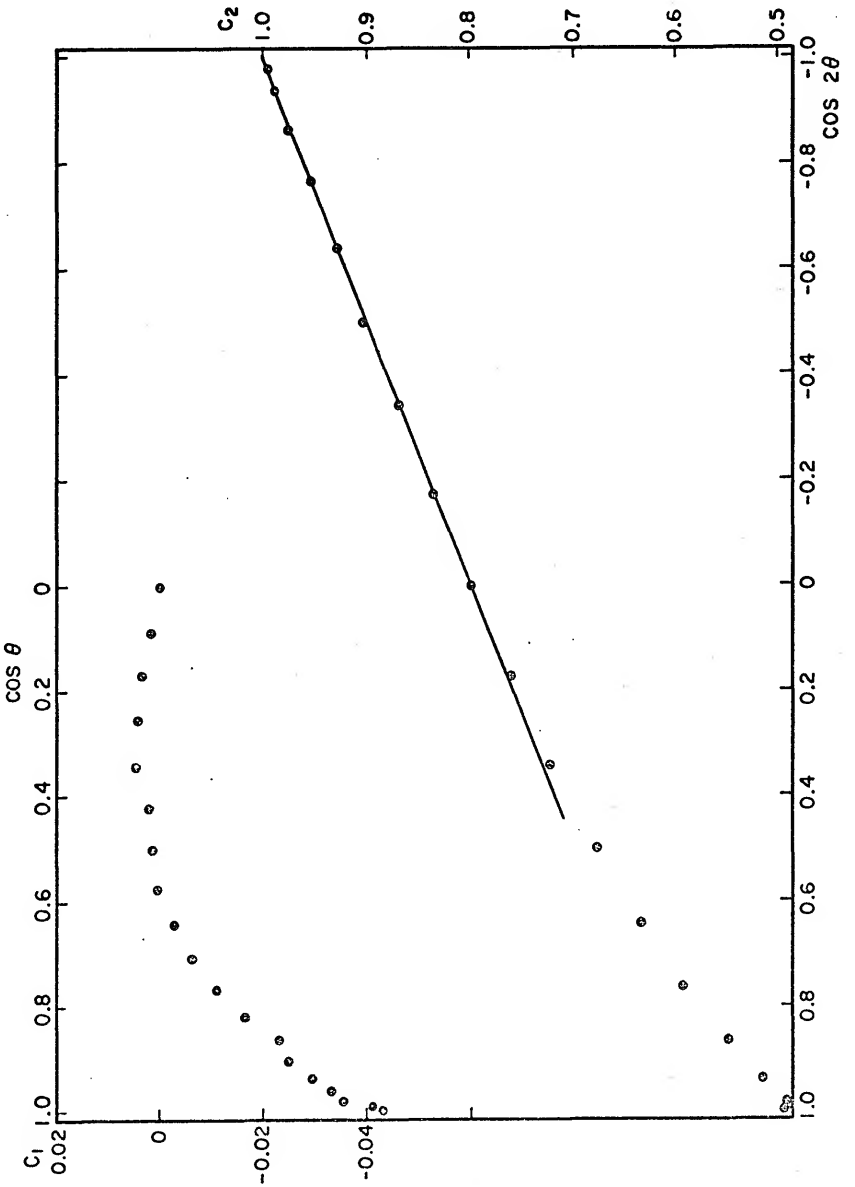
C_1
0.02
0
-0.02
-0.04
cos θ
1.0
0.8
0.6
0.4
0.2
0
C_2
1.0
0.9
0.8
0.7
0.6
0.5
cos 2θ
-1.0
-0.8
-0.6
-0.4
-0.2
0
0.2
0.4
0.6
0.8
1.0

TABLE II

Graphical Rectification Coefficients for
First Synthetic Light Curve

θ	a	b	C_1	C_2
0°	.4534	.5387	-.0432	.4956
5	.4522	.5353	-.0416	.4938
10	.4826	.5357	-.0356	.5182
15	.5188	.5851	-.0332	.5520
20	.5652	.6237	-.0293	.5945
25	.6109	.6602	-.0247	.6356
30	.6557	.7022	-.0233	.6790
35	.7051	.7382	-.0166	.7217
40	.7497	.7712	-.0108	.7605
45	.7927	.8053	-.0063	.7990
50	.8309	.8369	-.0030	.8339
55	.8692	.8681	.0006	.8687
60	.9045	.9014	.0016	.9030
65	.9294	.9355	.0020	.9275
70	.9564	.9477	.0044	.9521
75	.9775	.9695	.0040	.9735
80	.9912	.9847	.0033	.9880
85	.9963	.9934	.0015	.9949
90	1	1	0	1

$A_o = 0.7990$ $\quad C_o = 0.0354$

$A_1 = -0.0232$ $\quad C_1 = -A_1$

$A_2 = -0.2010$ $\quad C_2 = 0.0118$

$A_3 = -0.0147$

$A_4 = 0$

$$z = \begin{matrix} 0.3353 \\ 0.2724 \\ 0.2180 \end{matrix} \quad \text{for} \quad x = \begin{matrix} 0.6 \\ 0.8 \\ 1.0 \end{matrix}$$

Also listed in Table II is the value of z, given by

$$z = \frac{-4(A_2 - C_2)}{N(A_o - C_o - A_2 + C_2)}$$

where N depends on the assumed limb darkening (x); values were adopted such that N = 2.6, 3.2, or 4.0 when x is assumed to be 0.6, 0.8 or 1.0 respectively.

Fourier coefficients were also computed by a least squares Fourier analysis of the light outside of eclipses (45° to 135°). The results of this analysis are listed in Table III.

Both sets of rectification coefficients were then used to compute a rectified light curve. The rectified intensity is given by

$$I'' = \frac{I+C_o+C_1 \cos\theta+C_2 \cos 2\theta-A_3 \cos 3\theta-A_4 \cos 4\theta}{A_o+C_o+ (A_2+C_2) \cos 2\theta}$$

and the rectified phase by

$$\sin^2\theta = \frac{\sin^2 \theta}{1-z \cos^2\theta}$$

The rectified points are listed in Tables IV and V and plotted in Figures 3 and 4.

Several things are apparent from an examination of

TABLE III

Least Squares Rectification Coefficients for First Synthetic Light Curve

$A_o = 0.79532 \pm 0.00123$
$A_1 = -0.02208 \pm 0.00114$
$A_2 = -0.20699 \pm 0.00195$
$A_3 = -0.01304 \pm 0.00066$
$A_4 = -0.00350 \pm 0.00090$

OBSERVED INTENSITY	THEORETICAL INTENSITY	O-C	θ
0.7927	0.7924	0.0003	45.0000
0.8309	0.8317	-0.0008	50.0000
0.8692	0.8687	0.0005	55.0000
0.9045	0.9026	0.0019	60.0000
0.9294	0.9322	-0.0028	65.0000
0.9564	0.9570	-0.0006	70.0000
0.9775	0.9763	0.0012	75.0000
0.9912	0.9898	0.0014	80.0000
0.9963	0.9973	-0.0010	85.0000
1.0000	0.9988	0.0012	90.0000
0.9934	0.9944	-0.0010	95.0000
0.9847	0.9845	0.0002	100.0000
0.9695	0.9693	0.0002	105.0000
0.9477	0.9495	-0.0018	110.0000
0.9255	0.9257	-0.0002	115.0000
0.9014	0.8986	0.0028	120.0000
0.8681	0.8689	-0.0008	125.0000
0.8369	0.8375	-0.0006	130.0000
0.8053	0.8052	0.0001	135.0000

TABLE IV

Rectified First Synthetic Light Curve
Using Graphical Rectification Coefficients

θ(x=.6)	θ(x=.8)	θ(x=1)	I"(θ)	I"(180+θ)
0.000			0.8331	0.8493
3.066	2.931	2.826	0.8254	0.8413
6.125	5.857	5.651	0.8278	0.8410
9.173	8.775	8.468	0.8404	0.8480
12.204	11.680	11.277	0.8599	0.8599
15.212	14.570	14.074	0.8714	0.8703
18.194	17.439	16.857	0.8906	0.8916
21.143	20.286	19.624	0.9145	0.9124
24.058	23.108	22.371	0.9264	0.9268
26.933	25.901	25.099	0.9405	0.9388
29.768	28.665	27.803	0.9522	0.9517
35.405	34.092	33.141	0.9693	0.9778
40.658	39.382	38.373	0.9870	0.9905
45.825	44.540	43.498	0.9950	0.9959
50.810	49.536	48.513	0.9996	1.0003
55.573	54.406	53.423	0.9990	1.0009
60.279	59.152	58.234	1.0006	1.0014
64.793	63.781	62.953	1.0020	1.0054
65.000			0.9967	1.0018
70.000			0.9986	0.9995
75.000			1.0001	1.0009
80.000			1.0000	1.0001
85.000			0.9976	0.9983
90.000			1.0000	1.0000

TABLE V

Rectified First Synthetic Light Curve Using Least Squares Rectification Coefficients

I	I"	Θ
0.4524	0.8469	0.000
0.4483	0.8391	2.945
0.4522	0.8412	5.885
0.4643	0.8535	8.816
0.4826	0.8726	11.735
0.4973	0.8834	14.637
0.5188	0.9019	17.519
0.5452	0.9250	20.377
0.5652	0.9359	23.208
0.5881	0.9488	26.011
0.6109	0.9595	28.781
0.6557	0.9745	34.221
0.7051	0.9904	39.518
0.7497	0.9968	44.668
0.7927	1.0004	49.673
0.8309	0.9992	54.538
0.8692	1.0006	59.273
0.9045	1.0021	63.891
0.9294	0.9971	68.405
0.9564	0.9994	72.831
0.9775	1.0012	77.186
0.9912	1.0014	81.488
0.9963	0.9990	85.753
1.0000	1.0012	90.000
0.9934	0.9990	94.248
0.9847	1.0003	98.513
0.9695	1.0002	102.815
0.9477	0.9982	107.170
0.9255	0.9998	111.596
0.9014	1.0031	116.110
0.8681	0.9992	120.727
0.8369	0.9994	125.463
0.8053	1.0002	130.328

Table V continued.

I	I"	θ
0.7712	0.9977	135.332
0.7382	0.9952	140.483
0.7022	0.9857	145.780
0.6602	0.9631	151.220
0.6411	0.9521	153.990
0.6237	0.9417	156.792
0.6059	0.9290	159.624
0.5851	0.9097	162.482
0.5652	0.8897	165.364
0.5537	0.8804	168.266
0.5424	0.8694	171.185
0.5353	0.8630	174.116
0.5340	0.8639	177.056
0.5387	0.8722	180.000

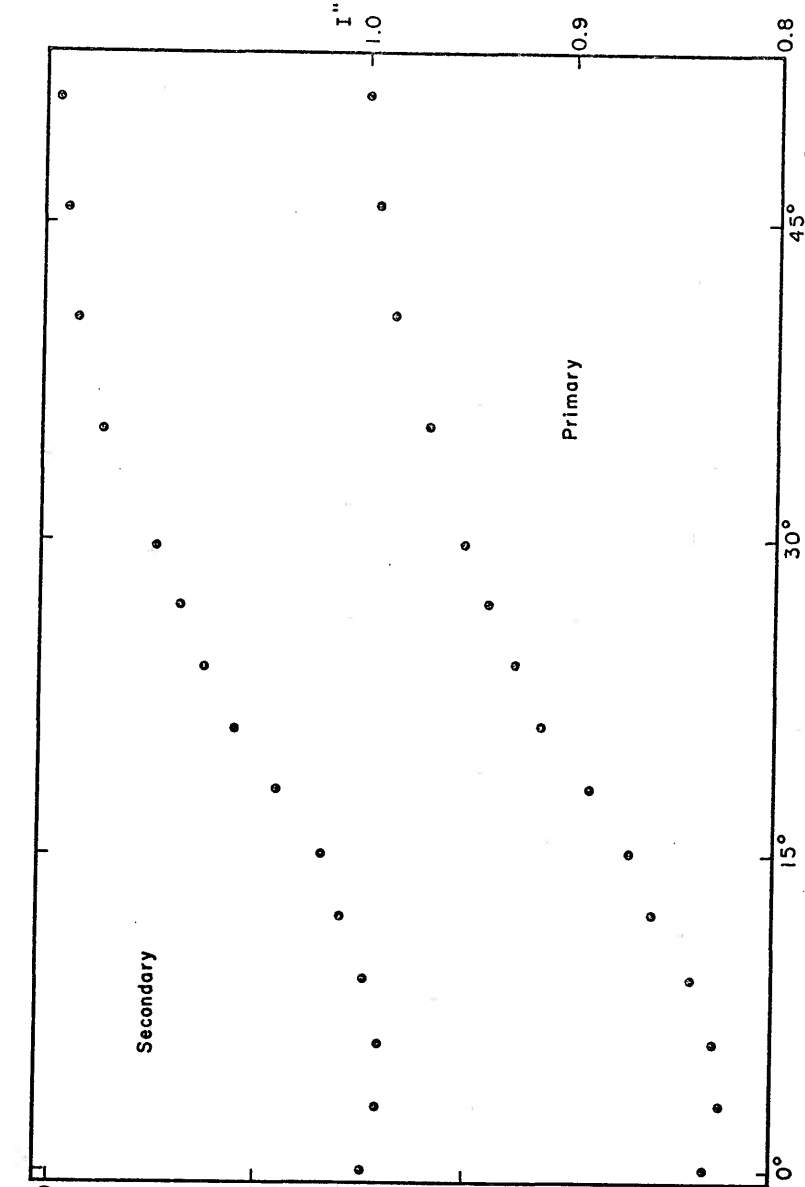

Figure 3. Rectified First Synthetic Light Curve Using Graphical Rectification Coefficients.

Figure 4. Rectified First Synthetic Light Curve Using Least Squares Rectification Coefficients: The solid circles are the rectified observations; the solid line is computed from the solution with k = 1; the plus signs are computed from the solution with k = 0.65, pr-tr; the open circles are computed from the solution with k = 0.65, pr-oc; and the X's are computed from the solution with k = 0.70, L_3 = 0.588.

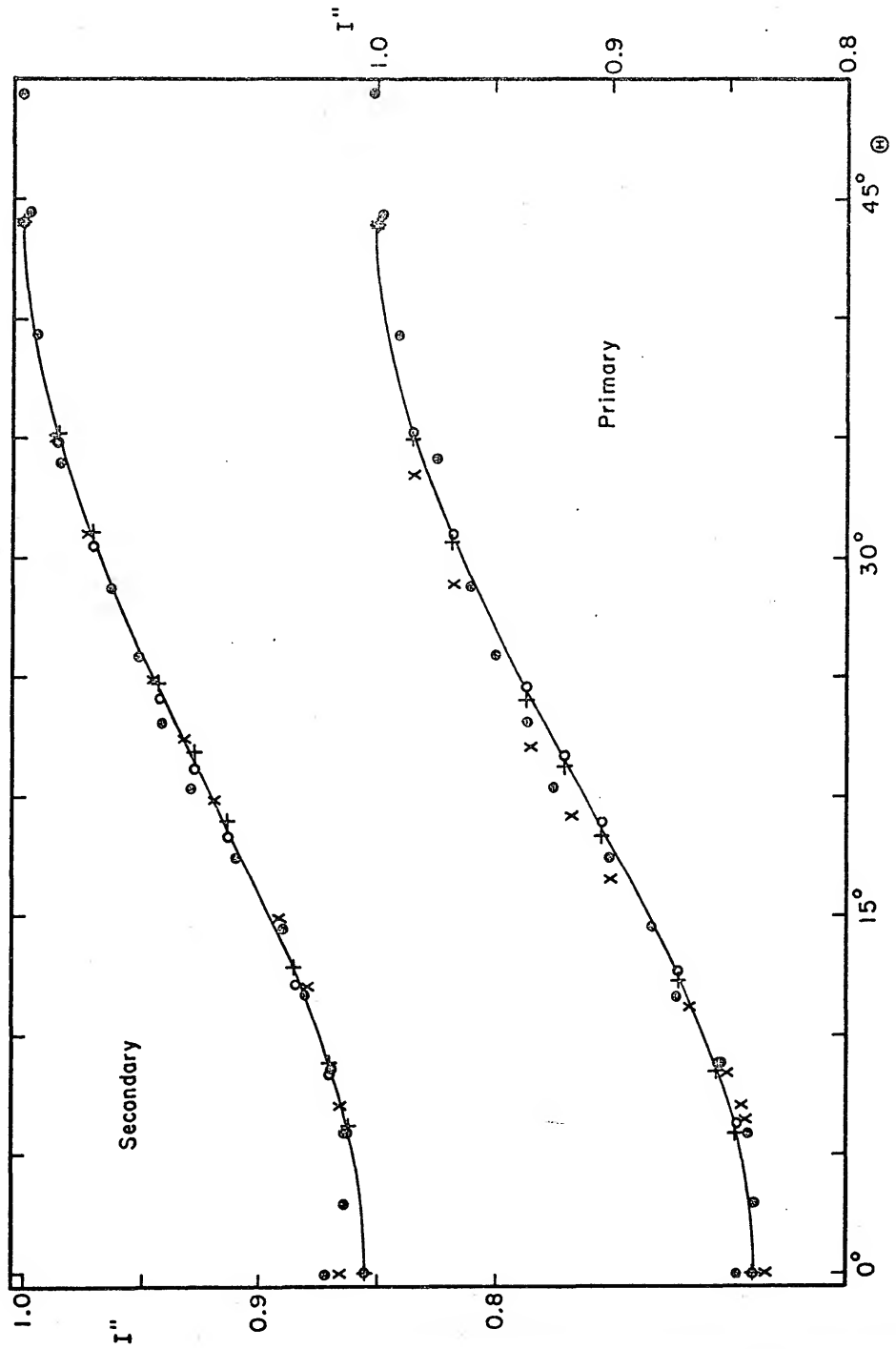
I"
1.0
0.9
0.8
Secondary
Primary
0°
15°
30°
45°
Θ

either of the rectified light curves. The first is that the amount of scatter of the data points in eclipse is much larger than was originally expected. This scatter will be treated as "observational" error for the present and no attempt will be made to explain it either in terms of the model or the method of computation of the data. Another obvious feature of the rectified minima is the "brightening" at the centers of the eclipses. Again no attempt will be made at present to explain this effect; however, its presence creates a serious uncertainty in both the depths of the eclipses and the credibility of the points near the center in terms of the Russell model.

Solutions from Graphical Rectification

The rectified light curve produced by applying the rectification coefficients derived by the graphical method was used for the first attempts at a solution. The phase was rectified with a z based on N = 2.6 corresponding to a darkening x = 0.6, and the first solutions were tried on the x = 0.6 nomograph. The depths of the eclipses were chosen as $1 - \ell_o^{pr} = 0.18$ and $1 - \ell_o^{sec} = 0.16$ and the following values were read off the plot of the rectified light curve:

n	Θ	$\sin^2\Theta$	χ^{pr}	Θ	$\sin^2\Theta$	χ^{sec}
0.2	33°0	.29663	2.268	32°6	.29027	1.901
0.5	21.2	.13077	1	23.0	.15267	1
0.8	12.2	.044658	.342	15.0	.066987	.439

By choosing values of $\Theta(n = .5)$ and $\Theta(n = .8)$ at $\Theta \pm 0°.5$, a permissible range of $.301 \leq \chi^{pr}(n = .8) \leq .387$ and $.394 \leq \chi^{sec}(n = .8) \leq .488$ was found. Since $\chi^{sec}(n = .8) > \chi^{pr}(n = .8)$, it appears that the primary eclipse is a transit and the secondary eclipse is an occultation. Then the values needed for the depth line on the nomograph are

$$(1 - \ell_o^{oc}) + (1 - \ell_o^{tr}) = 0.34$$

$$1 - \ell_o^{tr}/\ell_o^{oc} = 0.2142$$

$$1 - \ell_o^{tr}/\ell_o^{oc} + (1/50)\ 1 - \ell_o^{oc}/\ell_o^{oc} = 0.2180$$

Taking these values and the $\chi(n = 0.8)$ values given above to the $x = 0.6$ nomograph, an intersection of the depth line and the permissible values of both χ contours was found with $k = 0.45$, $p_o = -.98$, $\alpha_o^{oc} = .9987$, $\alpha_o^{tr} = .9928$. When these elements are taken to the χ tables, they produce the following points on the light curve:

n	χ^{oc}	$\sin^2\Theta$	Θ	χ^{tr}	$\sin^2\Theta$	Θ
0.0	2.823	.44122	41°.6	3.374	.44122	41°.6
0.2	1.725	.26961	31.3	1.913	.25016	30.0
0.5	1	.15629	23.3	1	.13077	21.2
0.8	.448	.070020	15.3	.376	.049170	12.8

Comparing these values with those taken from the "observed" light curve, several things are apparent. First,

the fit from the half-way point down is moderately satisfactory for this preliminary stage of solution. Second, the fit at the shoulders is very bad; the computed curve is much narrower than the "observed" curve. The $\chi(n < .5)$ values for both eclipses need to be increased a significant amount while making only small changes in the $\chi(n > .5)$ values, in order to fit the "observed" light curve with the chosen depths of the eclipses.

Since the nomographic solution on darkening $x = 0.6$ as described above was not satisfactory, other possibilities were explored. The first approach was to try nomographic solutions with other values of darkening. Table VI summarizes the results of these attempts. The main conclusion from this exploration of solutions with different values of darkening is that the fit will improve with increasing darkening. There are two reasons for this improvement. First the $\chi(n < .5)$ values for the transit eclipse tend to increase with increasing darkening, and second, the value of z is smaller for larger darkening. With a smaller z, the rectification of the phase tends to make the shoulders narrower relative to the half-width than with a larger z. Thus, it appeared that a darkening of $x = .8$ or $x = 1$ should be used for further trial solutions. The results of these solutions with $k = .45$ (see Tables VII and VIII and Figures 5 and 6) were not at all satisfactory. It was still not possible to fit the

TABLE VI

Solutions with Different Values of Limb Darkening

x	0.2	0.4	0.6	0.8	1.0
k	0.4625	0.4625	0.45	0.45	0.45
p_o	-0.93	-0.90	-0.98	-0.94	-0.90
$\alpha_o{}^{oc}$	0.9868	0.9799	0.9987	0.9943	0.9905
$\alpha_o{}^{tr}$	0.9809	0.9627	0.9928	0.9698	0.9375
χ^{oc}(n=.8)	0.401	0.405	0.448	0.452	0.452
χ^{tr}(n=.8)	0.383	0.370	0.376	0.361	0.351
χ^{oc}(n=.2)	1.812	1.799	1.725	1.712	1.703
χ^{tr}(n=.2)	1.867	1.908	1.913	1.957	1.991

TABLE VII

Solution for $x = 0.8$, $1 - \ell_o^{pr} = 0.18$, $1 - \ell_o^{sec} = 0.16$, $k = 0.45$, $p_o = -0.94$, $\alpha_o^{oc} = 0.9943$, $\alpha_o^{tr} = 0.9698$

n	χ^{oc}	$\sin^2\theta$	θ	χ^{tr}	$\sin^2\theta$	θ
0.0	2.827	.47732	43°7	3.650	.47732	43°7
0.1	2.047	.34562	36.0	2.464	.32222	34.6
0.2	1.712	.28905	32.5	1.957	.25592	30.4
0.4	1.203	.20312	26.8	1.265	.16542	24.0
0.5	1	.16884	24.3	1	.13077	21.2
0.6	.817	.13794	21.8	.766	.100170	18.5
0.8	.452	.076316	16.0	.361	.047208	12.6
0.9	.276	.044600	12.2	.181	.023669	8.9
0.95	.1734	.029277	9.9	.0925	.012096	6.3

TABLE VIII

Solution for $x = 1.0$, $1 - \ell_o^{pr} = 0.18$, $1 - \ell_o^{sec} = 0.16$, $k = 0.45$, $p_o = -0.90$, $\alpha_o^{oc} = 0.9905$, $\alpha_o^{tr} = 0.9375$

n	ψ^{oc}	χ^{oc}	$\sin^2\theta$	θ	ψ^{tr}	χ^{tr}	$\sin^2\theta$	θ
0.0	3.801	2.911	.47732	43°7	5.412	3.939	.47732	43.7
0.1	2.257	2.054	.33675	35.5	3.082	2.532	.30687	33.6
0.2	1.625	1.703	.27922	31.9	2.186	1.991	.24132	29.4
0.4	.7274	1.205	.19750	26.4	.9965	1.273	.15430	23.1
0.5	.3590	1	.16396	23.9	.5439	1	.12119	20.4
0.6	.0191	.811	.13302	21.4	.1465	.760	.092118	17.6
0.8	- .6275	.452	.074151	15.8	-.5306	.351	.042584	11.9
0.9	- .9684	.263	.043116	12.0	-.8290	.171	.20755	8.3
0.95	-1.1648	.1539	.025236	9.1	-.9717	.0851	.010315	5.8

Figure 5. Solution for $x = 0.8$, $1 - \ell_o^{pr} = 0.18$, $1 - \ell_o^{sec} = 0.16$, $k = 0.45$, $p_o = -0.94$, $\alpha_o^{oc} = 0.9943$, $\alpha_o^{tr} = 0.9698$: The solid circles are the rectified observations and the plus signs are computed from the solution.

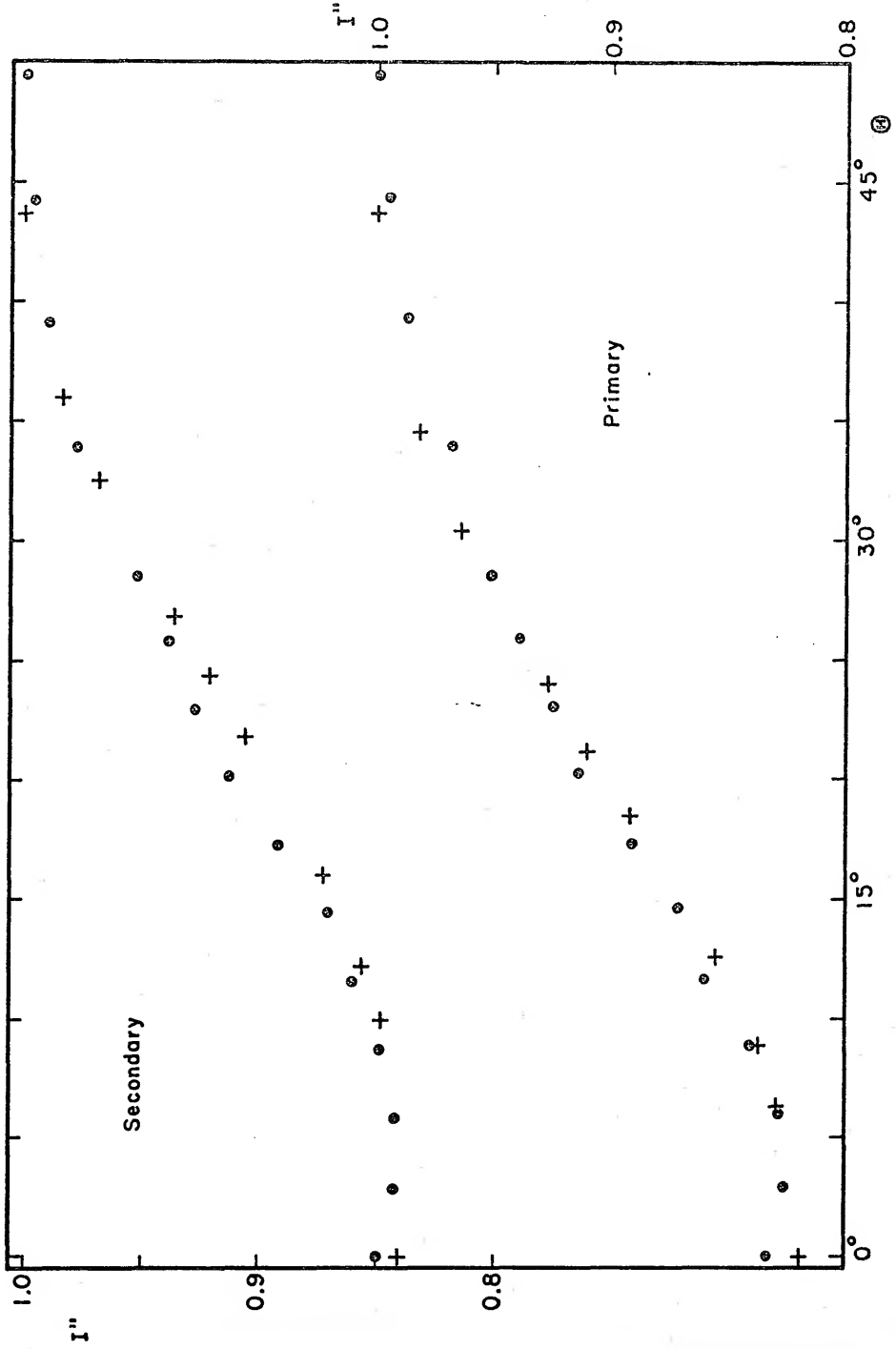
I"
1.0
0.9
0.8
Secondary
Primary
0°
15°
30°
45°
Θ

Figure 6. Solution for $x = 1.0$, $1 - \ell_o^{pr} = 0.18$, $1 - \ell_o^{sec} = 0.16$, $k = 0.45$, $p_o = -0.90$, $\alpha_o^{oc} = 0.9905$, $\alpha_o^{tr} = 0.9375$: The solid circles are the rectified observations and the plus signs are computed from the solution.

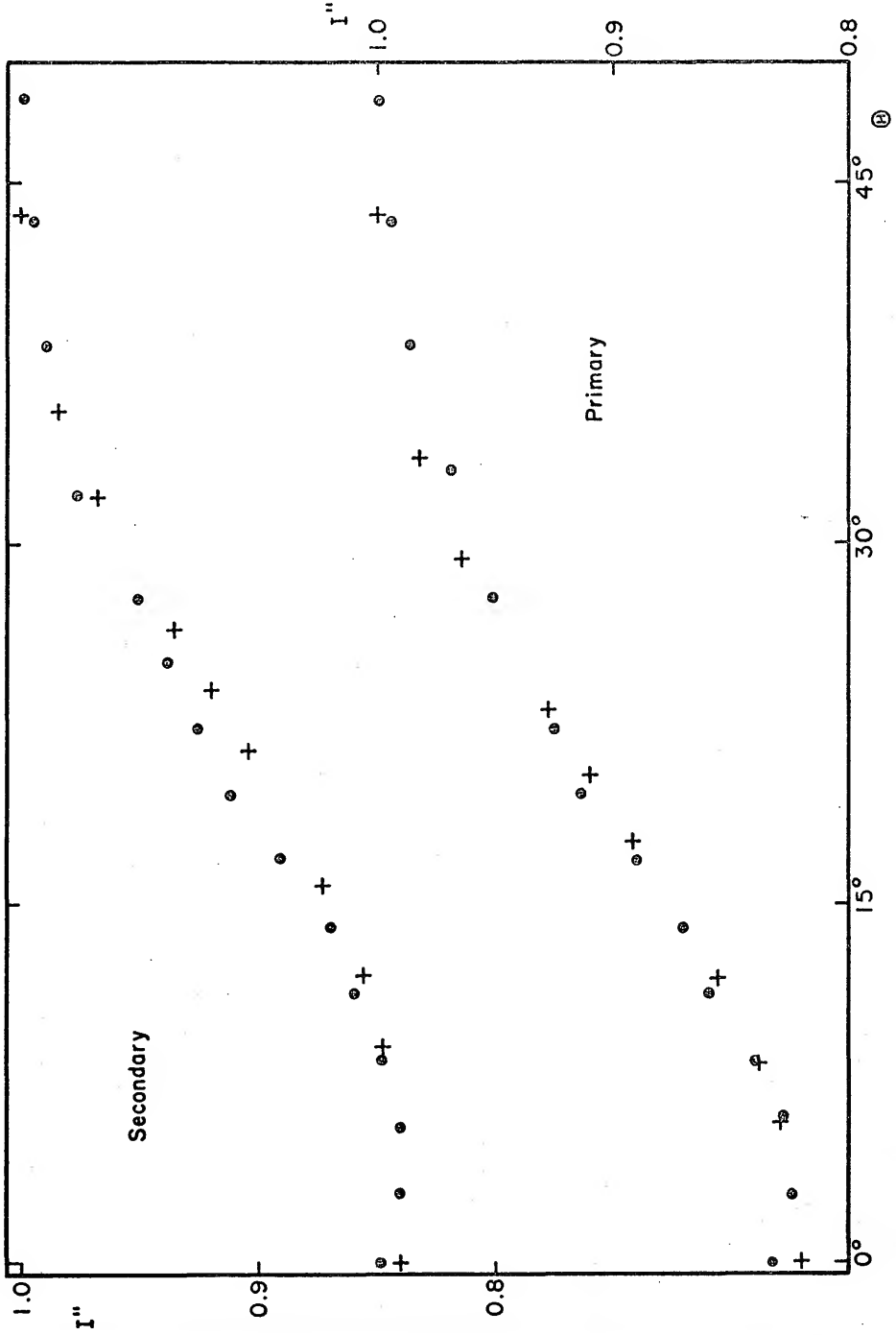
I"
1.0
0.9
0.8
0°
15°
30°
45°
Θ
Primary
Secondary

shoulders of the eclipses, especially the primary eclipse, while,at the same time, fitting the rest of the eclipse curves. In particular, with k = .45, the solutions for a circular orbit were too wide at the halfway point of the secondary eclipse and too narrow on the shoulders of the primary eclipse, with lesser problems elsewhere.

Because of the problems described above, it was necessary to abandon the chosen value of k = 0.45 and to explore other possibilities of k on the x = 0.6 nomograph, staying on the depth line given above. Table IX summarizes the results of these explorations. From an inspection of this table, it was decided to attempt trial solutions with k in the range .50 to .60 for darkenings x = 0.8 and total darkening. Some of these solutions are given in Tables X, XI, and XII. While these solutions are an improvement over previous ones, the major problem of the fit of the shoulders, especially in the primary eclipse, has not been alleviated.

Because of the recurrent problem with the fit of the shoulders of the eclipses, it was felt that a different approach might prove helpful. This approach was to choose a $\Theta(n = .5)$ for the primary eclipse and a Θ_e. From these values, $\chi(n = 0)$'s were derived. These χ's were taken to the x = 0.8 tables and values of k and α_o^{oc} were obtained and these shape curves were plotted (see Table XIII and Figure 7). The depth curve derived from

$$\alpha_o^{oc} = (1 - \ell_o^{oc}) + (1 - \ell_o^{tr})/q_o$$

TABLE IX

Solutions for $x = 0.6$, $1 - \ell_o^{tr}/\ell_o^{oc} = 0.2142$

$(1 - \ell_o^{tr}) + (1 - \ell_o^{oc}) = 0.34$

k	1.00	.85	.75	.60	.55	.50	.45
p_o	.0956	.0000	-.1000	-.3538	-.4820	-.6789	-.9800
$\alpha_o{}^{oc}$	.3400	.4136	.4900	.6800	.7700	.8900	.9987
$\alpha_o{}^{tr}$	.3400	.3788	.4363	.6018	.6897	.8224	.9928
$\chi^{oc}(n=.8)$	.346	.346	.347	.354	.361	.379	.448
$\chi^{tr}(n=.8)$	.346	.344	.343	.343	.344	.348	.376
$\chi^{oc}(n=.2)$	1.969	1.963	1.956	1.927	1.902	1.853	1.725
$\chi^{tr}(n=.2)$	1.969	1.976	1.982	1.986	1.983	1.972	1.913

TABLE X

Solution for $x = 0.8$, $1 - \ell_o^{pr} = 0.18$, $1 - \ell_o^{sec} = 0.16$, $k = 0.50$, $p_o = -0.6608$, $\alpha_o^{oc} = 0.89$, $\alpha_o^{tr} = 0.7915$

n	χ^{oc}	$\sin^2\theta$	θ	χ^{tr}	$\sin^2\theta$	θ
0.0	3.217	.47732	43°7	3.746	.47732	43°7
0.1	2.261	.33547	35.4	2.524	.32161	34.6
0.2	1.838	.27271	31.5	1.995	.25421	30.3
0.4	1.241	.18413	25.4	1.277	.16272	23.8
0.5	1	.14837	22.7	1	.12742	20.9
0.6	.781	.115880	19.9	.758	.096585	18.1
0.8	.384	.056976	13.8	.345	.043960	12.1
0.9	.195	.028933	9.8	.166	.021152	8.4
0.95	.0992	.014719	7.0	.0816	.010398	5.9

TABLE XI

Solution for $x = 0.8$, $1 - \ell_o^{pr} = 0.18$, $1 - \ell_o^{sec} = 0.16$, $k = 0.55$, $p_o = -0.4798$, $\alpha_o^{oc} = 0.78$, $\alpha_o^{tr} = 0.6659$

n	χ^{oc}	$\sin^2\theta$	θ	χ^{tr}	$\sin^2\theta$	θ
0.0	3.382	.47732	43°7	3.764	.47732	43°7
0.1	2.347	.33124	35.1	2.535	.32147	34.5
0.2	1.892	.26703	31.1	2.002	.25388	30.3
0.4	1.254	.17698	24.9	1.278	.15207	23.7
0.5	1	.141135	22.1	1	.126812	20.9
0.6	.771	.108815	19.3	.756	.095870	18.0
0.8	.366	.051655	13.1	.343	.043497	12.0
0.9	.180	.025404	9.2	.164	.020797	8.3
0.95	.0893	.012603	6.4	.0803	.010183	5.8

TABLE XII

Solution for $x = 1.0$, $1 - \ell_o^{pr} = 0.18$, $1 - \ell_o^{sec} = 0.16$, $k = 0.60$, $p_o = -0.3225$, $\alpha_o^{oc} = 0.68$, $\alpha_o^{tr} = 0.5332$

n	ψ^{oc}	χ^{oc}	$\sin^2\Theta$	Θ	ψ^{tr}	χ^{tr}	$\sin^2\Theta$	Θ
0.0	4.495	3.582	.47732	43°7	6.349	3.982	.47732	43°7
0.1	2.910	2.392	.31875	34.4	4.186	2.562	.30710	33.7
0.2	2.276	1.916	.25532	30.3	3.349	2.012	.24117	29.4
0.4	1.4016	1.259	.16777	24.2	2.233	1.280	.15343	23.1
0.5	1.0562	1	.133255	21.4	1.8073	1	.119869	20.3
0.6	.7471	.768	.102340	18.7	1.4350	.756	.090621	17.5
0.8	.2032	.360	.047972	12.7	.0843	.342	.040995	11.7
0.9	-.0424	.175	.023320	8.8	.5327	.163	.019539	8.0
0.95	-.1602	.0868	.011567	6.2	.4061	.0800	.009590	5.6

TABLE XIII

Shape Curve for $\Theta_e = 50°$, $\chi^{oc} = 3.955$, $\chi^{tr} = 4.605$, $x = 0.8$

k	α_o^{oc}(pr)	α_o^{oc}(pr)	α_o^{oc}(sec)
0.8	.9232	.8680	.8009
0.9	.8543	.8108	.6289
1.0	.8140	.8140	.5301

Shape Curve for $\Theta_e = 45°9$, $\chi^{oc} = 3.476$, $\chi^{tr} = 4.047$, $x = 0.8$

k	α_o^{oc}(pr)	α_o^{oc}(pr)	α_o^{oc}(sec)	
0.6	.9293	.8541	.6786	.8313
0.65			.4568	.9789
0.7	.7810	.6877	.3700	
0.8	.6862	.6092	.2767	
0.9		.5747	.2245	
1.0		.5828	.1913	

Figure 7. Depth Curve and Shape Curves: The solid circles are computed from the depth relation; the open circles are computed from the shape of the primary eclipse with $\Theta_e = 45°.9$; the squares are computed from the shape of the primary eclipse with $\Theta_e = 50°$; the asterisks are computed from the shape of the secondary eclipse with $\Theta_e = 45°.9$; and the plus signs are computed from the shape of the secondary eclipse with $\Theta_e = 50°$.

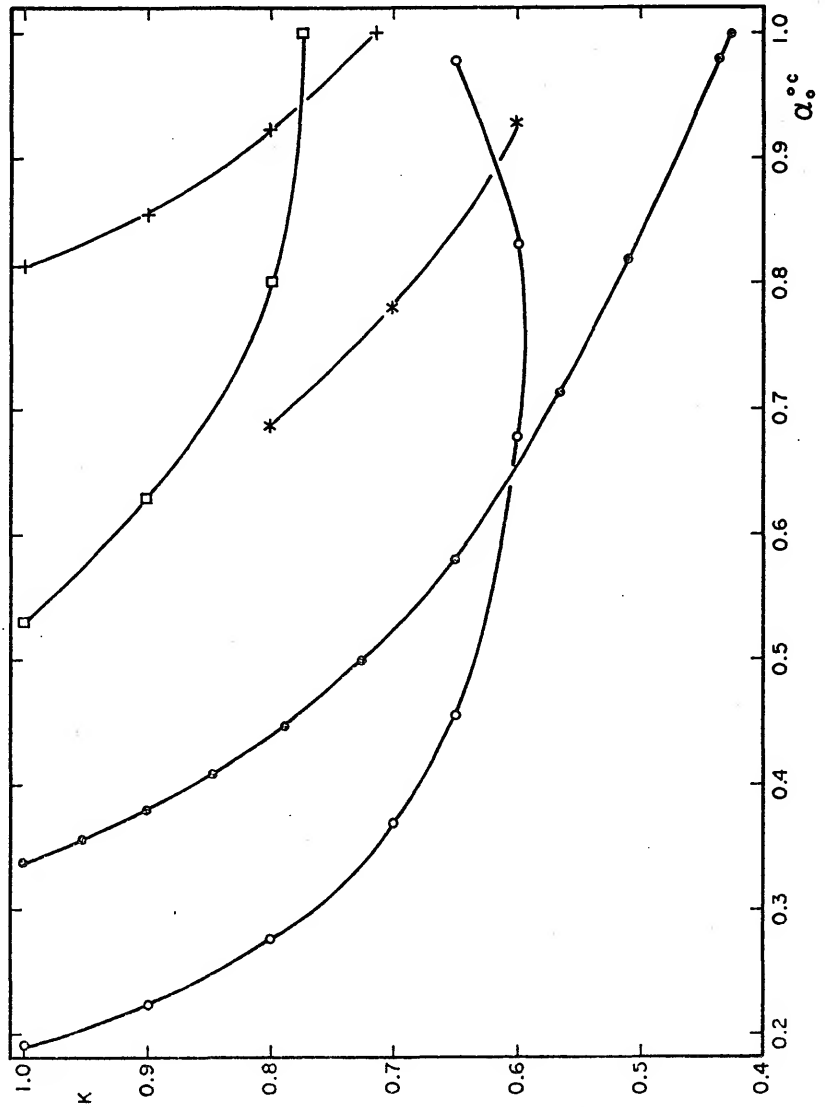
K
1.0
0.9
0.8
0.7
0.6
0.5
0.4
α_o°c
0.2
0.3
0.4
0.5
0.6
0.7
0.8
0.9
1.0

with $k(\alpha_o^{oc}, q_o)$ taken from the x = .8 tables was also derived and plotted (Table XIV and Figure 7). An inspection of this plot shows that for $\theta_e = 50°$ and $\theta_e = 45°.9$, the intersection of the shape curves for the two eclipses in both cases lies above the depth curve. This implies the possibility of a solution from the shapes alone, abandoning the depth curve and therefore the assumption that $L_1 + L_2 = 1$. This so-called third light solution is indeed one way to produce a theoretical light curve that will fit the observed curve. There is, however, no real justification for assuming the presence of this third light in the present case and therefore, this possibility was rejected.

It had been noticed from the first plotting of this rectified light curve that a number of the points in the primary and secondary eclipses were similar (i.e. for a given value of θ, I" was nearly the same for both eclipses). In attempting solutions for k = 1, this similarity became even more apparent and it was decided to superimpose the plots of the two eclipses (see Figure 8). The result was remarkable, from the shoulders down to a depth of approximately n = 0.8, the two eclipses were virtually identical; deeper than this point, there was a sharp divergence. Since this type of behavior is not possible in a system described by the Russell model, either the points near mid-eclipse had to be completely abandoned, or the rectification itself might be at fault, and a new rectification could be tried. It was decided to try to find a solution on the other

TABLE XIV

Depth Curve for $x = 0.8$, $1 - \ell_o^{oc} = 0.16$, $1 - \ell_o^{tr} = 0.18$

q_o	α_o^{oc}	k
0.195	1.00	.425
0.2	.98	.433
0.25	.82	.510
0.3	.713	.565
0.4	.58	.650
0.5	.50	.724
0.6	.447	.788
0.7	.408	.848
0.8	.38	.901
0.9	.357	.952
1.0	.34	1.000

Figure 8. Superpositions of Primary and Secondary Eclipses: The plus signs are the rectified observations of the primary eclipse and the open circles are the rectified observations of the secondary eclipse.

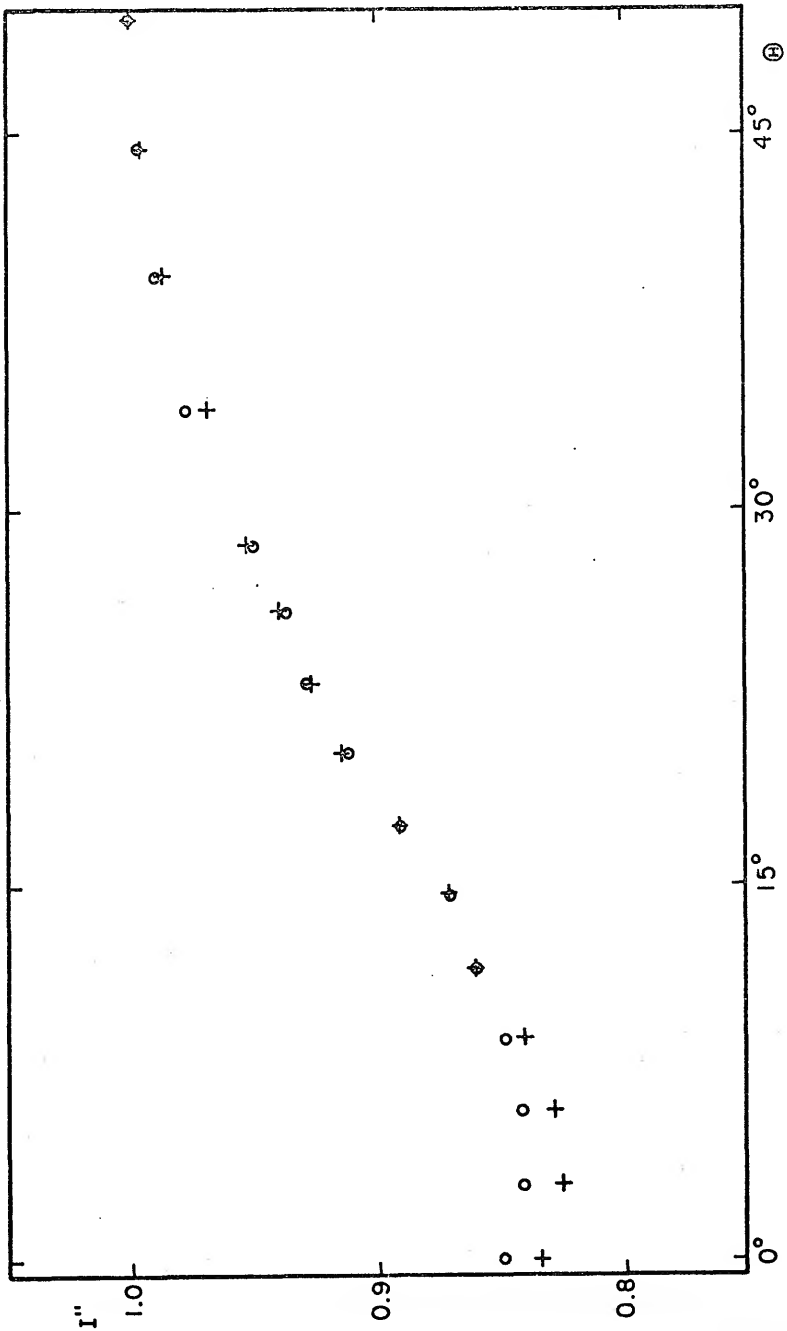
I''
1.0
0.9
0.8
0°
15°
30°
45°
Θ

rectification mentioned above, i.e. the one whose coefficients were derived by the least squares method of Fourier analysis.

Solutions from Least Squares Rectification

There are several differences apparent in looking at the two curves produced by the two different sets of rectification coefficients. Outside the eclipses, the residuals are more or less evenly distributed throughout the whole curve in the least squares rectification, with the sum of the squares of the residuals smaller than that from the graphical rectification, as expected. Inside the eclipses the two curves are no longer virtually identical from the shoulders down to an approximate level of n = 0.8; in general, for any given phase the primary is deeper than the secondary. The greatest change in the new rectification, however, is in the depths of the two eclipses. Both eclipses are significantly shallower, the depth of the primary eclipse going from about 0.18 to 0.16 and the depth of the secondary eclipse going from about 0.16 to 0.145.

A nomographic solution of this second rectified light curve was then attempted. The light curve was rectified in phase with a value of z based on N = 3.2 corresponding to a darkening x = 0.8 and the solution was tried on the x = 0.8 nomograph. The value of x = 0.8 was chosen for convenience since there is neither a nomograph nor a

set of χ tables for complete darkening and the previous explorations of the light curve seemed to indicate a large value for the darkening. The depths of the eclipses were chosen as $1 - \ell_o^{pr} = 0.16$ and $1 - \ell_o^{sec} = 0.14$ and the following values were read off the plot of the rectified light curve (Figure 4):

n	θ^{pr}	$\sin^2\theta^{pr}$	χ^{pr}	θ^{sec}	$\sin^2\theta^{sec}$	χ^{sec}
0.2	30°0	.25000	2.038	31°5	.27300	2.032
0.5	20.5	.12265	1	21.5	.13432	1
0.8	12.0	.043227	.352	13.5	.054497	.406

Since $\chi^{sec}(n = 0.8) > \chi^{pr}(n = 0.8)$, it seems that the primary eclipse is a transit and the secondary eclipse is an occultation as before. The values needed for the depth line on the nomograph are

$$(1 - \ell_o^{oc}) + (1 - \ell_o^{tr}) = 0.30$$

$$\frac{1 - \ell_o^{tr}}{\ell_o^{oc}} = 0.1860$$

$$\frac{1 - \ell_o^{tr}}{\ell_o^{oc}} + \frac{1}{50}\,\frac{1 - \ell_o^{oc}}{\ell_o^{oc}} = 0.1893$$

Taking these values and the $\chi(n = 0.8)$ values given above to the $x = 0.8$ nomograph, an intersection of the depth line and both χ contours was found with $k = 0.45$, $p_o = -0.75$, $\alpha_o^{oc} = 0.9395$, and $\alpha_o^{tr} = 0.8522$. Using the χ tables, the following points on the light curve were derived from these

parameters.

n	χ^{oc}	$\sin^2\theta$	θ	χ^{tr}	$\sin^2\theta$	θ
0.0	3.037	.44706	42°0	3.645	.44706	42°0
0.2	1.780	.26202	30.8	1.967	.24125	29.4
0.5	1	.14720	22.6	1	.12265	20.5
0.8	.407	.059912	14.2	.352	.043173	12.0

The situation here is quite similar to that found with the previous rectification. The computed curve is definitely narrower at the shoulders than the observed curve. The fit of primary eclipse from the half-way point down is fairly satisfactory. The lower half of the computed curve for the secondary eclipse is considerably wider than the observed curve.

These difficulties are basically the same as those encountered in the solution based on the first rectification. Furthermore, the situation here is one common to solutions of many systems with relatively shallow eclipses, i.e. solutions with a wide range of values of k differ very little in the light curves which they produce. For example, in this particular case, if the depths of the two eclipses and the value of the external tangency point, θ_e, are fixed, then solutions for the cases: 1) k = .65 primary-occultation, 2) k = .65 primary-transit, 3) k = 1 (see Tables XV, XVI, and XVII and Figure 4), differ in the whole course of the light curve by no more than approximately 0°6. This means that distinguishing among these possible solutions is quite

TABLE XV

Solution for x = 0.8, $1 - \ell_o^{pr} = 0.16$, $1 - \ell_o^{sec} = 0.145$, pr-oc, k = 0.65, $p_o = -0.1625$, $\alpha_o^{oc} = 0.55$, $\alpha_o^{tr} = 0.4548$

n	χ^{oc}	$\sin^2\theta$	θ	χ^{tr}	$\sin^2\theta$	θ
0.0	3.515	.48255	44°0	3.696	.48255	44°0
0.1	2.418	.331	35.2	2.507	.32731	34.9
0.2	1.935	.26564	31.0	1.986	.25929	30.6
0.4	1.264	.17353	24.6	1.275	.16646	24.1
0.5	1	.13728	21.7	1	.13056	21.2
0.6	.764	.104884	18.9	.758	.098064	18.3
0.8	.353	.048461	12.7	.344	.944913	12.2
0.9	.171	.023475	8.8	.165	.021542	8.4
0.95	.0840	.011532	6.2	.0807	.010536	5.9

TABLE XVI

Solution for x = 0.8, $1 - \ell_o^{pr} = 0.16$, $1 - \ell_o^{sec} = 0.145$, pr-tr, k = 0.65, $p_o = -0.1271$, $\alpha_o^{oc} = 0.525$, $\alpha_o^{tr} = 0.4314$

n	χ^{oc}	$\sin^2\theta$	θ	χ^{tr}	$\sin^2\theta$	θ
0.0	3.505	.48255	44°0	3.671	.48255	44°0
0.1	2.415	.33249	35.2	2.497	.32823	35.0
0.2	1.934	.26626	31.1	1.981	.26040	30.7
0.4	1.264	.17402	24.7	1.274	.16747	24.1
0.5	1	.13768	21.8	1	.13145	21.3
0.6	765	.105321	18.9	.758	.099638	18.4
0.8	.354	.048737	12.8	.345	.045350	12.3
0.9	.171	.023542	8.8	.165	.021689	8.5
0.95	.0841	.011578	6.2	.0811	.010661	5.9

TABLE XVII

Solution for $x = 0.8$, $1 - \ell_o^{pr} = 0.16$, $1 - \ell_o^{sec} = 0.145$, $k = 1.0$, $p_o = 0.1540$, $\alpha_o = 0.305$

n	χ	$\sin^2\theta$	θ
0.0	3.626	.48255	44°0
0.1	2.475	.32938	35.0
0.2	1.969	.26204	30.8
0.4	1.271	.16915	24.3
0.5	1	.133081	21.4
0.6	.760	.101142	18.5
0.8	.347	.046179	12.4
0.9	.167	.022225	8.6
0.95	.0818	.010886	6.0

difficult.

Because of the above difficulties, a provisional solution with the parameters $1 - \ell_o^{pr} = 0.16$, $1 - \ell_o^{sec} = 0.145$, $k = 1.0$, $\alpha_o = .305$, and $p_o = .1540$ was chosen. The computed curve was plotted (Figure 4) and values of observed minus computed (O - C) for each observed point were derived graphically. These (O - C) values are listed in Table XVIII and plotted as a function of phase in Figure 9. From an inspection of this plot, it appears that a higher order cosine term (e.g. cos 9 θ) is present, especially in the primary eclipse.

The possibility of using Kitamura's method for the solution of eclipsing binary light curves (11) was also explored. Kitamura's method has the advantage of using the whole light curve to find a provisional solution rather than using a few selected points as is done in the nomographic method. Since both methods of solution are based upon the same geometrical model for the eclipses, their final results should agree. Even though the two methods might produce different provisional solutions, a careful and thorough analysis based upon these different preliminary solutions should finally produce the same final solution. Any difference in the results has to be caused by improper application of one of the methods. Since solutions using Kitamura's method should not differ from those derived using the Russell-Merrill method, Kitamura's method was

TABLE XVIII

O-C's from Solution for k = 1, p_o = 0.1540, α_o = 0.305.

θ	O-C(θ)	O-C(180 +θ)
0.000	.007	.017
2.945	-.003	.007
5.885	-.007	.000
8.816	-.003	-.002
11.735	.003	-.002
14.637	.000	-.004
17.519	.003	.002
20.377	.011	.007
23.208	.006	.005
26.011	.004	.002
28.781	.001	.001
34.221	-.007	.003
39.518	-.006	-.001

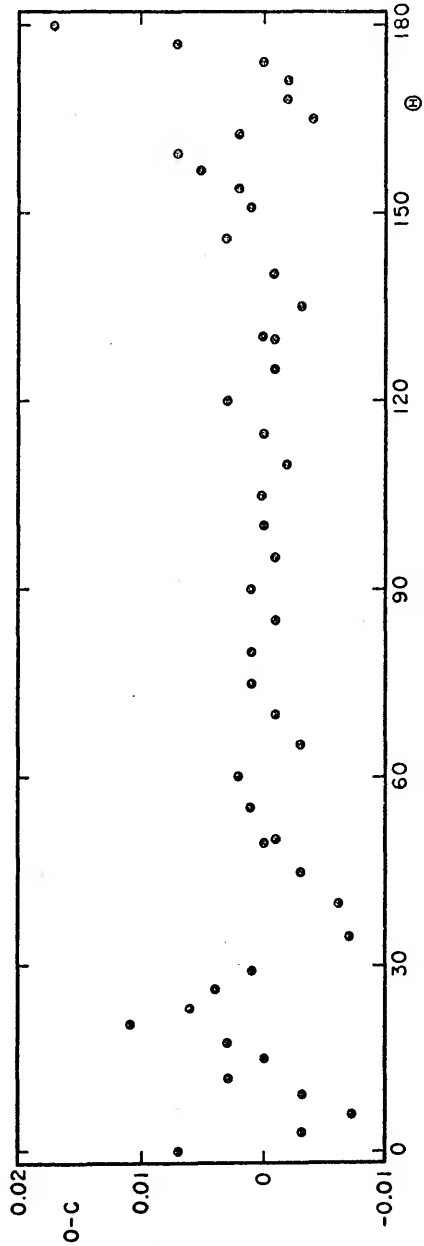

Figure 9. O-C's from Solution for k = 1, p_o = 0.1540, α_o = 0.305.

not pursued any further.

Before going on to find the geometrical elements corresponding to these possible solutions, a further exploration of the possibility that the eclipses are complete might be in order. By making this assumption, it is possible to find a solution from the shapes of the eclipses alone (i.e. by not assuming that $L_1 + L_2 = 1$). While this introduction of third light seems somewhat unwarranted, it is presented here for the sake of completeness. The shapes of the eclipses were used to derive the solution given in Table XIX and plotted in Figure 4. This solution assumes that the eclipses are complete and, in fact, takes the limiting situation of central eclipses (i.e. $i = 90°$). These assumptions require that more than half of the total light of the system come from some unknown third body ($L_3 = 0.588$). This solution seems to fit the light curve about as well as the previously mentioned solutions.

In rectifying the phase, the ellipticity z is a function of a parameter N which goes as

$$N = \frac{(15 + x)(1 + y)}{15 - 5x}$$

where x is the limb darkening and y is the gravity darkening of the star being eclipsed. In the rectification of the phase described above, a value of N = 2.6 corresponding to

TABLE XIX

Solution for $x = 0.8$, $1 - \ell_o^{pr} = 0.165$, $1 - \ell_o^{sec} = 0.145$, $k = 0.70$, $p_o = -1.429$, $\alpha_o^{oc} = 1.0$, $\alpha_o^{tr} = 1.067$, $\tau = 0.558590$, $L_3 = 0.588$.

n	χ^{oc}	$\sin^2\theta$	θ	χ^{tr}	$\sin^2\theta$	θ
0.0	3.339	.48255	44°0	4.481	.48255	44°0
0.1	2.281	.32965	35.0	2.833	.30508	33.5
0.2	1.834	.26505	31.0	2.163	.23293	28.9
0.4	1.231	.17790	24.9	1.307	.14075	22.0
0.5	1	.14452	22.3	1	.107688	19.2
0.6	.798	.11533	19.9	.745	.080228	16.5
0.8	.452	.065323	14.8	.350	.037691	11.2
0.9	.297	.042922	12.0	.196	.021107	8.4
0.95	.217	.031361	10.2	.1142	.012298	6.4
1.0	.1040	.015030	7.0			
$0.937=n_i$				.1396	.015033	7.0

a limb darkening of x = 0.6 implies that a gravity darkening of y = 1.0 was chosen. Dr. S. Rucinski (6) has suggested that a value of gravity darkening y = 0.32 might be more appropriate for this system. This possibility was explored and it was found to have no significant effect on the problems encountered in finding a solution for this system. Therefore, it was decided to proceed with the solutions already derived.

Orbital Elements

The next step was to derive orbital elements for the eclipsing system from the geometrical eclipse parameters. These elements can most easily be derived from the formulas given by Merrill (5):

$$a_g^2 = \frac{\sin^2\theta_e}{(1 + k)^2 - (1 + kp_o)^2\cos^2\theta_e}$$

$$a_s = ka_g$$

$$\cos i_r = (1 + kp_o)a_g$$

$$L_s = 1 - \ell_o^{oc}/\alpha_o^{oc}$$

$$L_g = 1 - L_s$$

The derived orbital elements for the various solutions are listed in Table XX.

Mean errors ($\mu = \sqrt{\Sigma(O - C)^2/(n - 1)}$) were derived for the "observed" points from each of the four possible solutions. These mean errors are listed in Table XX. The mean error has almost the same value for all three of the partial eclipse solutions (with no third light added). The value of the mean error for the complete eclipse solution (with third light) is slightly smaller than the values of the mean error for the other three solutions. Since these four solutions with very different values of the geometrical elements produce computed light curves which fit the observed light curve more or less equally well, it would not be meaningful to apply the method of differential corrections to find a least squares solution of the light curve. In the absence of a formal least squares solution, it is not possible to determine mean errors for each of the geometrical elements. From the results presented in Table XX, however, it is possible to estimate a reasonable range of each element. For the three partial eclipse solutions (without third light) the approximate ranges of these elements are: $.38 < a_g < .46$; $.29 < a_s < .38$; $64° < i_r < 66°$; $.53 < L_g < .72$; and $.27 < L_s < .48$. With the addition of third light the inclination can increase up to the limiting value of 90° and solutions are possible anywhere within this range of inclinations. In the solutions

TABLE XX

Orbital Elements for Solutions of First Synthetic Light Curve

	pr-oc		pr-tr	
k	.65	1.0	.65	.70
α_o^{oc}	.5500	.3050	.5250	1.0
α_o^{tr}	.4548	.3050	.4314	1.067
p_o	-.1625	+.1540	-.1271	-1.429
a_g	.457	.382	.459	.409
a_s	.297	.382	.299	.286
cos i_r	.40890	.44083	.42139	0
i_r	65°9	63°9	65°1	90°
L_g	.709	.525	.724	.277
L_s	.291	.475	.276	.135
L_3	0	0	0	.588
μ	.0045	.0044	.0044	.0037

presented here, the value of θ_e was chosen as 44° in order to best fit the whole light curve. The observations on the shoulders of the eclipses alone indicate that this value might be increased by several degrees. The effect of increasing θ_e is to increase the values of a_g and a_s (i.e., to increase the sizes of the stars relative to their separation) and to decrease the inclination of the orbit.

Figures of the Components

The figures of the components can now be computed from the formulas given by Merrill (10):

$$r_g + (0.17 + 1.19\ m_s/m_g) r_g^4 = a_g$$

$$b_g = a_g - 1.53 (m_s/m_g) r_g^4$$

$$c_g = 3r_g - a_g - b_g$$

These formulas require that the mass ratio of the components be known. Since this mass ratio was not known, a more indirect method was used to set limits on both the figures of the components and their mass ratios. This method assumes that no dimension of the star may exceed the size of the Roche lobe it is contained within. The dimensions of the Roche lobes for various mass ratios are

tabulated in the literature (e.g., Kopal (12)). The figures of the components were computed for a number of different mass ratios for each of the solutions. (The two solutions for k = .65 were combined for this purpose since the values of a_g and a_s in each were nearly equal.) These figures were compared with the size of the Roche lobe in order to determine the limiting mass ratios which would satisfy the criterion that the sizes of the stars must not exceed the sizes of their Roche lobes. These limiting mass ratios and the figures of the components derived using them for each of the solutions are listed in Table XXI.

Comparison of Solutions with Input Parameters

It is now possible to compare the solutions derived above with the parameters used to generate the light curve. The light curve was produced using Lucy's model for the light curves of W Ursae Majoris stars. In this model the surfaces of the two stars are Roche equipotential surfaces and for the Rucinski light curve the stars share a common envelope which fills the outer contact surface. The constant which defined this surface is C = 3.5591 with the mass ratio $q = m_s/m_g = 0.4$. The other parameters used in deriving the light curve are the inclination of the orbit i = 82°, the effective temperature of the surface T_e = 5700°, the wavelength of the light

TABLE XXI

Figures of the Components

k	.65	.65	1.0	1.0	.70	.70
m_s/m_g	.28	.57	.87	1.15	.25	.96
a_g	.458	.458	.382	.382	.409	.409
r_g	.439	.429	.361	.357	.397	.381
b_g	.442	.428	.359	.354	.400	.378
c_g	.417	.401	.342	.335	.382	.356
a_s	.298	.298	.382	.382	.286	.286
r_s	.273	.283	.357	.361	.263	.278
b_s	.267	.281	.354	.359	.257	.276
c_s	.254	.270	.335	.342	.246	.272

λ = 5500 Å, the limb darkening u = 0.6, and the gravity darkening y = 0.32. The size of the equipotential surface (and therefore the stars) was also given. These values are b_g = 0.531, c_g = 0.482, b_s = 0.363, and c_s = 0.337 (6).

These parameters can be compared with the results of the solutions as listed in Table XX and Table XXI. The inclination of the orbit suggests that a solution using the Russell-Merrill method which has this inclination will include the presence of some third light. The figures of the components (with q = 0.4) for such a solution can be of roughly the same shape in the yz-plane (the plane containing the b and c axes of the components) as the shapes of the lobes of the outer contact surface in the yz-plane. The Russell-Merrill dimensions of the components in this plane relative to the separation of the components are considerably smaller than the dimensions of the lobe of the outer contact surface in the yz-plane. Although it is possible, as previously mentioned, to increase slightly the dimensions of the components by increasing the values of Θ_e in the solution, it is not possible to increase the dimensions of the components to anywhere near the size of the outer contact surface and still have the value of Θ_e compatible with the light curve. Using the Russell model of similar prolate ellipsoids, it is possible to propose a system consisting of two components whose dimensions in the yz-plane are nearly as large as the dimensions of the

lobes of the outer contact surface in the yz-plane. These prolate ellipsoids would be in contact (i.e., $a_g + a_s = 1$). There are a number of objections to this proposed system. First of all, it is not possible for real stars in contact to have ellipsoidal shapes. Even if such a system were physically possible, it would produce eclipses with $\theta_e = 90°$, in contrast with the values ($44° \lesssim \theta_e < 50°$) given by the light curve. Even the physically realistic system with the two components filling their Roche lobes (inner contact surfaces) produces eclipses that are wider (for i = 82°) than those in the light curve (12). In this case the sizes of the components in the yz-plane are also considerably smaller than the sizes of the lobes of the outer contact surface in the yz-plane.

As the above discussion indicates, the solutions produced by applying the Russell-Merrill method to the light curve give very different values for the orbital elements than the parameters used to generate the light curve. This is especially true if third light is not included in the solution. Then, not only are the stars much smaller than the outer contact surface, but the inclination of the orbit is also quite different from the inclination used in deriving the light curve. Leaving aside the question of third light, since the amount of third light cannot be determined from the light curve alone, it is apparent that the Russell-Merrill solution of the light curve is completely unsuccessful in predicting the elements used to derive the light curve from Lucy's model. Thus these two

models for the light curves of W Ursae Majoris stars seem to be incompatible. While the models can produce similar light curves, both of which resemble the light curves observed for W Ursae Majoris type stars, the orbital elements which they use to produce these similar light curves are quite different. Since most of the solutions of the light curves of W Ursae Majoris type stars which are in the literature are based upon the geometrical model lying behind the Russell-Merrill method of solution (or, equivalently, other methods based upon the same model), much caution is in order in looking at these solutions. If Lucy's model represents the actual physical situation for a W Ursae Majoris type star, then most of the solutions in the literature probably do not realistically represent the actual physical situation present in the W Ursae Majoris type stars.

CHAPTER III

SECOND SYNTHETIC LIGHT CURVE

A second synthetic light curve for a W Ursae Majoris type eclipsing binary was generated from a theoretical model by Dr. R. E. Wilson (9). The "observational" data for this light curve consisted of 51 values of the differential stellar magnitude as a function of phase, with the phases given in intervals of one-hundredth of the period from phase 0.00 to phase 0.50. The remaining half of the light curve from phase 0.50 to phase 1.00 was assumed to be symmetrical. This "observational" data is plotted in Figure 10 and listed in Table XXII. (A normalization constant equal to 0.2049 was subtracted from each of the magnitudes.) Also listed in this table are the corresponding light values and phase angles in degrees for each data point. The synthetic light curve was to be treated as observational data and a solution was to be obtained by using the standard Russell-Merrill method of solution for light curves of eclipsing binaries. No additional information about the nature of the derivation of this light curve was to be used in the solution.

Figure 10. Observations of Second Synthetic Light Curve.

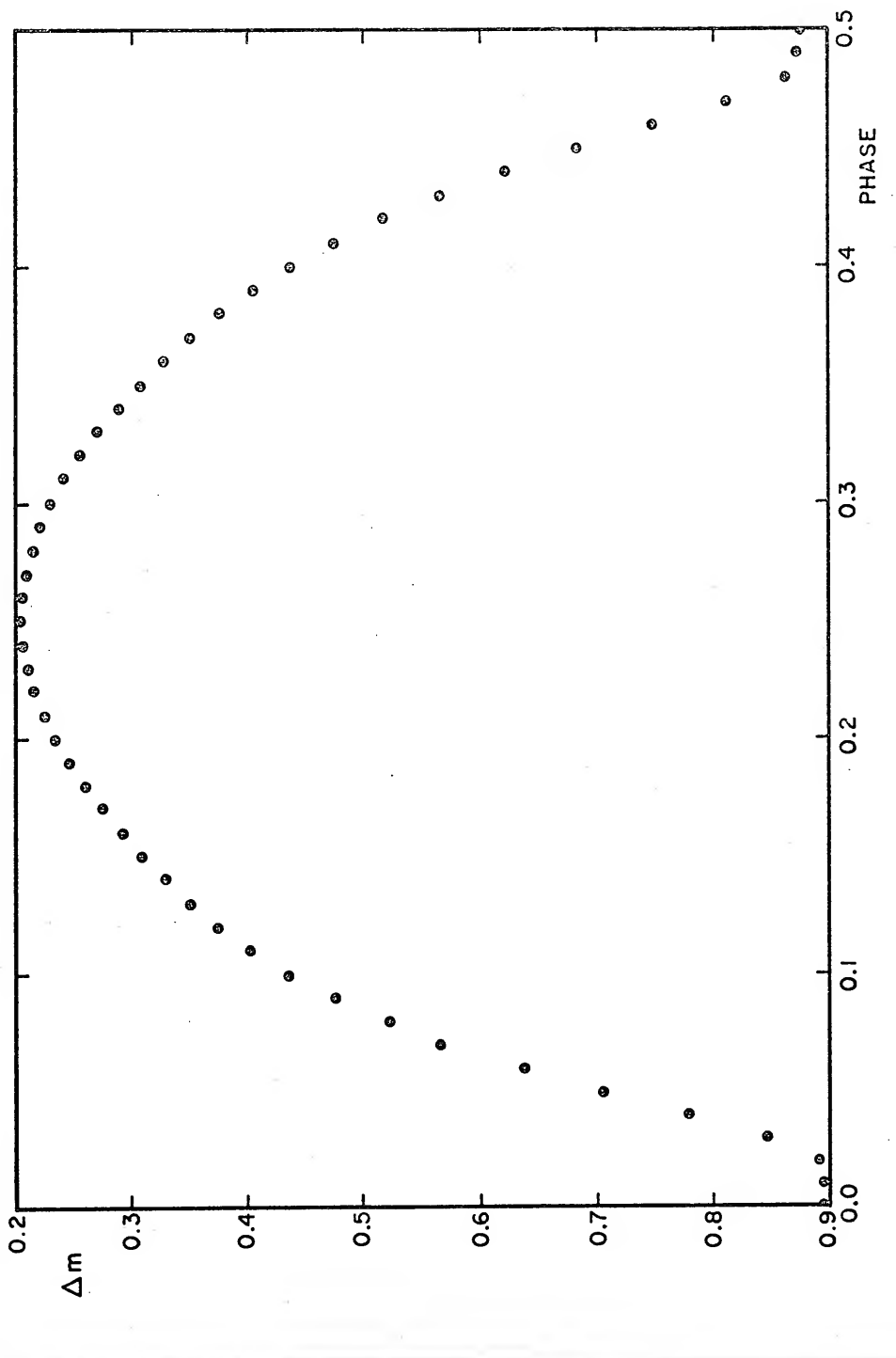
0.2
0.3
0.4
0.5
0.6
0.7
0.8
0.9
Δm
0.0
0.1
0.2
0.3
0.4
0.5
PHASE

TABLE XXII

Observations of Second Synthetic Light Curve

PHASE	$\Delta m-0.2049$	I	θ
0.00	0.6900	0.5297	0.0
0.01	0.6893	0.5300	3.6
0.02	0.6857	0.5318	7.2
0.03	0.6398	0.5547	10.8
0.04	0.5725	0.5902	14.4
0.05	0.5012	0.6303	18.0
0.06	0.4333	0.6709	21.6
0.07	0.3718	0.7100	25.2
0.08	0.3176	0.7464	28.8
0.09	0.2707	0.7793	32.4
0.10	0.2308	0.8085	36.0
0.11	0.1972	0.8339	39.6
0.12	0.1691	0.8558	43.2
0.13	0.1457	0.8744	46.8
0.14	0.1252	0.8911	50.4
0.15	0.1060	0.9070	54.0
0.16	0.0881	0.9221	57.6
0.17	0.0712	0.9365	61.2
0.18	0.0557	0.9500	64.8
0.19	0.0419	0.9621	68.4
0.20	0.0298	0.9729	72.0
0.21	0.0197	0.9820	75.6
0.22	0.0115	0.9895	79.2
0.23	0.0057	0.9948	82.8
0.24	0.0016	0.9985	86.4
0.25	0.0000	1.0000	90.0
0.26	0.0006	0.9994	93.6
0.27	0.0037	0.9966	97.2
0.28	0.0087	0.9920	100.8
0.29	0.0160	0.9854	104.4
0.30	0.0256	0.9767	108.0
0.31	0.0374	0.9661	111.6
0.32	0.0510	0.9541	115.2

Table XXII continued.

PHASE	Δm-0.2049	I	θ
0.33	0.0667	0.9404	118.8
0.34	0.0841	0.9255	122.4
0.35	0.1028	0.9097	126.0
0.36	0.1231	0.8928	129.6
0.37	0.1459	0.8743	133.2
0.38	0.1715	0.8539	136.8
0.39	0.1998	0.8319	140.4
0.40	0.2322	0.8075	144.0
0.41	0.0694	0.7803	147.6
0.42	0.3115	0.7506	151.2
0.43	0.3621	0.7164	154.8
0.44	0.4172	0.6810	158.4
0.45	0.4779	0.6439	162.0
0.46	0.5426	0.6067	165.6
0.47	0.6066	0.5720	169.2
0.48	0.6574	0.5458	172.8
0.49	0.6672	0.5409	176.4
0.50	0.6693	0.5399	180.0

Rectification

As in the previous synthetic light curve solution, the first step is an analysis of the light outside the eclipses in order to rectify the light curve to the spherical model. This analysis was done by a least-squares Fourier analysis of the light outside of eclipse (48° to 132°). The results of this analysis are listed in Table XXIII. The light values were then rectified by the formula:

$$I'' = \frac{I+C_o+C_1 \cos \theta+C_2 \cos 2\theta-A_3 \cos 3\theta-A_4 \cos 4\theta}{A_o+C_o+ (A_2+C_2) \cos 2\theta}$$

and the phase angles were rectified by the formula

$$\sin^2\theta'' = \sin^2\theta/(1 - z \cos^2\theta)$$

where $z = -4(A_2 - C_2)/N(A_o - C_o - A_2 + C_2)$ with $N = 2.2$, corresponding to a limb darkening $x = 0.4$. The rectification coefficients for reflection were determined from the statistical formula given by Russell and Merrill (2): $C_o = 0.072 \sin^2\theta_e = 0.0398$, $C_1 = -A_1$, and $C_2 = 0.024 \sin^2\theta_e = 0.0133$, with $\theta_e = 48°$. Following Merrill (10), the A_3 and A_4 terms were removed by subtraction. The rectified points are listed in Table XXIV and plotted in Figure 11.

TABLE XXIII

Rectification Coefficients for Second Synthetic Light Curve

$A_o' = 0.86563 \pm 0.00012$

$A_1 = 0.00390 \pm 0.00009$

$A_2 = -0.13528 \pm 0.00018$

$A_3 = 0.00382 \pm 0.00005$

$A_4 = -0.00098 \pm 0.00007$

OBSERVED INTENSITY	THEORETICAL INTENSITY	O-C	θ
0.8911	0.8910	0.0001	50.4000
0.9070	0.9069	0.0001	54.0000
0.9221	0.9222	-0.0001	57.6000
0.9365	0.9366	-0.0001	61.2000
0.9500	0.9500	-0.0000	64.8000
0.9621	0.9622	-0.0001	68.4000
0.9729	0.9729	0.0000	72.0000
0.9820	0.9820	-0.0000	75.6000
0.9895	0.9894	0.0001	79.2000
0.9948	0.9949	-0.0001	82.8000
0.9985	0.9984	0.0001	86.4000
1.0000	0.9999	0.0001	90.0000
0.9994	0.9994	0.0000	93.6000
0.9966	0.9967	-0.0001	97.2000
0.9920	0.9920	-0.0000	100.8000
0.9854	0.9853	0.0001	104.4000
0.9767	0.9767	0.0000	108.0000
0.9661	0.9662	-0.0001	111.6000
0.9541	0.9541	0.0000	115.2000
0.9404	0.9405	-0.0001	118.8000
0.9255	0.9256	-0.0001	122.4000
0.9097	0.9096	0.0001	126.0000
0.8928	0.8928	0.0000	129.6000

TABLE XXIV

Rectified Second Synthetic Light Curve

I	I"	Θ
0.5297	0.7353	0.000
0.5300	0.7347	4.233
0.5318	0.7341	8.453
0.5547	0.7583	12.647
0.5902	0.7960	16.805
0.6303	0.8370	20.917
0.6709	0.8760	24.972
0.7100	0.9106	28.965
0.7464	0.9396	32.889
0.7793	0.9624	36.741
0.8085	0.9792	40.518
0.8339	0.9905	44.219
0.8558	0.9970	47.845
0.8744	0.9996	51.398
0.8911	1.0001	54.881
0.9070	1.0002	58.298
0.9221	1.0000	61.653
0.9365	0.9999	64.950
0.9500	1.0000	68.196
0.9621	1.0000	71.397
0.9729	1.0001	74.559
0.9820	1.0000	77.687
0.9895	1.0002	80.789
0.9948	1.0000	83.870
0.9985	1.0001	86.939
1.0000	1.0001	90.000
0.9994	1.0001	93.062
0.9966	0.9999	96.130
0.9920	1.0000	99.212
0.9854	1.0002	102.314
0.9767	1.0001	105.442
0.9661	0.9999	108.604
0.9541	1.0001	111.804

Table XXIV continued.

I	I"	Θ
0.9404	1.0000	115.051
0.9255	1.0000	118.348
0.9097	1.0002	121.703
0.8928	1.0001	125.119
0.9743	0.9989	128.602
0.8539	0.9958	132.156
0.8319	0.9908	135.782
0.8075	0.9826	139.483
0.7803	0.9701	143.260
0.7506	0.9533	147.112
0.7164	0.9291	151.036
0.6810	0.9012	155.028
0.6439	0.8686	159.084
0.6067	0.8331	163.195
0.5720	0.7979	167.354
0.5458	0.7708	171.548
0.5409	0.7681	175.768
0.5399	0.7681	180.000

Figure 11. Rectified Second Synthetic Light Curve: The solid circles are the rectified observations; the plus signs are computed from the solution without third light; and the open circles are computed from the solution with third light.

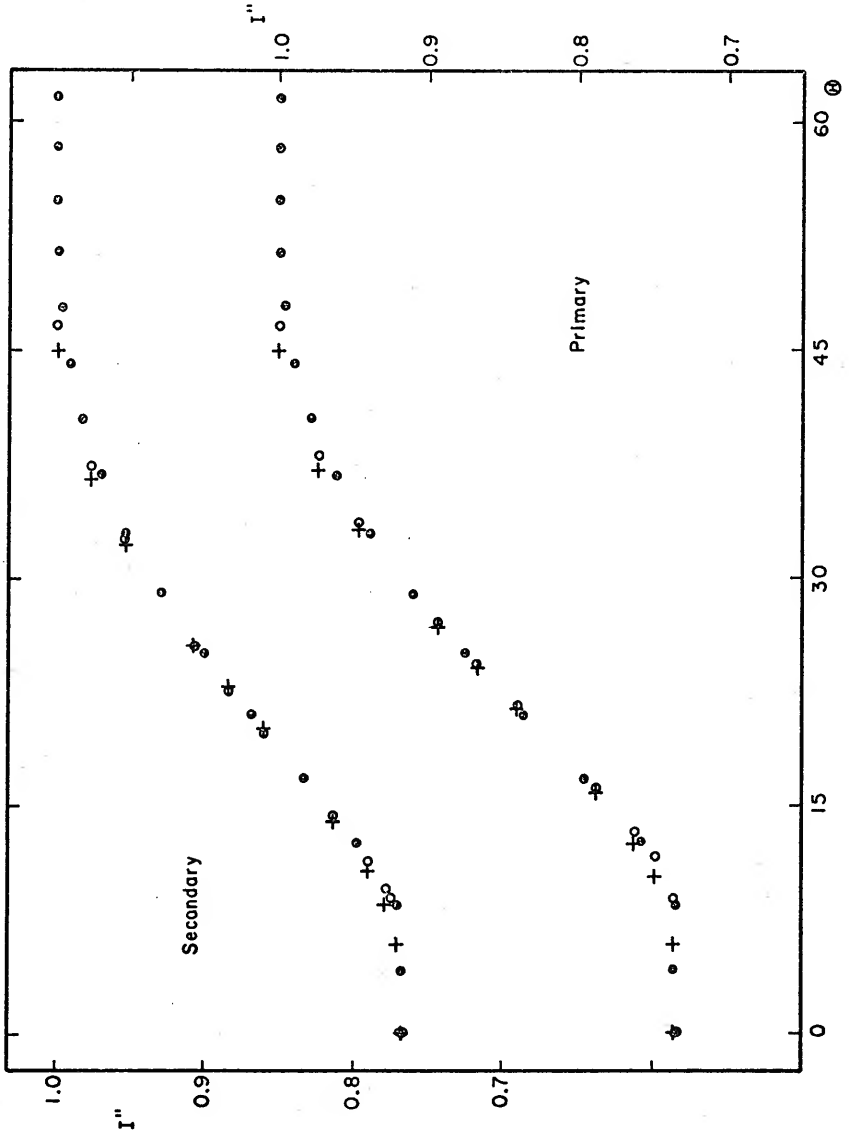
I"
1.0
0.9
0.8
0.7
Secondary
Primary
0
15
30
45
60 θ

Solutions

An examination of the rectified light curve reveals several things. The most obvious is that the eclipses are apparently complete. Furthermore it appears that the primary eclipse is the occultation (total) eclipse and the secondary eclipse is the transit (annular) eclipse. Closer examination reveals a very slight brightening in the center of the primary eclipse. The flatness of both eclipses indicates that the limb darkening is probably small. The depths of the two eclipses were chosen as $1 - \ell_o^{pr} = 0.265$ and $1 - \ell_o^{sec} = 0.233$ for the purpose of obtaining a preliminary nomographic solution. Then the following values were read off the plot of the rectified light curve:

n	θ^{pr}	$\sin^2\theta$	χ^{pr}	θ^{sec}	$\sin^2\theta$	χ^{sec}
0.2	33.5	.30463	1.841	33.1	.29823	1.986
0.5	24.0	.16543	1	22.8	.15017	1
0.8	15.8	.074137	.448	14.4	.061847	.412

$\chi^{pr}(n = 0.8) > \chi^{sec}(n = 0.8)$, confirming that the primary eclipse is the occultation eclipse and the secondary eclipse is the transit eclipse. These χ values along with a depth line $1 - \ell_o^{tr}/\ell_o^{sec} = 0.3176$ were taken to the total eclipse portion of the x = 0.4 nomographs and a satisfactory intersection of the three curves was found. This intersection implied a solution with the values k = 0.545, $\alpha_o^{oc} = 1.0$, $\alpha_o^{tr} = 1.016$, $p_o = -1.10$, and $\tau = 0.3126$. The results of this solution are listed in Table XXV and plotted in Figure 11.

TABLE XXV

Solution for $x = 0.4$, $k = 0.545$, $\alpha_o^{oc} = 1.0$, $\alpha_o^{tr} = 1.016$, $p_o = -1.10$, $\bar{\tau} = 0.3126$, $1 - \ell_o^{pr} = 0.265$, $1 - \ell_o^{sec} = 0.233$

n	χ^{oc}	$\sin^2\theta$	θ	χ^{tr}	$\sin^2\theta$	θ
0.0	2.977	.50000	45°0	3.364	.50000	45°0
0.1	2.180	.36613	37.2	2.395	.35597	36.6
0.2	1.785	.29979	33.2	1.921	.28552	32.3
0.4	1.224	.20557	27.0	1.256	.18668	25.6
0.5	1	.16795	24.2	1	.14863	22.7
0.6	.800	.13436	21.5	777	.11549	19.9
0.8	.447	.075074	15.9	.398	.059155	14.1
0.9	.279	.046858	12.5	.231	.034334	10.7
0.95	.190	.031911	10.3	.1426	.021195	8.4
1.0	.0623	.010463	5.9			
$0.984 = n_i$				.069	.010255	5.8

A brief inspection of this plot shows that the fit is reasonably satisfactory except at the shoulders of the eclipses. At the shoulders, the computed curve is significantly narrower than the "observed" points. This, in essence, is the same situation that was found in the solution of the first synthetic light curve. Further refinements of the solution, consistent with the assumption of complete eclipses and the retention of the depth line $\frac{1 - \ell_o^{tr}}{\ell_o^{oc}} = 0.3176$, will not significantly improve this situation. It seems that there is probably some incompatibility between the Russell model of prolate spheroids as rectified to the spherical model and the theoretical model which was used to generate the light curves. If the assumption that the theoretical model more closely approximates physical reality for W Ursae Majoris stars is warranted, then the Russell model has serious faults when applied to these systems. It is well known, of course, that the Russell model is only a rough approximation to the very close binary systems. The real question, which this study will attempt to answer partially, is whether a solution of such a system derived from the Russell model will provide an adequate representation of the true orbital elements of the binary system.

One way to somewhat improve the fit of a solution to the "observed" points is to abandon the depth line and

do a solution only from the shapes of the eclipses. This may mean the introduction of the light of a third body to the system. In the present case, the introduction of third light ($L_3 = 0.234$) yields the central eclipse solution listed in Table XXVI and plotted in Figure 11. This solution improves the fit somewhat, though the shoulders of the computed curve are still too narrow. There seems to be no sound observational reason for adding this third light. In about 20% of the solutions of eclipsing binary light curves in the literature (13), some third light is present. This third light solution is presented here in order to demonstrate how the addition of third light affects the solution. Unless there is some real physical source of this third light, however, the necessity for its introduction to improve the solution only serves to point out the inadequacies of the model on which the solution is based.

Orbital Elements and Figures of the Components

These two solutions, from the formulas given above, were then used to derive orbital parameters and limiting mass ratios for the assumption that neither component exceeds the size of its Roche lobe. The results of these derivations are listed in Tables XXVII and XXVIII.

Comparison of Solutions with Input Parameters

It is now possible to compare the solutions derived

TABLE XXVI

Solution for $x = 0.4$, $k = 0.65$, $\alpha_o^{oc} = 1.0$, $\alpha_o^{tr} = 1.039$, $p_o = -1.538$, $\tau = 0.447537$, $1 - \ell_o^{pr} = 0.265$, $1 - \ell_o^{sec} = 0.233$, $L_3 = 0.234$

n	χ^{oc}	$\sin^2\theta$	θ	χ^{tr}	$\sin^2\theta$	θ
0.0	3.131	.52965	46°7	3.600	.52965	46°7
0.1	2.250	.38061	38.1	2.502	.36812	37.4
0.2	1.822	.30821	33.7	1.976	.29073	32.4
0.4	1.229	.20790	27.1	1.265	.18612	25.6
0.5	1	.16916	24.3	1	.14713	22.6
0.6	.800	.13533	21.6	.775	.11403	19.8
0.8	.462	.078152	16.2	.413	.060765	14.3
0.9	.314	.053116	13.3	.263	.038695	11.3
0.95	.240	.040598	11.6	.1867	.027469	9.5
1.0	.141	.023852	8.9			
$0.962 = n_i$				.162	.023835	8.9

TABLE XXVII

Orbital Elements for Solutions of Second Synthetic Light Curve

k	0.545	0.65
α_o^{oc}	1.0	1.0
α_o^{tr}	1.016	1.039
p_o	-1.10	-1.538
a_g	0.466	0.441
a_s	0.254	0.287
$\cos i_r$	0.18663	0
i_r	79°2	90°
L_g	0.735	0.501
L_s	0.265	0.265
L_3	0	0.234

TABLE XXVIII

Figures of the Components

m_s/m_g	.52	.17	.66	.25
a_g	.466	.466	.441	.441
r_g	.437	.451	.413	.426
b_g	.437	.455	.412	.429
c_g	.408	.432	.386	.408
a_s	.254	.254	.287	.287
r_s	.245	.233	.276	.264
b_s	.244	.228	.274	.258
c_s	.237	.217	.267	.247

above with the parameters used to generate the light curve. The theoretical light curve is a trial and error match to Broglia's observations of RZ Comae (14). This light curve was generated by Dr. R. E. Wilson from the parameters listed in Table XXIX. In this model, as in the model used to generate the first synthetic light curve, the sizes of both the components exceed the sizes of their Roche lobes. In this case the boundary of the components lies along a common envelope which is smaller than the outer contact surface. Broglia's observations of RZ Comae were solved by Binnendijk (15). The solution of the synthetic light curve (without third light) as listed in Table XXVII and Table XXVIII is fairly close to Binnendijk's solution of the real observations of RZ Comae. This would seem to indicate that this solution is the one which follows from the Russell model and that it is not greatly sensitive to effects of judgment and details of procedure. However the true parameters used to derive the synthetic light curve are not at all close to the solution given above or to Binnendijk's. In fact, it is possible to derive a theoretical light curve from the true parameters using the Russell model. Such a light curve would look very different from the synthetic light curve derived from the same parameters using Wilson's model. The most obvious difference is that the Russell model theoretical light curve would have significantly wider and deeper eclipses than those

TABLE XXIX

Input Parameters for Second Synthetic Light Curve

i	86°.00
L_1	0.3149
L_2	0.6851
x_1	0.40
x_2	0.40
r_1(pole)	0.2992
r_i(side)	.3132
r_1(back)	.3505
λeff	5500 Å
g_1	1.00
g_2	1.00
T_1	5500K (polar)
T_2	5563K(polar)
m_2/m_1	2.200
r_2(pole)	0.4287
r_2(side)	.4579
k	0.69
r_2(back)	.4880
Ω_1	5.449
Ω_2	5.449
A_1	1.00
A_2	1.00
ℓ_3	0.000

present in the given synthetic light curve. The difference in depth is especially obvious since the light lost in the total eclipse is equal to the light of the smaller star. In addition the annular eclipse in the theoretical Russell Model light curve derived from the true parameters would be deeper than the total eclipse, the reverse of the situation in the synthetic light curve.

A comparison of the solutions derived above using the Russell-Merrill method (Table XXVII and Table XXVIII) with the true parameters used to derive the synthetic light curve (Table XXIX) reveals that the Russell-Merrill solution of the light curve is completely unsuccessful in predicting the elements used to derive the light curve from Wilson's model. The situation here is similar to that found in the solution of the first synthetic light curve. Wilson's model, like Lucy's model, seems to be incompatible with the Russell model as applied to the light curves of W Ursae Majoris stars. Again, although Wilson's model and the Russell model will produce similar light curves, both of which resemble the light curves observed for W Ursae Majoris type stars, the orbital elements which they use to produce these similar light curves are quite different. Unfortunately, there is no way to determine from the two synthetic light curves whether Lucy's model and Wilson's model are compatible. The evidence of the solutions of the two synthetic light curves makes it clear that some

caution is in order in looking at published solutions for the light curves of W Ursae Majoris type stars. Most of these solutions are based on the geometrical model which lies behind the Russell-Merrill method of solution (or, equivalently, other methods based upon the same model). The solutions from this geometrical model (i.e. the Russell model) are not compatible with the parameters used to derive similar theoretical light curves from astrophysical models such as Lucy's or Wilson's. While it is not possible to determine in this study which of the three models best represent the real situation in W Ursae Majoris type stars, there is little doubt that there are serious problems in applying the Russell model to these stars.

One of the problems encountered in the solutions of both synthetic light curves was the fit of the solutions at the shoulders of the eclipses. In both cases the "observations" at the shoulders lie below the theoretical curves, and the eclipses seem to be of longer duration observationally than predicted by the Russell model. According to Bookmyer "this particular discrepancy between the Russell model and observations occurs in many W Ursae Majoris systems" (16). Binnendijk also reports that "it has been determined that in many light curves the observations defining the shoulders of the eclipse curves are fainter than expected from the Russell model" (1). Both authors interpret this effect as evidence for a permanent distortion

in the shapes of the components; the facing hemispheres of the components are more elongated than the Russell model ellipsoids. Since the synthetic light curves show this feature which is common to most W Ursae Majoris systems, perhaps this is further evidence that the Russell model does not apply to these systems.

CHAPTER IV

THE SYSTEM OF 44i BOOTIS

History

The system of 44i Bootis was discovered as a visual binary by William Herschel in 1781. On the discovery night he entered in his observing book:

> Double. Considerably unequal. Both white. With 227 they seem almost to touch, or at most 1/4 diameter of S. asunder; with 460, 1/2 or 3/4 diameter of S. This is a fine object to try a telescope, and a miniature of Alpha Geminorum. Position 29° 54' n. following (17).

The variation of one or both components was suspected by several early observers of the visual pair. These early observations are summarized by Miss Agnes Clerke as follows:

> On June 16, 1819, Struve noted a difference of two magnitudes between the components; of one invariably 1822-33, but of only half a magnitude 1833-38. Argelander found them exactly equal, June 6, 1830. To Dawes in April 1841, the attendant star seemed a shade brighter than its primary, which was rated as of fifth magnitude. Duner's observations at Lund, 1868-75, confirm their relative variability, causing the disparity between them to range from 0.4 to

> 1.3 magnitude; and he points out that they appeared to Herschel considerably unequal in 1781, but perfectly matched in 1787. Both stars were yellow in 1875, but the tint of the smaller was at times less deep than at others. Admiral Smyth marked it as "lucid gray" in 1842; Webb and Secchi respectively found it blue in 1850 and 1859; Webb and Engelmann reddish in 1856 and 1865. The principal star has often been considered as pure white. The spectrum belongs to Class I. The photographic magnitudes of the pair, as determined at Paris in 1886, are 5.3 and 6. Engelmann concluded the smaller component to vary from magnitude 5 to 7, the larger from 5 to 6. They revolve in a period of 261 years, the plane of their orbit passing nearly through the sun. The periastron passage was in 1783. They possess at least four times the solar luminous intensity (18).

The fainter component of the visual pair was found to have a spectrum resembling that of W Ursae Majoris by members of the Mount Wilson staff in 1921. In 1926 J. Schilt observed the star photographically and found that this component is an eclipsing variable, as suspected, with a period a little greater than a quarter of a day. In 1929 G. P. Kuiper confirmed the variability found by Schilt from older plates of the visual pair taken by Hertzsprung in 1915 and Münch in 1922 and 1926. There have been many investigations of the light variation of the fainter component of the visual double since that time (19).

Visual Binary

44i Bootis is a well known visual binary, Σ1909-ADS 9494. The most recent discussion of the orbit was by W. D. Heintz in 1963. His final elements as reported by J. Meeus (20) are

P	=	246.20 years	a	=	4".100
T	=	2042.00	i	=	±84°.50
e	=	0.360	ω	=	237°.90
π_d	=	0".080	Ω	=	228°.50

where P is the period of revolution, a is the semi-major axis of the orbit, T is the year of periastron passage, i is the inclination of the orbit, e is the eccentricity of the orbit, ω is the longitude of periastron, π_d is the dynamical parallax, and Ω is the position angle of the ascending node. Because of the high inclination the apparent ellipse is very elongated and the angular distance between the components is less than one-half second of arc at this time (see Figure 12). The dynamical parallax agrees well with the trigonometric and spectroscopic parallaxes quoted by Binnendijk (19).

$$\pi_{tr} = 0".076 \pm 0".005$$

$$\pi_{sp} = 0".073 \pm 0".005$$

We will call the brighter component star A. Its spectral

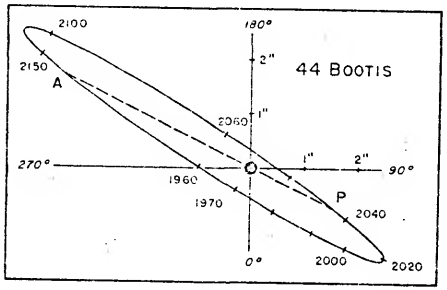

Figure 12. Visual Binary Orbit of 44i Bootis (20).

type is F9 (21) and, according to Binnendijk, there are indications that its light shows a slight variability. The fainter component of the visual double star has a spectral type G4 (21) with rotationally broadened absorption lines like those found in W Ursae Majoris stars. We will call the fainter component (the eclipsing variable) star B, and its brighter and fainter components star B1 and star B2 (or sometimes star 1 and star 2) respectively. From the visual orbit and a mean parallax of 0".076 we find for the sum of the masses:

$$M_A + M_{B1} + M_{B2} = 2.59 \odot .$$

Spectroscopic Binary

The eclipsing system is also a spectroscopic binary. D. M. Popper (22) observed the radial velocity curves and found the following results:

$K_{B1} = 115.4 \pm 1.6$ km/sec	$K_{B2} = 231.1 \pm 1.9$ km/sec
$e = 0$	$M_{B2}/M_{B1} = 0.50 \pm .03$
$a_{B1} \sin i = 0.43 \times 10^6$ km	$a_{B2} \sin i = 0.85 \times 10^6$ km
$M_{B1} \sin i = 0.77 \odot$	$M_{B2} \sin i = 0.39 \odot$

where K is the amplitude of the radial velocity variation, e is the eccentricity of the orbit, M is the mass of the

star, a is the semi-major axis of the orbit, and i is the inclination of the orbit. A more recent solution of the radial velocity curves was made by L. Binnendijk; however, it is based on older observations made by W. E. Harper. Following A. H. Batten (23), Popper's solution was chosen because it is based on a greater number of observations.

From the line intensities Popper extimated that the luminosity ratio of the components is 0.6 and most certainly lies between the values 0.5 and 0.85. Therefore in our notation $L_1 = 0.62$ and $L_2 = 0.38$. On the other hand, Petrie gives .06 $\pm$ .05 for the magnitude difference between the components of the spectroscopic binary or 0.95 $\pm$ 0.04 for the luminosity ratio; thus $L_1 = 0.51$ and $L_2 = 0.49$.

Eclipsing Variable

A large number of observations of the light variation of 44i Bootis B have been made since this variation was discovered. These observations have shown the presence of strange deviations from the mean light curve. There have also been several apparently abrupt changes in the period of the system. There are no published solutions made from observations in more than one color. For these reasons, it was decided that further observations were in order.

Instrumentation

The observations were taken at the Rosemary Hill Observatory of the University of Florida. The telescope used was a 30-inch reflector manufactured by the Tinsley Company. The telescope has a prime focal length of 120 inches. It has interchangeable secondary mirrors which allow observing at either the Newtonian focus or the Cassegrain focus. A six-inch refractor is mounted alongside the reflector for use as a finder-scope. The photometer was mounted at the Cassegrain focus with an effective focal ratio of f/16.

The optical and mechanical parts of the photometer were built by Astromechanics. As the light rays pass from the telescope into the photometer, they travel first through a small aperture, then through a filter, and finally through a Fabry lens before impinging on the phototube. The diaphragm which provides aperture of 0.33, 0.51, 0.93, 1.52, 1.98, 2.54, 2.89, 3.90, 4.89, and 5.85 millimeters, which, with a focal length of 480 inches, correspond to angular aperture of 5.4, 8.3, 15.2, 25, 32.5, 41.5, 47, 64, 80, and 96 seconds of arc. The 32.5-second aperture was used in these observations. A diagonal mirror may be placed in the light path following the aperture. When the diagonal mirror is in the light path, the light rays are deflected to a viewing eyepiece. The outline of

the particular aperture in use can be seen when the eyepiece is in use, as the aperture is illuminated by a small bulb. This facilitates centering the star in the aperture. When the diagonal mirror is withdrawn from the light path, the light path is unobstructed and a signal can be generated. When the mirror is withdrawn to take a photoelectric reading, the bulb is switched off by a micro-switch. The starlight then passes through a filter.

The filters are mounted on a wheel so that the observer can select one of the ultraviolet (Corning 9863), blue (Corning 5030 and Schott GG 13), and yellow (Corning 3389) filters, which correspond to the Johnson-Morgan UBV system (24). The Fabry lens serves to keep the same portion of the photocathode illuminated despite the effect of seeing. The filtered light rays impinge on the cathode of the EMI 6256B multiplier phototube at the end of the light path. A high voltage power supply was used to provide a potential difference of 1500 volts between the cathode and the anode of the photomultiplier. (Unfortunately, the photometer was not wired properly by Astromechanics and there was no potential applied to the cathode. Thus there was no potential difference between the cathode and the first dynode; the whole 1500 volts' potential difference was applied between the first dynode and the anode. This fault was not discovered until after the observations had been completed; however, the quality of the observations does

not seem to have been affected by the lack of potential on the cathode of the phototube.) The output of the photomultiplier tube is fed into a DC amplifier.

The DC amplifier is used to amplify the small current from the phototube to a level detectable by the recorder. The amplifier was of standard design with an electric circuit similar to the one described by Whitford (25). The size of the resistors is determined so as to change the amplification in coarse steps of 2.5 magnitudes, from 0 to 12.5 and in fine steps of 0.25 magnitudes from 0 to 2.50, where magnitude here refers to stellar magnitude. Different combinations of these resistors are used to produce the suitable signal on the recorder chart. The combination of resistors desired is selected with two rotary switches mounted on the amplifier. The time constant is controlled by a third rotary switch which gives a choice of four time constants.

The output of the DC amplifier is used to drive the pen of the dual-channel recorder built by Honeywell. Only one channel of the recorder was used; it has a pen which marks a continuous strip-chart to correspond with the signal current from the amplifier. The chart is set to run at a rate of one inch per minute. The observatory is equipped with a high frequency receiver for receiving WWV time signals; the time was recorded on the chart several times during the night. Readings of a barometer, a thermometer, and a hygrometer were also made several times a

night and recorded on the chart.

Observations

The light of the triple system was measured by centering the system in a diaphragm approximately thirty seconds of arc in diameter. Observations were obtained on five nights in the spring and summer of 1969 and 1970. Additional observations were made in the spring of 1971 for times of minimum light. The star HR 5581 was used as a comparison star throughout. Its constancy had been thoroughly checked by J. Stebbins and C. M. Huffer, and later by O. J. Eggen, by comparing it with star HR 5635 (26)(see Table XXX). Binnendijk (19) later reconfirmed the constancy of the comparison star; thus, only one check star reading was taken each night. The observations were taken in a regular sequence: comparison star, sky deflection, variable star, sky, variable, comparison, etc. Each object was observed through both blue and yellow filters,with individual readings lasting approximately thirty seconds. Ultraviolet observations were made on only one night. It was decided to observe only in blue and yellow light, since the short period of the system requires observations closely spaced in time. The star deflections were read from the chart to an accuracy of three places (e.g. 54.7) with the sky plus dark current deflections subtracted. The time for each observation

TABLE XXX

Comparison Stars

STAR	RA(1900)	DEC(1900)	m_v	Sp(27)
44i Bootis (HR 5618, HD 133640, BD +48°2259)	$15^h00^m.5$	+48°13'	4.86	GO
Comparison (HR 5581, HD 132254, BD +50°2126)	14 53.0	50 03	5.68	F5
Check (HR 5635, HD 134190, BD +55°1730)	15 03.4	55 56	5.21	G5

was read from the chart to the nearest 5 seconds. A series of programs for the IBM 360 computer was used to convert the raw data read from the charts into the final light curve. The difference in magnitude, Δm, between the variable star and the comparison star at the time of a variable star reading was determined from the following relation:

$$\Delta m = 2.5 \log \frac{\ell(\text{comp.})}{\ell(\text{var.})}$$

where ℓ(comp.) is the apparent light of the comparison star and ℓ(var.) that of the variable star; and this ratio is, of course, equal to the ratio of chart-readings of the two stars with sky readings subtracted. Linear interpolation was used wherever values between readings were needed. The magnitude differences together with the times of observation in heliocentric Julian days are given in Table XXXI. These magnitude differences were corrected for first-and second-order extinction and transformed to the Johnson-Morgan UBV standard system in the manner described below.

Reduction of Data

After observations have been made of the variable and comparison stars, it is necessary to remove the effects of the earth's atmosphere from these observations. It is also most useful to transform the data to a standard

TABLE XXXI

Observations of 44i Bootis

Yellow Observations

Hel JD 2440000+	PHASE	Δm
339.63161	0.93314	-0.780
.63491	0.94546	-0.779
.64741	0.99213	-0.757
.65048	0.00359	-0.770
.66084	0.04228	-0.817
.66396	0.05393	-0.841
.67444	0.09306	-0.878
.67704	0.10277	-0.881
.68630	0.13734	-0.870
.68879	0.14664	-0.875
.71530	0.24563	-0.862
.71825	0.25664	-0.907
346.61210	0.99751	-0.765
.61395	0.00442	-0.767
.62355	0.04026	-0.802
.62488	0.04523	-0.814
.63183	0.07118	-0.826
.63368	0.07809	-0.845
.64005	0.10187	-0.857
.64173	0.10814	-0.865
.64728	0.12887	-0.882
.64971	0.13794	-0.882
.65579	0.16064	-0.885
.65747	0.16691	-0.893
.66360	0.18980	-0.901
.66545	0.19671	-0.901
.67807	0.24383	-0.899
.67969	0.24988	-0.909
.69861	0.32053	-0.878
.70064	0.32811	-0.881
.70214	0.33371	-0.887
.70804	0.35574	-0.878
.70920	0.36007	-0.881
.71059	0.36526	-0.867

Table XXXI continued.

Hel JD 2440000+	PHASE	Δm
.71806	0.39315	-0.863
.71985	0.39983	-0.869
.75596	0.53467	-0.820
.75868	0.54482	-0.826
.77622	0.61031	-0.871
.77801	0.61700	-0.876
.77980	0.62368	-0.881
392.57818	0.62973	-0.888
.57997	0.63641	-0.895
.59051	0.67577	-0.935
.59219	0.68204	-0.940
.60029	0.71229	-0.960
.60220	0.71942	-0.970
.63269	0.83326	-0.929
.63455	0.84021	-0.928
.64676	0.88580	-0.903
.64872	0.89312	-0.895
.65781	0.92706	-0.834
.65943	0.93311	-0.838
.67019	0.97329	-0.826
.67210	0.98042	-0.832
715.59120	0.99047	-0.786
.59462	0.00324	-0.781
.60816	0.05380	-0.859
.61076	0.06351	-0.861
.62262	0.10779	-0.892
.62546	0.11840	-0.885
.63727	0.16249	-0.910
.63975	0.17175	-0.908
.65081	0.21305	-0.928
.65376	0.22407	-0.943
.66481	0.26533	-0.927
.66765	0.27593	-0.926
.67928	0.31935	-0.928
.68188	0.32906	-0.911
.69421	0.37510	-0.883
.69664	0.38417	-0.879
.70735	0.42416	-0.856
.71007	0.43432	-0.855
.72147	0.47689	-0.830
.72506	0.49029	-0.814
769.59105	0.35379	-0.944
.59325	0.36200	-0.924
.59829	0.38082	-0.878
.60066	0.38967	-0.871

Table XXXI continued.

Hel JD 2440000+	PHASE	Δm
.60610	0.40998	-0.842
.60847	0.41883	-0.859
.61304	0.43589	-0.835
.61507	0.44347	-0.828
.61906	0.45837	-0.801
.62259	0.47155	-0.826
.62786	0.49123	-0.811
.63035	0.50053	-0.796
.63533	0.51912	-0.815
.63712	0.52581	-0.821
.64175	0.54309	-0.827
.64372	0.55045	-0.828
.64864	0.56882	-0.864
.65089	0.57722	-0.879
.65500	0.59257	-0.883
.65703	0.60015	-0.890
.66142	0.61654	-0.892
.66304	0.62259	-0.916
.66652	0.63558	-0.890
.66860	0.64335	-0.907
.67184	0.65545	-0.930
.67392	0.66321	-0.917
.67769	0.67729	-0.937
.68006	0.68614	-0.931
.68463	0.70320	-0.942
.68642	0.70989	-0.967
.68932	0.72072	-0.931
.69117	0.72762	-0.924
.69539	0.74338	-0.894
.69725	0.75033	-0.908
.70147	0.76608	-0.907
.70326	0.77277	-0.916
.70651	0.78490	-0.913
.70813	0.79095	-0.926
.71154	0.80368	-0.928
.71362	0.81145	-0.907
.71681	0.82336	-0.906
.71872	0.83049	-0.921
.72317	0.84711	-0.917
.72462	0.85252	-0.913
.72867	0.86764	-0.919
.73046	0.87433	-0.914
.73428	0.88859	-0.870
.73590	0.89464	-0.844
.73984	0.90935	-0.860

Table XXXI continued.

Hel JD 2440000+	PHASE	Δm
.74134	0.91495	-0.865
.74632	0.93355	-0.839
.74782	0.93915	-0.780
.75280	0.95774	-0.815
.75448	0.96402	-0.824
.75969	0.98347	-0.800
.77175	0.02850	-0.805
.78324	0.07140	-0.857
1102.58471		-0.905
.58749		-0.899
.59392		-0.908
.59606		-0.915
.60022		-0.915
.60283		-0.898
.60833		-0.902
.61053		-0.892
.61463		-0.886
.61735		-0.880
.62135		-0.872
.62366		-0.866
.62713		-0.865
.62916		-0.855
.63333		-0.835
.63558		-0.829
.64015		-0.808
.64230		-0.787
.65636		-0.759
.65908		-0.761
.66568		-0.789
.66840		-0.794
.67331		-0.816
.67557		-0.825
.68043		-0.851
.68321		-0.863
.68715		-0.867
.68952		-0.868
.69380		-0.880
.69571		-0.885
.69988		-0.901
.70237		-0.875
	Blue Observations	
339.62768	0.91846	-0.683
.63590	0.94915	-0.649

Table XXXI continued.

Hel JD 2440000+	PHASE	Δm
.64672	0.98956	-0.647
.65158	0.00770	-0.651
.65951	0.03731	-0.661
.66466	0.05654	-0.688
.67346	0.08940	-0.744
.67797	0.10624	-0.734
.68549	0.13432	-0.734
.68977	0.15030	-0.744
.71449	0.24260	-0.748
.71906	0.25966	-0.786
346.61123	0.99426	-0.638
.61499	0.00830	-0.643
.62292	0.03791	-0.671
.62558	0.04784	-0.690
.63102	0.06815	-0.698
.63443	0.08089	-0.720
.63947	0.09970	-0.727
.64236	0.11050	-0.739
.64664	0.12648	-0.750
.64902	0.13536	-0.751
.65509	0.15803	-0.746
.65816	0.16949	-0.755
.66285	0.18700	-0.775
.66615	0.19932	-0.773
.67732	0.24103	-0.762
.68044	0.25268	-0.770
.71742	0.39076	-0.723
.72072	0.40308	-0.720
.75521	0.53186	-0.688
.75799	0.54225	-0.696
392.57749	0.62715	-0.751
.58055	0.63858	-0.768
.58987	0.67338	-0.800
.59276	0.68417	-0.813
.59959	0.70967	-0.829
.60283	0.72177	-0.829
.63206	0.83091	-0.805
.63530	0.84301	-0.799
.64606	0.88319	-0.768
.64942	0.89573	-0.758
.65717	0.92467	-0.726
.66007	0.93550	-0.699
.66962	0.97116	-0.696
.67280	0.98303	-0.700

Table XXXI continued.

Hel JD 2440000+	PHASE	Δm
715.59016	0.98659	-0.674
.59566	0.00713	-0.676
.60723	0.05033	-0.731
.61163	0.06676	-0.753
.62181	0.10477	-0.768
.62650	0.12228	-0.762
.63634	0.15902	-0.774
.64051	0.17459	-0.774
.65011	0.21044	-0.777
.65474	0.22772	-0.787
.66400	0.26230	-0.777
.66846	0.27895	-0.763
.67847	0.31633	-0.774
.68275	0.33231	-0.767
.69334	0.37185	-0.755
.69651	0.38742	-0.728
.70659	0.42133	-0.718
.71105	0.43798	-0.710
.72072	0.47409	-0.694
.72592	0.49350	-0.678
769.59152	0.35554	-0.793
.59291	0.36073	-0.777
.59875	0.38254	-0.720
.60020	0.38795	-0.718
.60656	0.41170	-0.705
.60795	0.41689	-0.705
.61357	0.43787	-0.689
.61467	0.44198	-0.680
.61953	0.46013	-0.660
.62080	0.46487	-0.643
.62850	0.49362	-0.658
.62983	0.49859	-0.663
.63573	0.52062	-0.698
.63677	0.52450	-0.701
.64215	0.54459	-0.710
.64331	0.54892	-0.703
.64921	0.57095	-0.732
.65060	0.57614	-0.736
.65541	0.59410	-0.757
.65645	0.59798	-0.751
.66177	0.61785	-0.760
.66258	0.62087	-0.776
.66686	0.63685	-0.772

Table XXXI continued.

Hel JD 2440000+	PHASE	Δm
.66820	0.64186	-0.777
.67236	0.65739	-0.802
.67352	0.66172	-0.772
.67821	0.67923	-0.779
.67954	0.68420	-0.797
.68504	0.70473	-0.813
.68614	0.70884	-0.819
.68967	0.72202	-0.799
.69071	0.72591	-0.797
.69580	0.74491	-0.777
.69638	0.74708	-0.770
.70182	0.76739	-0.794
.70292	0.77150	-0.781
.70685	0.78617	-0.796
.70778	0.78964	-0.789
.71200	0.80540	-0.788
.71322	0.80996	-0.790
.71721	0.82485	-0.770
.71831	0.82898	-0.762
.72352	0.84841	-0.791
.72502	0.85402	-0.763
.72902	0.86895	-0.775
.73006	0.87283	-0.776
.73480	0.89053	-0.723
.73561	0.89356	-0.694
.74013	0.91043	-0.725
.74105	0.91387	-0.715
.74673	0.93508	-0.689
.74754	0.93810	-0.651
.75321	0.95927	-0.717
.75408	0.96252	-0.694
.76004	0.98478	-0.689
.77263	0.03179	-0.692
.78284	0.06991	-0.721
1102.58535		-0.763
.58686		-0.751
.59444		-0.776
.59559		-0.772
.60080		-0.776
.60231		-0.770
.60873		-0.764
.61006		-0.758

Table XXXI continued.

Hel JD 2440000+	PHASE	Δm
.61515		-0.739
.61660		-0.745
.62187		-0.732
.62314		-0.733
.62766		-0.723
.62870		-0.725
.63385		-0.695
.63506		-0.702
.64073		-0.668
.64183		-0.654
.65694		-0.611
.65850		-0.616
.66625		-0.654
.66770		-0.665
.67384		-0.681
.67505		-0.691
.68101		-0.714
.68263		-0.716
.68761		-0.718
.68900		-0.727
.69432		-0.737
.69519		-0.735
.70051		-0.749
.70184		-0.739
	Ultraviolet Observations	
715.58808	0.97882	-0.600
.59658	0.01056	-0.610
.60619	0.04644	-0.677
.61250	0.07001	-0.710
.62089	0.10133	-0.718
.62749	0.12598	-0.684
.63547	0.15577	-0.696
.64137	0.17780	-0.690
.64936	0.20764	-0.703
.65590	0.23206	-0.729
.66325	0.25950	-0.733
.66944	0.28261	-0.716
.67760	0.31308	-0.715
.68362	0.33556	-0.713

Table XXXI continued.

Hel JD 2440000+	PHASE	Δm
.69247	0.36860	-0.828
.69832	0.39045	-0.689
.70567	0.41789	-0.648
.71203	0.44164	-0.644
.71996	0.47125	-0.642
.72702	0.49761	-0.634

observational system. This transformation makes the results independent of the choice of telescope-photometer system, thereby making direct comparison of data taken with different instrumental systems feasible. The methods used for these reductions will closely correspond to those described by Hardie (28).

Passage through the earth's atmosphere has two effects on the light from a star. First, it is diminished and second, it is reddened. The magnitude of these effects is dependent on the amount of atmosphere the light passes through. These extinction effects can be expressed as

$$m_o = m - k'X - k''CX \qquad (1)$$

where m_o is the magnitude of the star outside the atmosphere, m is the magnitude observed after the light has passed through a path length X of the atmosphere, with X expressed in units of air mass at the zenith of the observer, C is the color index of the star, and k' and k" we shall call the first and second order extinction coefficients.

The relative air mass, X, in units of the air mass at the zenith is a function of the secant of the zenith distance, z. The value of sec z may be determined through the relation

$$\sec z = (\sin\phi \sin\delta + \cos\rho \cos\phi \cosh)^{-1} \qquad (2)$$

in which ϕ is the observer's latitude, while δ and h are the declination and hour angle of the star. After sec z is found as above, then X may be determined by the formula (28)

$$X = \sec z - 0.0018167\ (\sec z - 1) - 0.002875\ (\sec z - 1)^2 - 0.0008083\ (\sec z - 1)^3 \qquad (3)$$

To determine the first-order (or principal) extinction one may measure a non-variable star over a wide range of air mass. Then the extinction coefficient may be derived from a plot of the measured magnitude of the star, m, versus the air mass X. In differential photometry of variable stars, the comparison star may serve as the constant star used to determine the first-order extinction coefficients, provided that the observations cover a sufficiently large range of air mass. Only on one of the five nights of observation discussed above (July 1, 1970) were the observations taken through a sufficiently large range of air mass for extinction to be determined accurately. The values so determined (by a least squares fit of the data) were $k'_y = 1.15$ and $k'_b = 1.53$. Plots of the comparison star magnitude versus air mass for that night are shown in Figure 13. For the other four nights, it was necessary to adopt the following mean extinction coefficients: $k'_v = 0.4$, $k'_b = 0.6$, $k'_u = 1.0$.

The second-order extinction coefficients are a

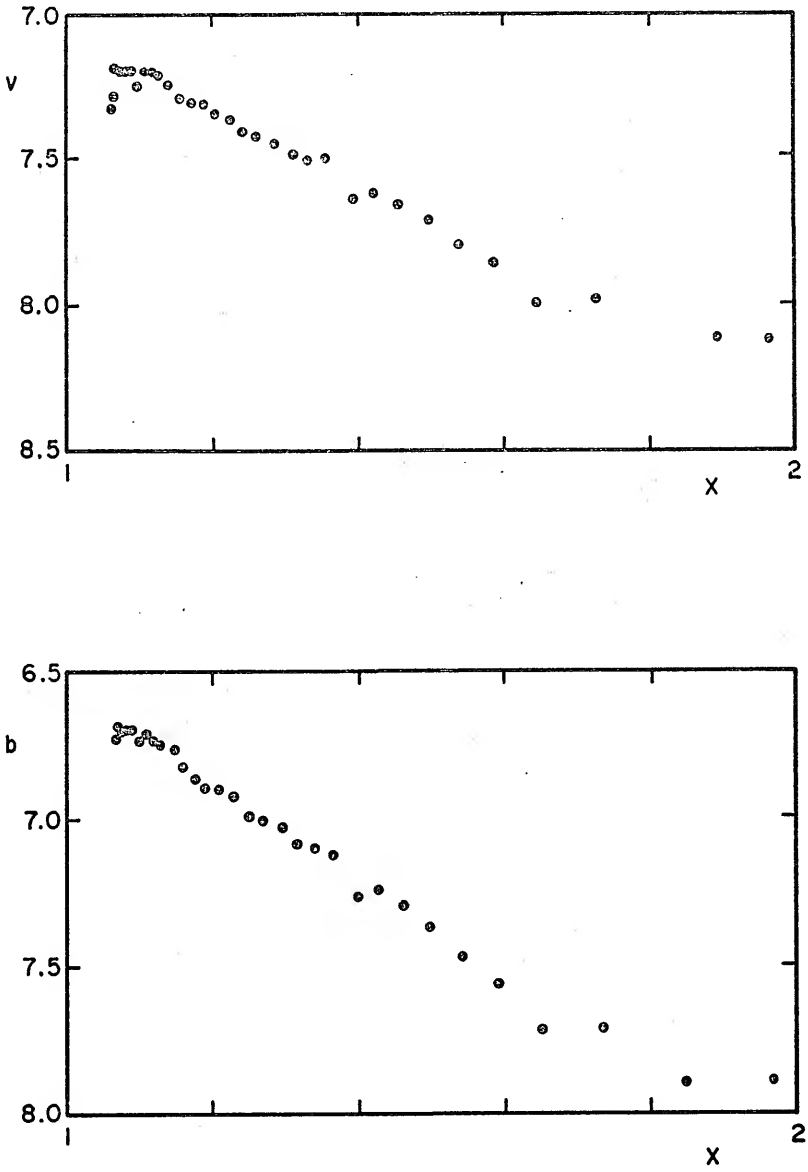

Figure 13. Comparison Star Extinction for July 1, 1970.

measure of the wavelength dependence of the extinction. They may be determined by observing a pair of stars of widely differing color index over a large range of air mass. Then if the two stars have essentially the same position, the differential measures of their magnitude and color will follow these relations:

$$\Delta m_o = \Delta m - k'' \Delta CX \quad (4)$$

$$\Delta C_o = \Delta C - k''_c \Delta CX \quad (5)$$

Therefore, plots of Δm versus (ΔCX) and of ΔC versus (ΔCX) will give lines whose slopes are k'' and k''_c. These second-order extinction coefficients are substantially constant over short periods of time (e.g. one observing season). The two stars of the visual binary Albireo (Beta Cygni AB) were used to determine the second-order coefficients. This system was chosen since both stars are relatively bright, one star is blue and the other is red, and both stars are Johnson-Morgan standard stars (see Table XXXII). The two stars were observed on two nights (July 19, 1970 and August 16, 1970) through a total range of about four air masses. When the data was reduced and plotted (Figure 14), it showed the presence of a non-negligible second-order extinction in the V (visible or yellow) wavelength band. This extinction is not expected; however, it might be attributed to the high water vapor

TABLE XXXII

Standard Stars

STAR	Sp	RA(1970)	Dec(1970)	V	B-V	U-B
o Tau	G8III	$3^h23^m11^s.7$	8°55'.5	3.59	0.89	0.62
ε Tau	KOIII	4 26 51.7	19 06.9	3.54	1.02	0.88
π^3Ori	F6V	4 48 12.6	6 54.6	3.19	0.45	-0.01
ζ Oph	09.5V	16 35 30.2	-10 30.5	2.56	0.02	-0.86
α Oph	A5III	17 33 32.4	12 34.8	2.08	0.15	0.10
β Oph	K2III	17 41 59.3	4 34.7	2.77	1.16	1.24
γ Lyr	B9III	18 57 49.2	32 38.8	3.25	-0.05	-0.09
β Cyg A	(KO)	19 29 31.8	27 53.8	3.07	1.12	0.62
β Cyg B	B8V	19 29 31.8	27 53.8	5.11	-0.10	-0.32
κ Aql	BO.5III	19 35 16.1	- 7 05.3	4.96	-0.01	-0.87
β Aql	C8IV	19 53 50.3	6 19.8	3.71	0.86	0.48
α Del	B9V	20 38 14.6	15 48.3	3.77	-0.06	-0.22
ε Aqr	AlV	20 46 03.1	- 9 36.4	3.77	0.01	0.04
μ Cep	M2IA	21 42 35.2	58 38.5	3.99	2.41	2.40
74Aqr	(B9)	22 51 51.8	-11 46.4	5.81	-0.08	-0.32
α Peg	B9V	23 03 15.8	15 02.6	2.49	-0.05	-0.06
ι Psc	F7V	23 38 24.3	5 27.8	4.13	0.51	0.00

Figure 14. Second-order Extinction for Albireo: Solid circles--July 19, 1970; open circles--August 6, 1970.

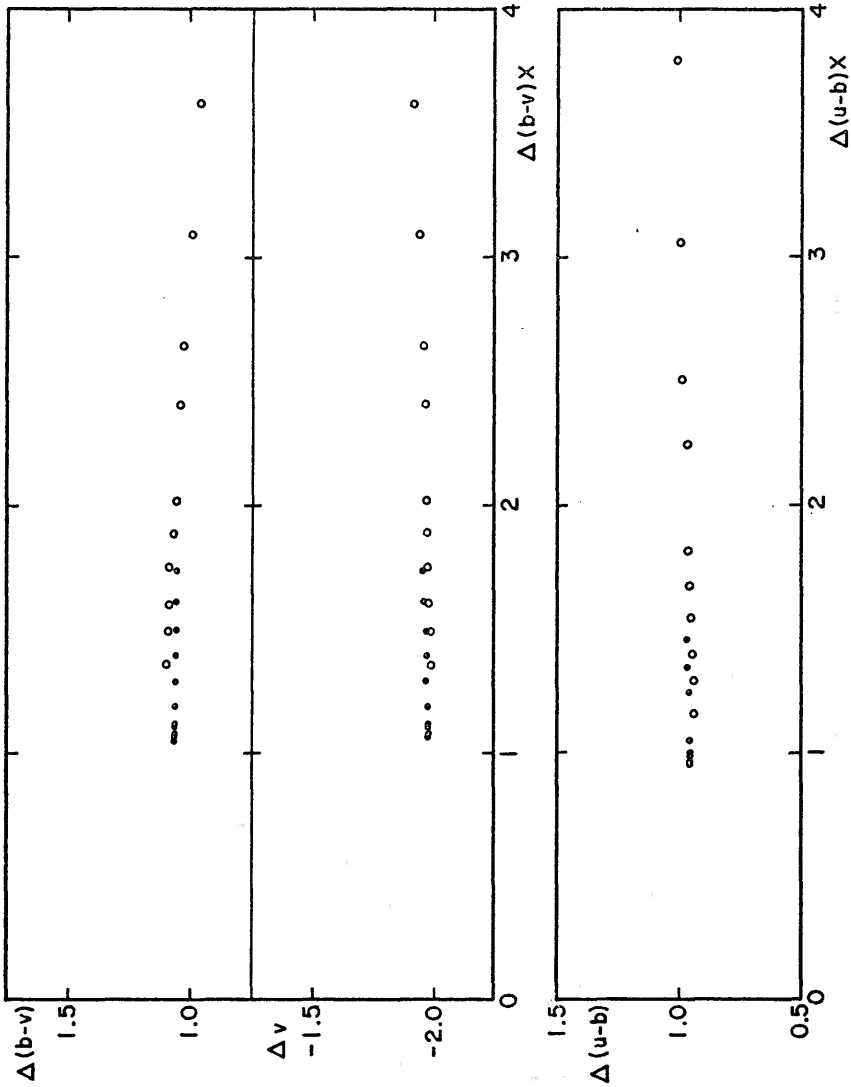
Δ(b-v)
1.5
1.0
Δ v
-1.5
-2.0
0
1
2
3
4
Δ(b-v)X
Δ(u-b)
1.5
1.0
0.5
0
1
2
3
4
Δ(u-b)X

content of the atmosphere at the time the observations were taken (relative humidity usually greater than 95%). Since this effect appeared to be an atmospheric effect, the $k"_v$ term was retained and the working equations used were modified to include it. The second-order extinction coefficients derived from the data by a least squares fit were $k"_v = 0.028$, $k"_{bv} = -0.034$, and $k"_{ub} = 0.022$. Principal extinction coefficients were also derived from the observations of Albireo in order to better determine mean values for these coefficients. This data is plotted in Figures 15-17.

Once the extinction coefficients have been determined, they may be applied to the observed magnitudes in the three UBV color bands (u, b, v) to obtain the extra-atmosphere values of the stellar magnitudes denoted by the zero subscripts:

$$v_o = v - k'_v X - k"_v (b - v) X \qquad (6a)$$

$$b_o = b - k'_b X - k"_b (b - v) X \qquad (6b)$$

$$u_o = u - k'_u X - k"_u (u - b) X \qquad (6c)$$

where $k"_b = k"_{bv} + k"_v$ and $k"_u = k"_{ub} + k"_b$.

In order to be able to compare observations taken with different equipment, it is necessary to transform these quantities to a standard system (i.e. the Johnson-Morgan UBV system). This transformation can be represented

Figure 15. First-order Yellow Extinction for Albireo: Triangles--Beta Cygni A, July 19, 1970; open circles--Beta Cygni A, August 16, 1970; X's--Beta Cygni B, July 19, 1970; solid circles--Beta Cygni B, August 16, 1970.

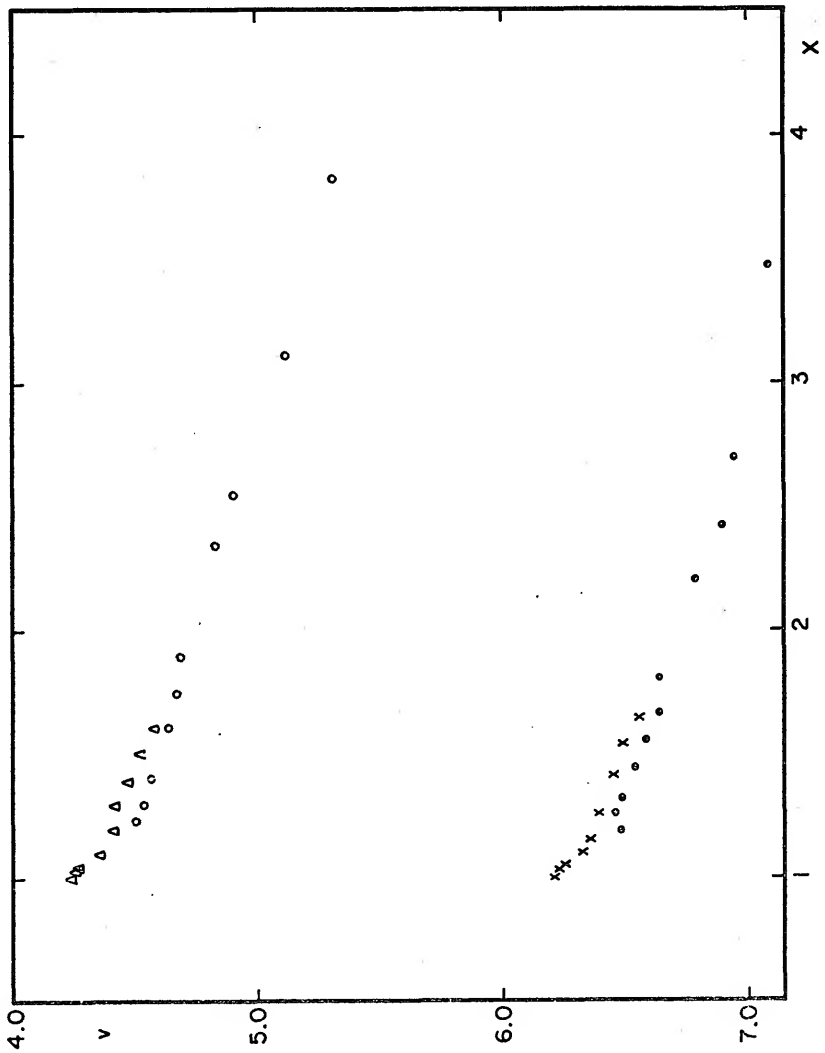
4.0
5.0
6.0
7.0
V
1
2
3
4
X

Figure 16. First-order Blue Extinction for Albireo: Triangles--Beta Cygni A, July 19, 1970; open circles--Beta Cygni A, August 16, 1970; X's--Beta Cygni B, July 19, 1970; solid circles--Beta Cygni B, August 16, 1970.

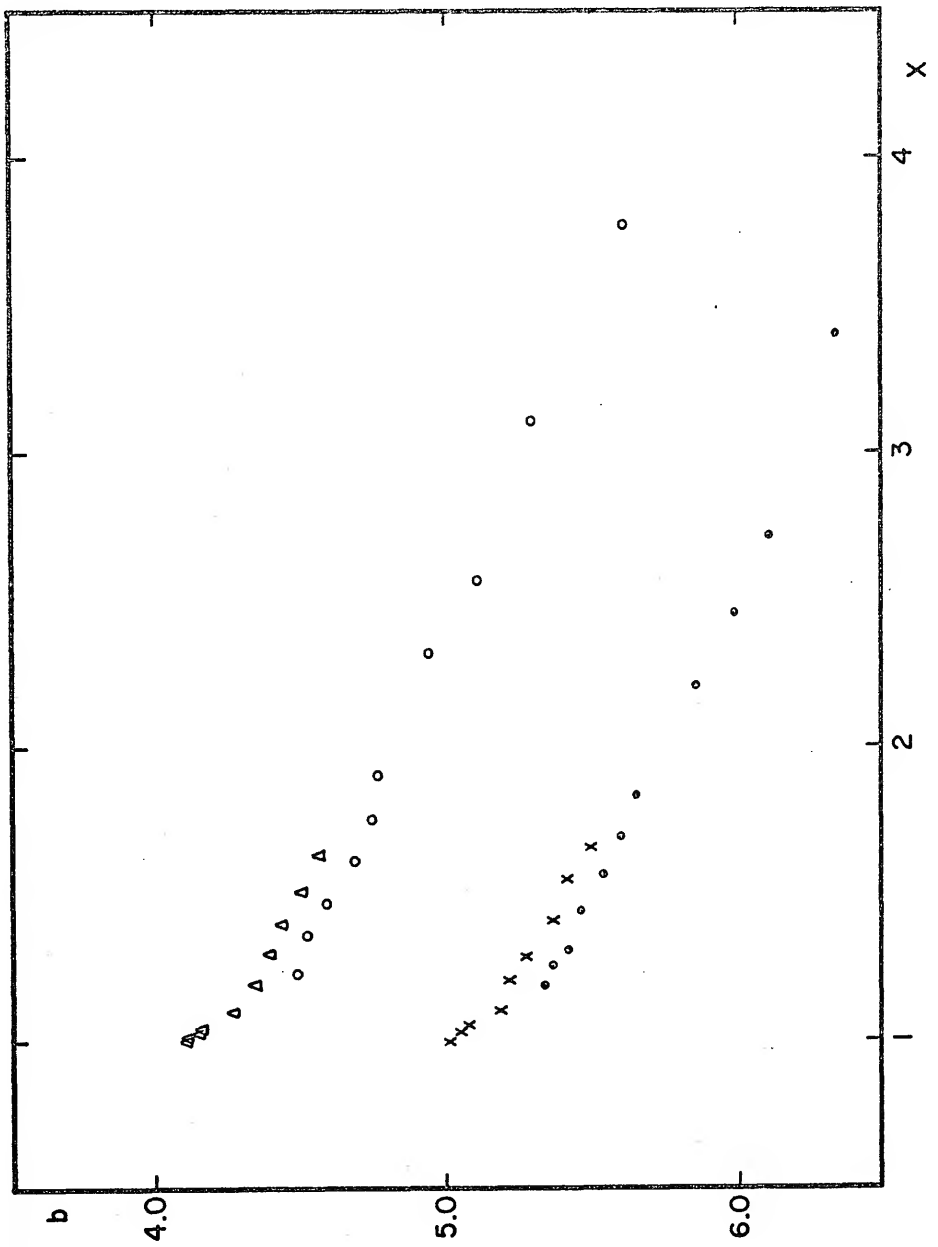
b
4.0
5.0
6.0
1
2
3
4
X

Figure 17. First-order Ultra-Violet Extinction for Albireo: Triangles--Beta Cygni A, July 19, 1970; open circles-- Beta Cygni A, August 16, 1970; X's--Beta Cygni B, July 19, 1970; solid circles--Beta Cygni B, August 16, 1970.

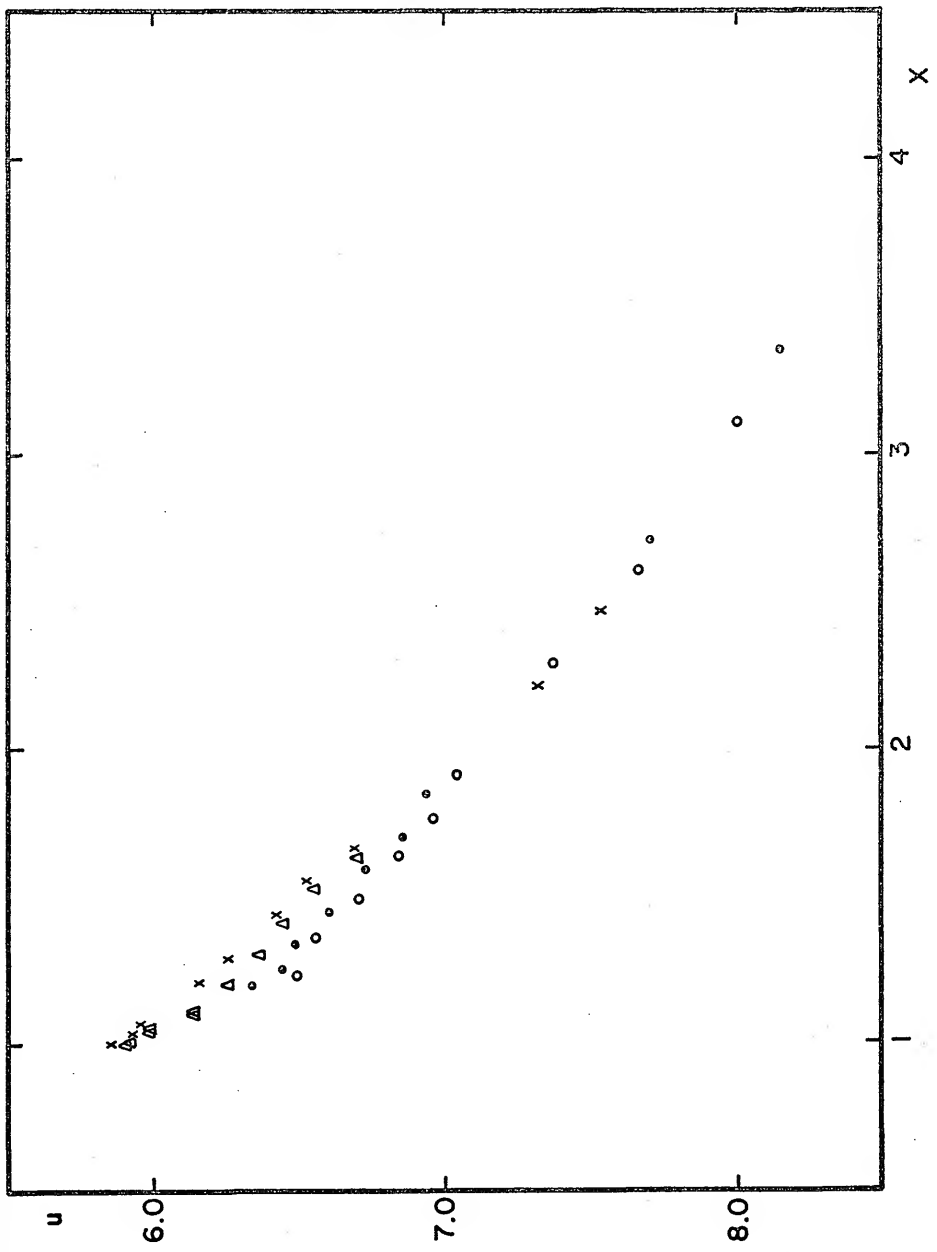
u
6.0
7.0
8.0
1
2
3
4
X

by the following equations:

$$V = v_o + \varepsilon(B - V) + \zeta_v \tag{7a}$$

$$B - V = \mu(b - v)_o + \zeta_{bv} \tag{7b}$$

$$U - B = \psi(u - b)_o + \zeta_{ub} \tag{7c}$$

where U, B, and V are the magnitudes on the standard system; ε, μ, and ψ are the transformation coefficients; and the ζ's represent zero-point differences between the natural system and the standard system.

One way to determine these transformation coefficients is to observe a number of stars with known standard magnitudes and color indices. These stars should be chosen to cover as wide a range of color indices as possible. The plots of $V - v_o$ versus $B - V$, $B - V$ versus $(b - v)_o$, and $U - B$ versus $(u - b)_o$ for each star will have slopes of ε, μ, and ψ respectively. Seventeen stars chosen from the list of Johnson (29) were observed and used to determine the transformation coefficients. These stars with their standard magnitudes and colors are listed in Table XXXII. The observations were corrected for extinction and plots were made of $V - v_o$ versus $B - V$, $(B - V) - (b - v)_o$ versus $B - V$, and $(U - B) - (u - b)_o$ versus $U - B$ (see Figure 18). Then ε, μ, and ψ were determined by a least squares method. The zero-point coefficients were not determined. The values of the transformation coefficients were $\varepsilon = -0.134$, $\mu = 1.072$ and $\psi = 1.020$.

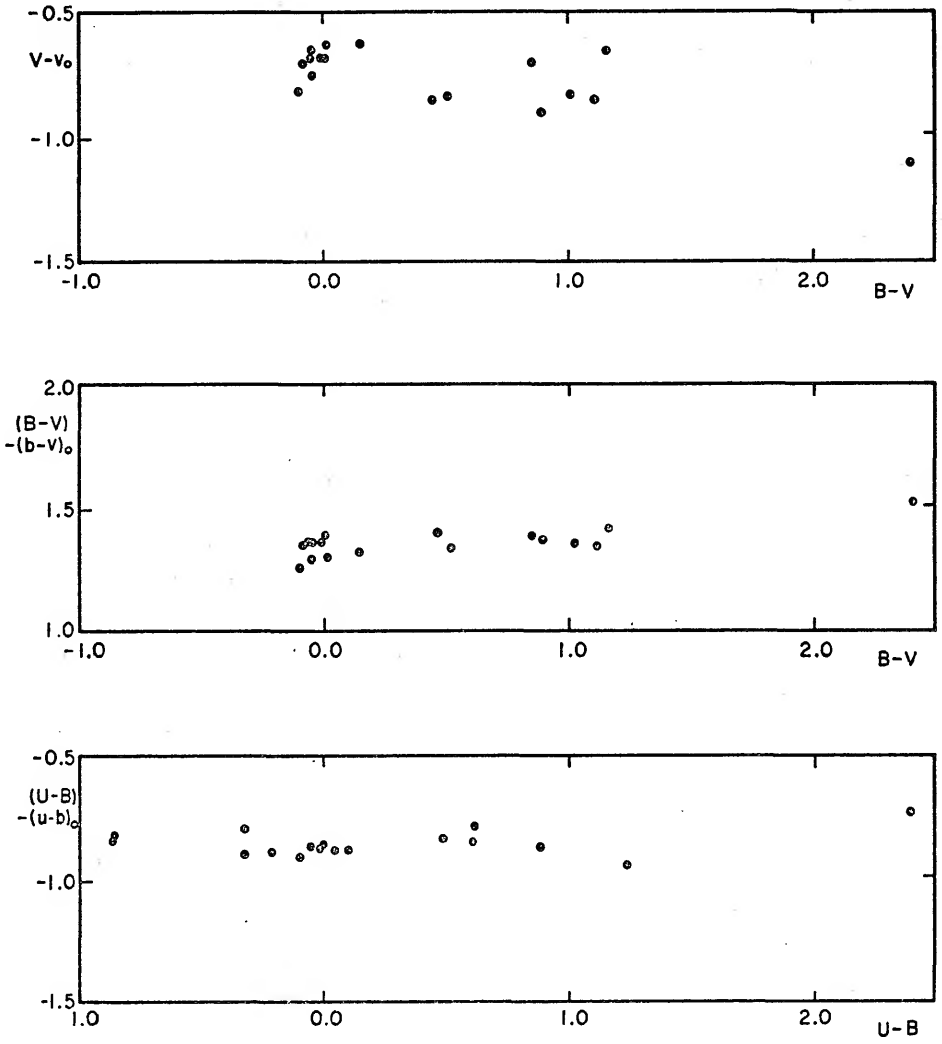

Figure 18. UBV Transformation Coefficients.

Once the extinction and transformation coefficients have been determined, it is useful to have a set of working equations which combine all the reductions. In the study of variable stars, it is customary to select a comparison star close to the variable in the sky and similar in color and magnitude. By doing this the differential measures are less dependent on extinction, thereby the extinction corrections are usually small. Considering equations (6) as applied to both variable and comparison star and expressing them in differential magnitudes and color indices:

$$\Delta v_o = \Delta v - k'_v \Delta X - k''_v \Delta(b - v)\overline{X} \qquad (8a)$$

$$\Delta b_o = \Delta b - k'_b \Delta X - k''_b \Delta(b - v)\overline{X} \qquad (8b)$$

$$\Delta u_o = \Delta u - k'_u \Delta X - k''_u \Delta(u - b)\overline{X} \qquad (8c)$$

where $\overline{X}$ is the mean air mass and third-order terms are ignored. Considering equations (7) as applied to both stars, and rewriting them in terms of standard magnitudes:

$$\Delta V = \Delta v_o + \varepsilon\mu\Delta(b - v)_o \qquad (9a)$$

$$\Delta B = \Delta v_o + (\mu + \varepsilon\mu)\,\Delta(b - v)_o \qquad (9b)$$

$$\Delta U = \Delta v_o + (\mu + \varepsilon\mu)\,\Delta(b - v)_o + \psi\Delta(u - b)_o \qquad (9c)$$

Equations (8) and (9) may be combined to give the final

working equations used in the reductions:

$$\Delta V = \Delta v + (\varepsilon\mu(1 - k''_v\bar{X}) - k''_v\bar{X})\Delta(b - v) - k'_v\Delta X \qquad (10a)$$

$$\Delta B = \Delta v + (\mu + \varepsilon\mu(1 - k''_{bv}\bar{X}) - k''_v\bar{X})\Delta(b - v) - k'_b\Delta X \qquad (10b)$$

$$\Delta U = \Delta v + (\mu + \varepsilon\mu(1 - k''_{bv}\bar{X}) - k''_v\bar{X})\Delta(b - v) + \psi(1 - k''_{ub}\bar{X})\Delta(u - b) - k'_u\Delta X \qquad (10c)$$

The time is the most accurately observed quantity. The time in hours, minutes, and seconds was converted into decimals of a day with the day itself denoted by its Julian Day number. These times in geocentric Julian day must be converted into heliocentric Julian days because of the varying position of the earth in its orbit around the sun. The light from a star may reach the earth as much as eight minutes earlier and eight minutes later than it reaches the sun, due to the finite velocity of light. This correction must be made in order not to introduce a period change in the observed variable star. This correction is:

$$t = -0^d.005775((\cos\delta\ \cos\alpha)X + (\tan\varepsilon\ \sin\delta + \cos\delta\ \sin\alpha)Y)$$

where α and δ are the right ascension and declination of the star, ε is the obliquity of the ecliptic, X and Y are the rectangular coordinates of the sun for the given date, and $0^d.005775$ is the time in which light travels one astronomical unit (see Binnendijk (30) for derivation).

Times of Minimum Light and the Period

The times of minimum light were obtained from the curves of magnitude difference as a function of time by the tracing paper method (31) for the five nights of observation. An additional time of minimum light was obtained from the observations made on May 30, 1971 by the method of Kwee and Van Woerden (32). The times of minimum light are averages of the values obtained with the blue and yellow filters. They are listed in Table XXXIII along with other recent times of minimum light. Tabulations of earlier times of minimum light are given by Purgathofer and Prochazka (33) and by Schneller (34).

Variation in the period caused by motion in a visual binary system

Since 44i Bootis B is one component of a visual binary system, the observed times of minimum light will vary sinusoidally about the true time of minimum light measured with respect to the center of gravity of the binary system. That is, the observed time of minimum light will differ from the true time with respect to the center of gravity of the system by an amount equal to the stellar light time corresponding to the distance of the variable from the center of gravity projected on the line of sight. Figure 19 shows the effect of this correction on the selected times of minimum light listed in Table XXXIV. The correc-

TABLE XXXIII

Recent Times of Minimum Light

Hel JD 2400000+	E[a]	O-C[a]	E[b]	O-C[b]	REFERENCES
37362.4855	-4297.5	+0.0009			34
7362.6171	-4297	-0.0015			34
7364.493	-4290	-0.0003			34
7365.5641	-4286	-0.0004			34
7439.6151	-4009.5	-0.0001			35
7443.6322	-3994.5	-0.0002			35
7443.7660	-3994	-0.0003			35
7449.6577	-3972	-0.0005			35
7449.7917	-3971.5	-0.0004			35
7472.6889	-3886	-0.0013			35
7472.8228	-3885.5	-0.0013			35
7740.5042	-2886	-0.0003			34
7743.4498	-2875	-0.0007			34
7779.4695	-2740.5	-0.0020			34
7780.4080	-2737	-0.0009			34
7826.4719	-2565	-0.0010			34
7835.4445	-2531.5	-0.0002			34
7852.4510	-2468	-0.0001			36
7853.3867	-2464.5	-0.0016			36
7853.5203	-2464	-0.0019			36
7855.3959	-2457	-0.0010			34
7860.4856	-2438	+0.0003			36
7862.4927	-2430.5	-0.0012			36
7867.4522	-2412	+0.0037			36
8241.439	-1015.5	-0.0122			37
8540.4649	101	-0.0009			38
8902.4155	1452.5	-0.0014			34
8910.4510	1482.5	-0.0003			34
8915.4011	1501	-0.0048			34
8941.3798	1598	-0.0040			33
9210.3994	2602.5	-0.0039			39
9224.4624	2655	-0.0012			39
9242.4050	2722	-0.0021			40
9243.3465	2725.5	+0.0021			40
9245.3520	2733	-0.0011			40

Table XXXIII continued.

Hel JD 2400000+	E^a	$O-C^a$	E^b	$O-C^b$	REFERENCES
9245.4865	2733.5	-0.0005			40
9247.3600	2740.5	-0.0017			40
9247.360	2740.5	-0.0017			41
9248.428	2744.5	-0.0049			41
9248.4310	2744.5	-0.0019			40
9252.4480	2759.5	-0.0022			39
9260.484	2789.5	-0.0006			41
9261.421	2793	-0.0009			41
9290.3455	2901	-0.0004			39
9380.328	3237	-0.0035			41
9391.305	3278	-0.0069			41
9633.423	4182	+0.0070			41
9665.421[c]	4301.5	+0.0012	-2516.5	+0.0015	41
9671.445[c]	4324	-0.0006	-2494	-0.0004	41
9673.454[c]	4331.5	-0.0002	-2486.5	-0.0000	41
9760.358[c]	4656	-0.0020	-2162	-0.0027	41
9922.9250[c]	5263	+0.0017	-1555	-0.0008	42
9935.9136[c]	5311.5	+0.0013	-1506.5	-0.0013	42
9940.8686	5330	+0.0018	-1488	-0.0009	43
9945.4222[c]	5347	+0.0025	-1471	-0.0002	44
9948.363	5358	-0.0026	-1460	-0.0054	45
9952.9210[c]	5375	+0.0025	-1443	-0.0003	42
9956.400	5388	0.0000	-1430	-0.0029	45
9959.349	5399	+0.0030	-1419	+0.0001	45
9959.481	5399.5	+0.0010	-1418.5	-0.0018	45
9968.453	5433	+0.0013	-1385	-0.0017	45
9977.292	5466	+0.0024	-1352	-0.0007	45
9998.7166	5546	+0.0019	-1272	-0.0015	43
40312.4589	6717.5	-0.0003	- 100.5	-0.0071	46
312.5972	6718	+0.0041	- 100	-0.0028	46
313.4043	6721	+0.0078	- 97	+0.0009	46
316.346	6732	+0.0035	- 86	-0.0034	45
319.296	6743	+0.0076	- 75	+0.0006	45
325.4556[c]	6766	+0.0074	- 52	+0.0004	47
331.346	6788	+0.0059	- 30	-0.0012	45
333.3541[c]	6795.5	+0.0054	- 22.5	-0.0017	47
339.3816[c]	6818	+0.0071	0	-0.0001	47
339.6493[c]	6819	+0.0070	1	-0.0002	d
346.6161[c]	6845	+0.0106	27	+0.0033	d
346.7482[c]	6845.5	+0.0088	27.5	+0.0015	d
363.484	6908	+0.0062	90	-0.0013	45
382.7676	6980	+0.0072	162	-0.0005	48
390.8020	7010	+0.0072	192	-0.0006	48
392.5449[c]	7016.5	+0.0093	198.5	+0.0015	d

Table XXXIII continued.

Hel JD 2400000+	E^a	O-C^a	E^b	O-C^b	REFERENCES
392.6820[c]	7017	+0.0125	199	+0.0047	d
420.7971	7122	+0.0071	304	-0.0011	48
661.4273	8020.5	+0.0061	1202.5	-0.0047	49
675.4875	8073	+0.0071	1255	-0.0049	46
675.6200	8073.5	+0.0046	1255.5	-0.0063	46
678.5661	8084.5	+0.0048	1266.5	-0.0062	46
679.3684	8087.5	+0.0036	1269.5	-0.0074	46
679.5037	8088	+0.0050	1270	-0.0060	46
681.3774	8095	+0.0040	1777	-0.0070	46
681.5119	8095.5	+0.0046	1277.5	-0.0064	46
682.4502	8099	+0.0056	1281	-0.0055	46
686.4668	8114	+0.0050	1296	-0.0061	46
697.7184	8156	+0.0084	1338	-0.0029	43
697.8526	8156.5	+0.0087	1338.5	-0.0026	43
698.7890	8160	+0.0077	1342	-0.0035	43
698.9213	8160.5	+0.0061	1342.5	-0.0051	43
699.7284	8163.5	+0.0098	1345.5	-0.0015	43
699.8617	8164	+0.0092	1346	-0.0021	43
700.3943	8166	+0.0061	1348	-0.0051	50
700.6648	8167	+0.0089	1349	-0.0025	43
700.8009	8167.5	+0.0110	1349.5	-0.0003	43
700.9324	8168	+0.0086	1350	-0.0027	43
701.7347	8171	+0.0075	1353	-0.0038	43
701.8709	8171.5	+0.0097	1353.5	-0.0015	43
714.5891[c]	8219	+0.0068	1401	-0.0046	d
714.7299[c]	8219.5	+0.0137	1401.5	+0.0023	d
753.4231	8364	+0.0077	1546	-0.0043	49
769.6286[c]	8424.5	+0.0104	1606.5	-0.0016	d
769.7628[c]	8425	+0.0107	1607	-0.0013	d
780.471	8465	+0.0064	1647	-0.0058	49
1055.3820	9491.5	+0.0060	2673.5	-0.0093	46
1055.5165	9492	+0.0066	2674	-0.0087	46
1102.6556	9668	+0.0103	2850	-0.0054	d
1138.406	9801.5	+0.0075	2983.5	-0.0086	51
1139.345	9805	+0.0092	2987	-0.0070	51
1141.4886	9813	+0.0103	2995	-0.0059	51

a Computed from min = JD 2438513.4166 + $0^d.2678143E$
b Computed from min = JD 2440339.3817 + $0^d.26781731E$
c Used to compute new light elements
d Present work

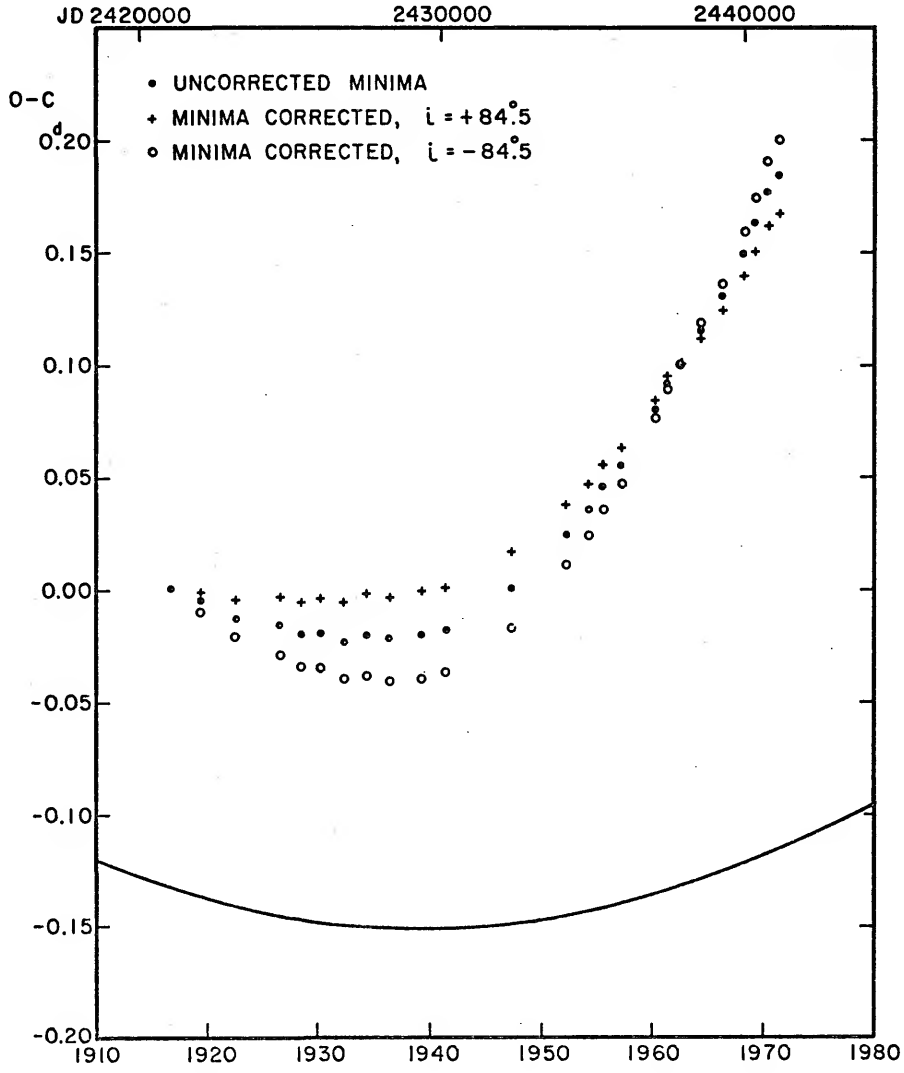

Figure 19. Variation in the Period of 44i Bootis B Caused by Motion in a Visual Binary System.

TABLE XXXIV

Times of Minimum Light with Corrections for Motion in a Visual Binary Orbit

Hel JD 240000+	E[a]	YEAR	LIGHT TIME CORRECTION	O-C[a]	O-C[b]	O-C[c]	REFERENCES
21113.2588	0	1916.7	0	0	0	0	34
2090.4863	3649	1919.4	.0045	-.0051	-.0006	-.0096	34
3215.4075	7849.5	1922.5	.0082	-.0127	-.0045	-.0209	34
4616.4322	13305	1926.5	.0126	-.0163	-.0037	-.0289	34
5398.4398	16001	1928.4	.0143	-.0199	-.0056	-.0342	52
6058.8554	18467	1930.2	.0157	-.0196	-.0039	-.0353	34
6864.4194	21475	1932.4	.0171	-.0231	-.0060	-.0402	34
7568.4902	24104	1934.4	.0181	-.0203	-.0022	-.0384	53
8314.6026	26890	1936.4	.0188	-.0219	-.0031	-.0407	34
9337.6320	30710	1939.3	.0192	-.0203	-.0011	-.0395	34
30152.5752	33753	1941.5	.0190	-.0178	+.0012	-.0368	22
2339.7838	41920	1947.4	.0170	+.0003	+.0173	-.0167	26
4132.5171	48614	1952.3	.0133	.0246	.0379	+.0113	34
4845.7017	51277	1954.3	.0113	.0357	.0470	.0243	19
5341.4252	53128	1955.6	.0100	.0460	.0560	.0360	54
5932.4875	55335	1957.3	.0079	.0553	.0632	.0474	54
7026.5094	59420	1960.3	.0037	.0802	.0839	.0765	34
7449.6577	61000	1961.4	.0022	.0914	.0936	.0892	35
7855.3959	62515	1962.5	.0004	.1000	.1004	.0996	34
8540.4646	65073	1964.4	-.0029	.1150	.1121	.1179	34
9224.4624	67627	1966.3	-.0062	.1303	.1241	.1365	39
9922.9250	70235	1968.3	-.0099	.1488	.1389	.1587	42
40339.6493	71791	1969.3	-.0120	.1634	.1514	.1754	d
769.7628	73397	1970.5	-.0144	.1767	.1623	.1911	d
1102.6556	74640	1971.4	-.0163	.1838	.1675	.2001	d

a Computed from min = JD 2421113.2588 + 0^d.26780832E

b Corrected, i positive

c Corrected, i negative

d Present work

tions correspond to the visual orbital elements given above with the reasonable mass ratio $M_A/(M_A + M_{B1} + M_{B2}) = 0.4$ with both positive and negative inclinations of the visual binary system being plotted. The computed times of minimum light are derived from an early set of light elements given by Eggen (26):

$$\text{Min} = \text{JD}2421113.2588 + 0^{d}.26780832\ E$$

The plot shows several things. First of all, the sinusoidal variation of the period is overshadowed by a number of apparently sudden period changes; the first one occuring approximately in 1940. These intrinsic period changes make it difficult to be certain of the proper choice for the sign of the inclination of the visual binary orbit and make determination of the mass ratio of the components of the visual binary unfeasible. It appears likely, however, from the observations before 1940, that the positive sign for the inclination is the proper choice. Because the light time changes are nearly linear over the last several years, the uncorrected times of minimum light will be used in all further discussion.

A recent period change

The (O-C) values for all the recent times of minimum light (listed in Table XXXIII) were calculated using the most recent light elements available as given

by Pohl (41):

$$\text{Primary minimum} = \text{JD}2438573.4166 + 0^{d}.26781430\ E$$

These (O-C) values are listed in Table XXXIII along with the number of elapsed periods since the given epoch. Figure 20 is a plot of these (O-C) values as a function of the number of elapsed periods. From this plot it seems apparent that a sudden increase in the period occurred sometime in 1967. Twenty times of minimum light observed after this time were used to derive new light elements:

$$\text{Primary minimum} = \text{JD}2440339.3817 + 0^{d}.26781731\ E$$
$$\pm 3 \qquad\qquad \pm 24$$

The (O-C) values and the number of elapsed periods from these light elements are listed in Table XXXIII and plotted in Figure 21. This new period represents an increase of about 0.26 seconds from Pohl's period. The phases of the observations were now computed from these light elements and are listed in Table XXXI.

Light Variations

When the results of the individual nights were plotted as a function of phase and combined (see Figures 22 and 23), several things became apparent. The first was the expected general shape of the light curve; i.e. typical of a W Ursae Majoris type variable. The second was an apparent shift of the zero-point of the magnitudes from

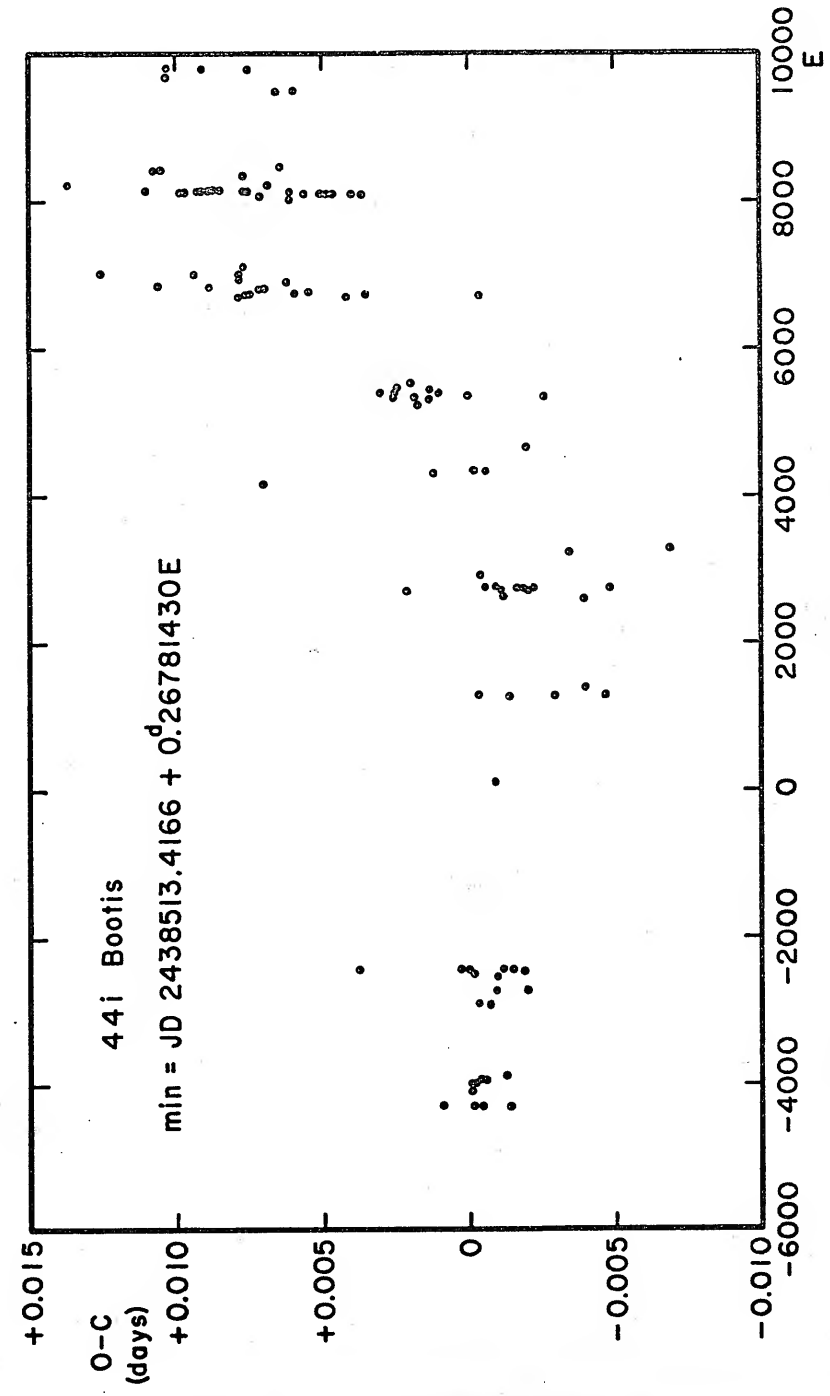

Figure 20. O-C's from Pohl's Light Elements.

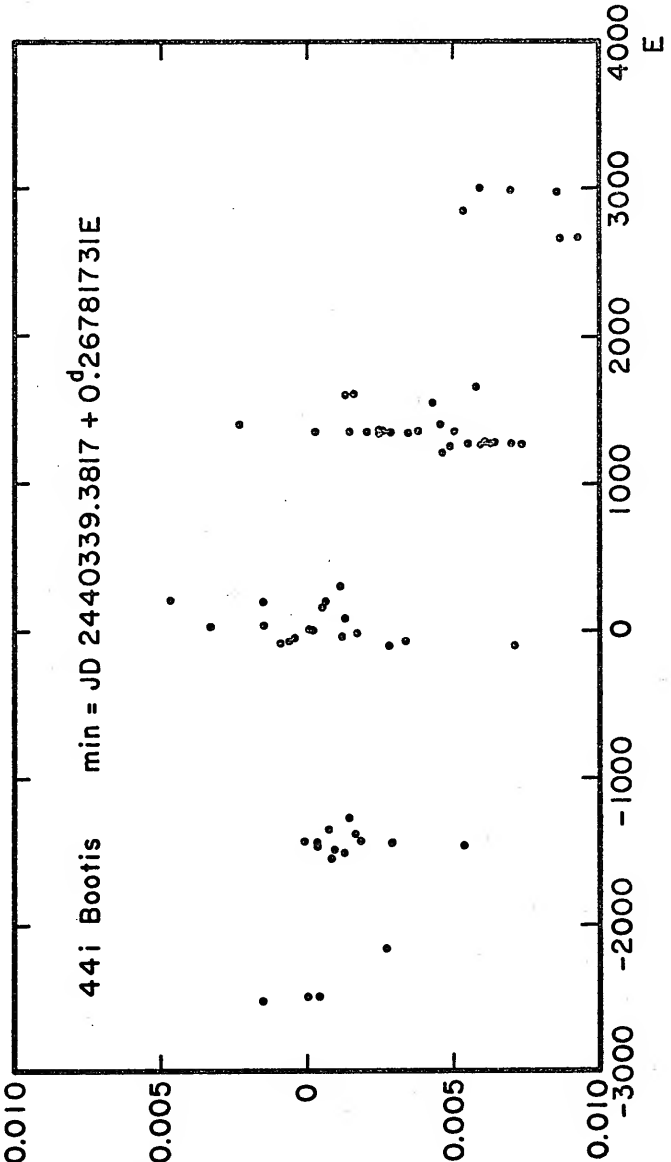

Figure 21. O-C's from New Light Elements.

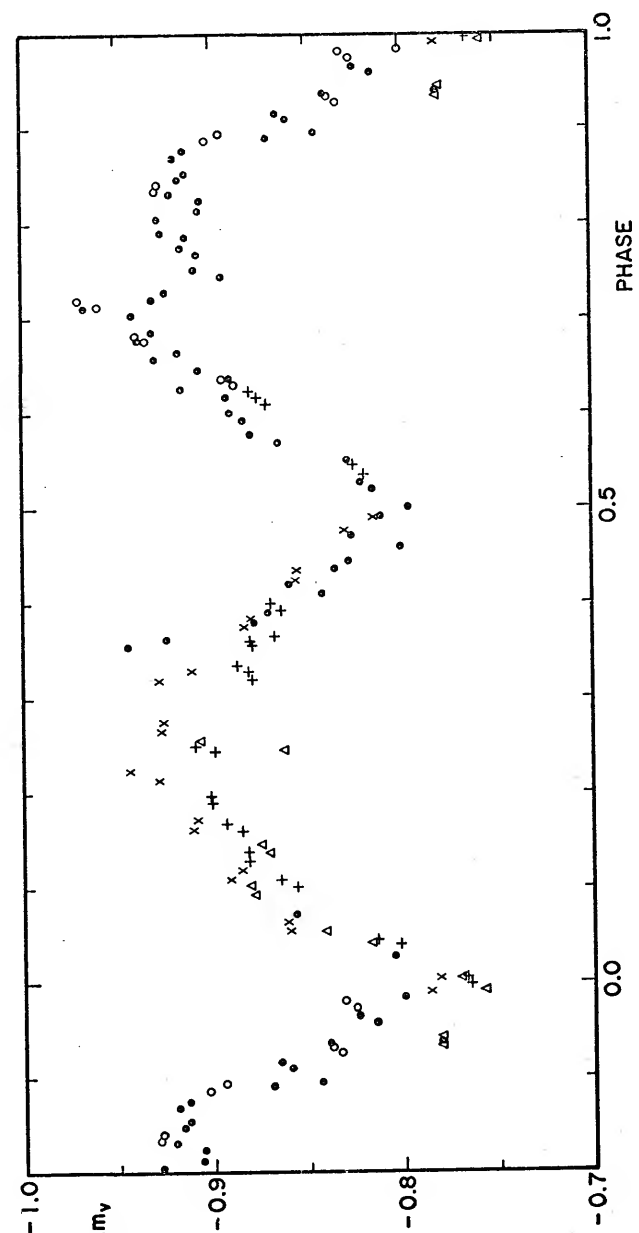

Figure 22. Yellow Light Curve of 44i Bootis: Triangles--April 27, 1969; plus signs--May 4, 1969; open circles--June 19, 1969; X's--May 7, 1970; solid circles--July 1, 1970.

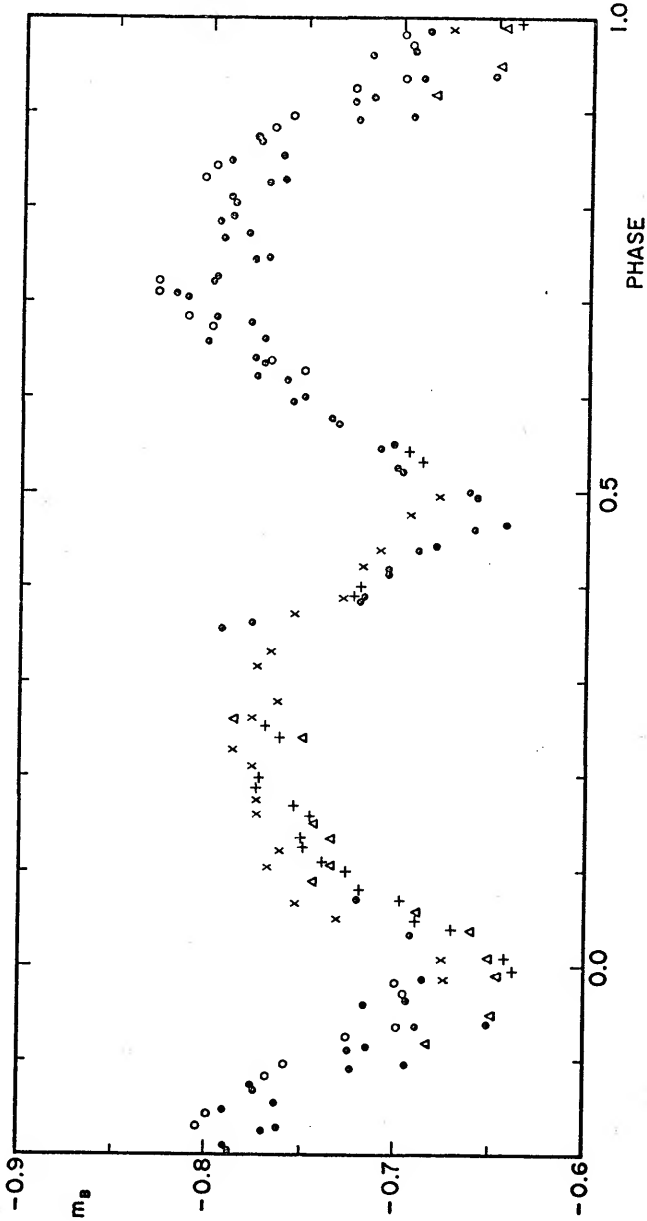

Figure 23. Blue Light Curve of 44i Bootis: Triangles--April 27, 1969; plus signs--May 4, 1969; open circles--June 19,1969; X's--May 7, 1970; solid circles--July 1, 1970.

night to night; that is, the whole light curve goes slightly up and down. The third feature which appears in the light curve is a slight depression shortly after maximum light in the observations taken on the night of July 1, 1970.

The main feature in the mean light curve is the difference in the height of the two maxima. The secondary maximum (i.e. the one following the shallower eclipse) is obviously higher than the primary maximum. This has not been true in all previous observations of the system. In fact, the light curve is subject to change as is shown by Figures 24 and 25 which give the mean light curves of the different authors who have observed the system. The earlier light curves up to and including Binnendijk's are reproduced from Binnendijk's paper (19). All phases are made zero at primary minimum. The zero points of the magnitudes are adjusted to give the best agreement with Binnendijk's mean light curve, but the magnitude scale of the authors was not altered.

Schilt observed the eclipsing star with respect to the bright visual component photographically. To produce the light curve shown in Figure 24 Binnendijk made normal points from these long runs which gave a good light curve. Following Kuiper he omitted three short runs of plates of poor quality. The light of star 1 was added in the computation to arrive at the combined light of the system using Schilt's value of 0.76 mag. for the difference

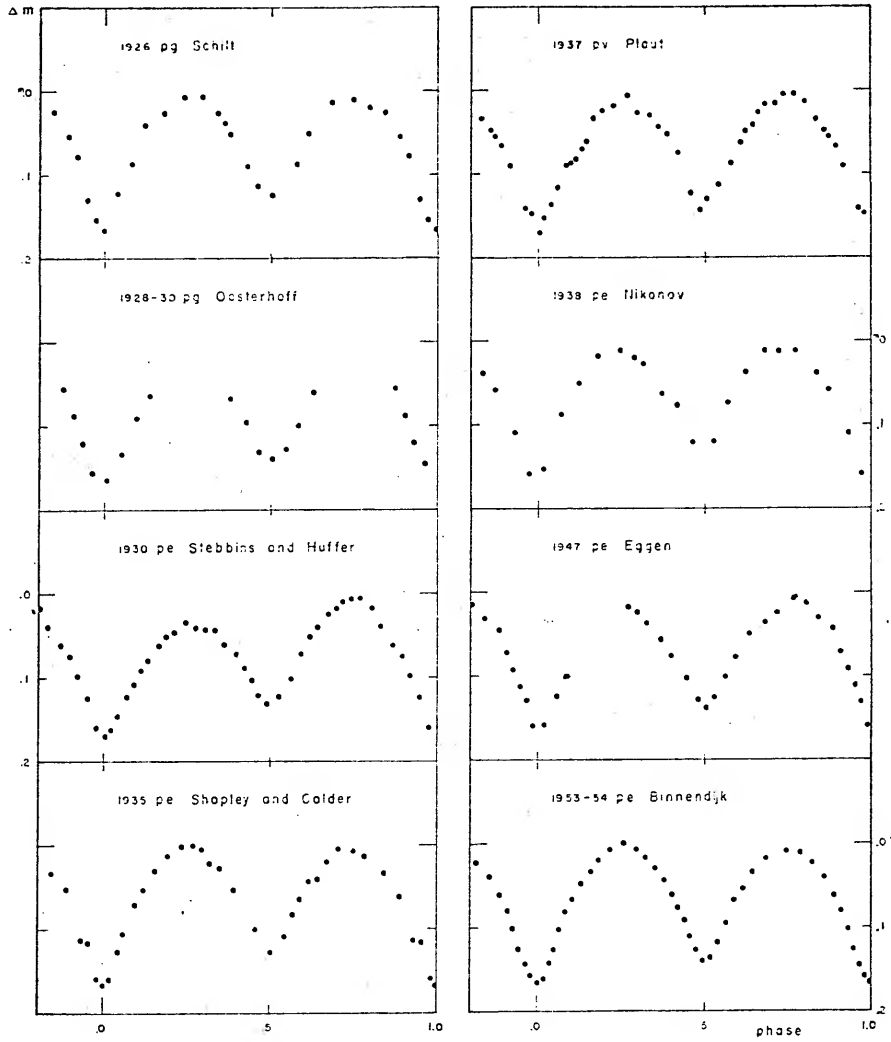

Figure 24. The Light Curves of Different Authors (19).

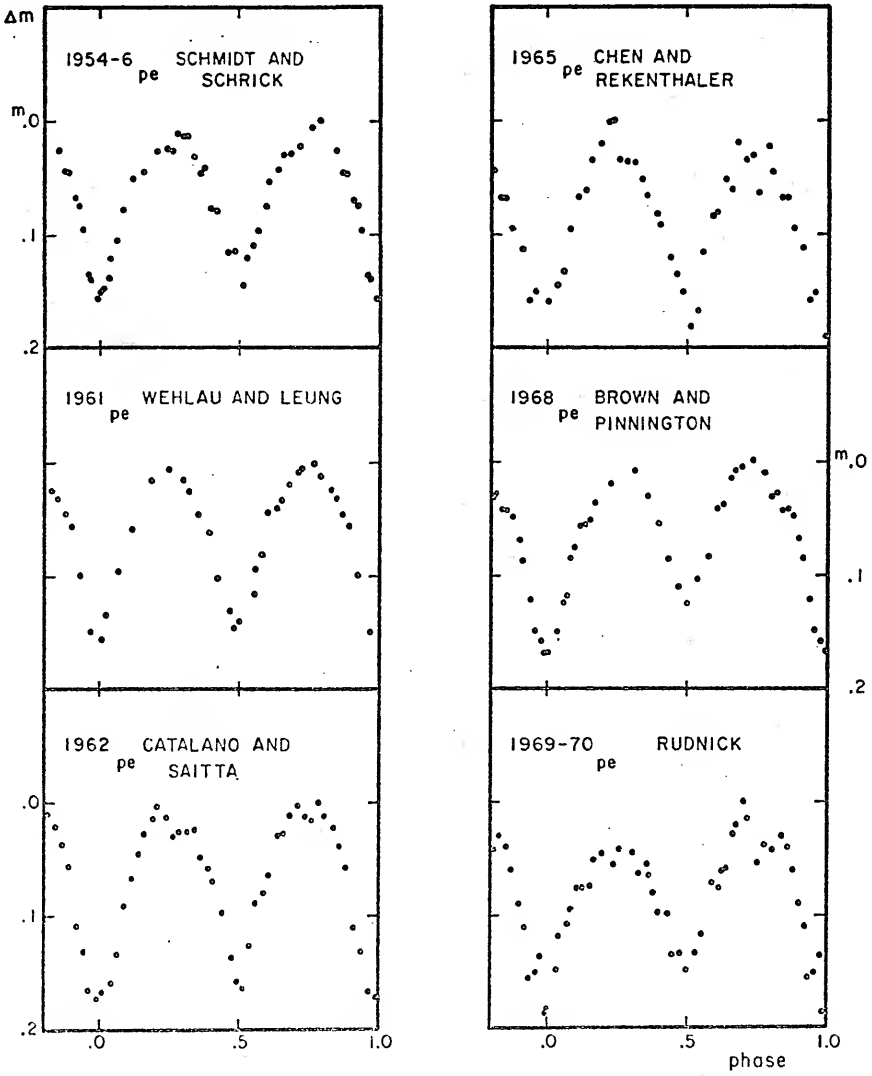

Figure 25. The Light Curves of Different Authors.

between the visual components. The same was done with the observations of the minima by Oosterhoff (52). All later authors had to measure this combined light because the separation of the stars became too small. The light curve by Stebbins and Huffer, observed in 1930, was computed by Eggen (26). The normal points of the light curve of Shapley and Calder were only computed for the observations taken in 1935. In Plaut's light curve (53) Binnendijk recomputed the normals around the maxima. Nikonov gives light curves in the blue and infrared; Binnendijk reproduces the former. Normal points were made from the published graphs of Eggen's observations. This was possible except for the gap in the figure, where the deviations from a mean curve are as large as 0.04 mag. Binnendijk also omitted the deep and shifted secondary minimum which Eggen observed on March 6, 1947 from this mean curve. Binnendijk computed the normal points of his own observations after the zero points of each night's observations had been adjusted to force agreement of the maxima. Schmidt and Schrick (54) observed the system in three colors and gave their observations in two groups: Group I included only good observations; and Group II included the remaining poorer observations. The normal pointsgiven here were computed from the Group I observations taken at an effective wavelength of 450 mμ. Wehlau and Leung (35) give light curves in yellow and blue light; the former is reproduced here. Catalano and Saitta (36)

observed the system in Hα light; their normal points are reproduced here. Chen and Rekenthaler (55), Brown and Pinnington (42), and the author observed the system in yellow and blue light. In all cases normal points were computed from the yellow observations.

An inspection of these mean light curves shows that both the relative heights of the maxima and the shape of the light curve change. It seems apparent from reading the literature that the changes in the shape of the light curve occur on a very short time scale. Chen and Rekenthaler (56) reported a variation in the depth of the secondary minimum of approximately 0.033 mag. from one cycle to the next, i.e. in a period of less than six and one-half hours. Other authors have also reported night to night changes in the light curve. Eggen, for example, observed a deepened (0.04 mag) and shifted secondary minimum on the night of March 16, 1947. Both Brown and Pinnington and the author have observed similar slight depressions shortly after secondary maximum on the nights of March 6, 1968 and July 1, 1970 respectively (see Figure 26). These variations in the light curve and especially the deformity of the light curve at maximum light seem to be present in most of the observations of the system. Variations of light curves of eclipsing binaries of the W Ursae Majoris type are not uncommon. In fact, the many irregular period changes of the system suggest that the system is unstable, and there-

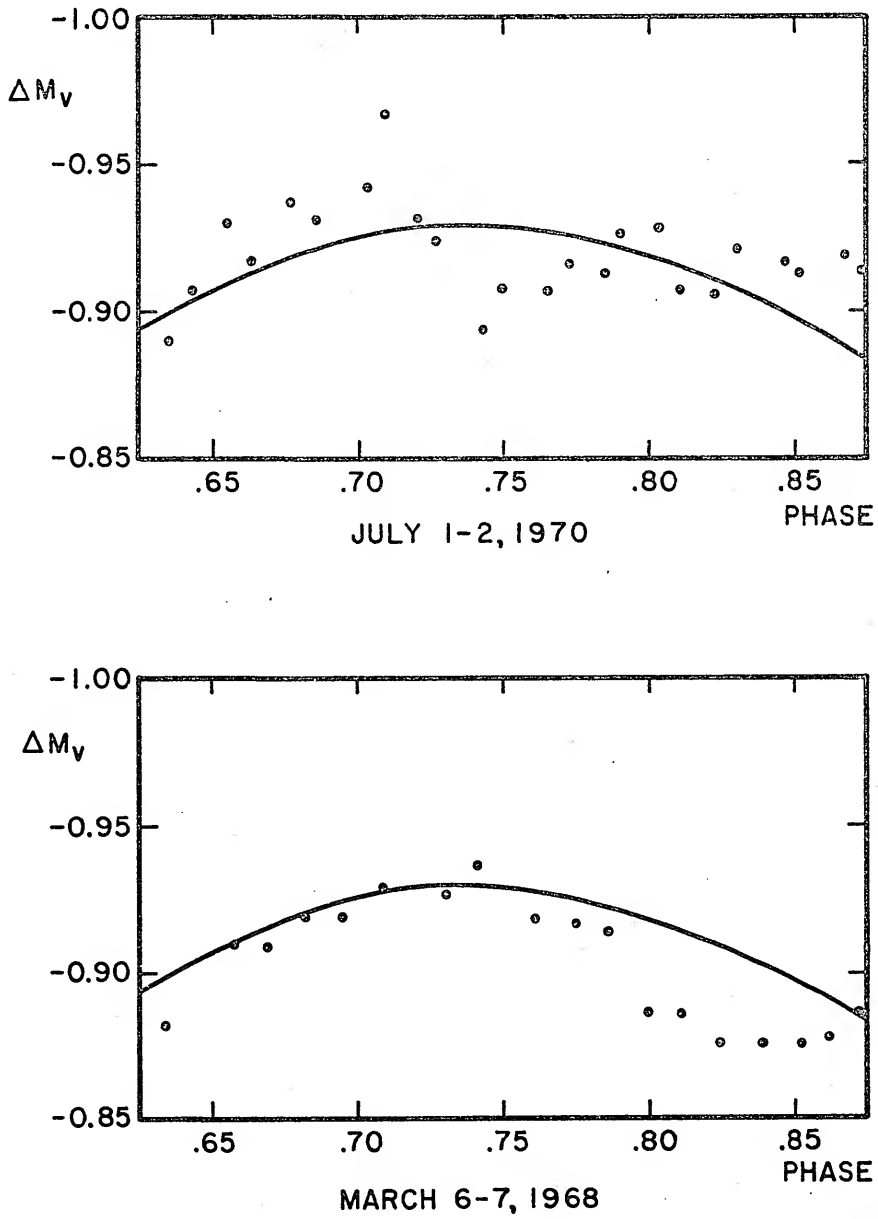

Figure 26. Deformities of the Light Curve of 44i Bootis on Two Nights.

fore that variability of the light curve is not unexpected. In this case, however, the picture is further complicated by several indications in earlier observations that the brighter non-eclipsing component of the visual pair is slightly variable. Untangling these two effects on the combined light will probably not be possible until the two components of the visual binary can be observed separately.

Rectification

In order to proceed conveniently towards a solution of the light curve, it was necessary to convert the data from stellar magnitudes to light values and to free the observations from the light of star A. There are three independent measures of the difference in magnitude Δm_{AB} between component A and the eclipsing system B at maximum light (21):

λ	Δm_{AB}	Author
B	0.76	Schilt
V	0.63	Kuiper
V	0.70	Wallenquist

A difference of 0.76 mag. in blue light and 0.66 mag. in yellow light was used to remove the light of component A from the light curves. These values are also consistent with the spectral types of the stars as reported by Kurpinska and Van't Veer (21).

The yellow light curve was chosen for the first attempts at a solution. The light in the maxima of the eclipsing system was now written in the form:

$$I = A_o + A_1\cos\theta + A_2\cos 2\theta + A_3\cos 3\theta + A_4\cos\theta$$

$$+ B_1\sin\theta + B_2\sin 2\theta + B_3\sin 3\theta + B_4\sin 4\theta.$$

The coefficients were then derived by using Merrill's graphical method as follows:

$A_o = 0.7985$

$A_1 = -0.0038$ $\qquad$ $B_1 = -0.0253$

$A_2 = -0.0976$ $\qquad$ $B_2 = 0.0050$

$A_3 = 0.0055$ $\qquad$ $B_3 = 0$

$A_4 = 0$ $\qquad$ $B_4 = 0$

The intensities were then rectified by the formula:

$$I'' = \frac{I - A_1\cos\theta - A_3\cos 3\theta - B_1\sin\theta - B_2\sin 2\theta}{A_o + A_2\cos 2\theta}$$

and the phase angles were rectified by the formula

$$\sin^2\Theta = \sin^2\theta/(1 - z\cos^2\theta)$$

where $z = -4A_2/N(A_o - A_2)$ with $N = 2.6$ corresponding to a limb darkening $x = 0.6$.

Orbital Elements

The rectified light curve shows two unequal minima with light losses of $1 - \ell_o^{pr} = 0.23$ and $1 - \ell_o = 0.13$. After a coefficient of limb darkening $x = 0.6$ was assumed for each component, solutions were made with several values of k, the ratio of radii. As the Merrill nomographs reveal, for shallow minima of partial eclipses a large change in k introduces only a slight change in the shape of the eclipses. This means that for a great part of the partial eclipse portion of the nomographs, the shape (χ) curves run nearly parallel to or coincident with the depth line. If the differences in the depths of the two eclipses are not great, then the depth lines for the two possible cases (the primary eclipse either an occultation or a transit with the secondary eclipse the other) will not differ greatly, becoming coincident when the two eclipses are equally deep. This indeterminacy, which is illustrated by the nomographs, means that solutions must be tried for a large range of values of k.

Solutions were made for $k = 1.0$ and for the two cases of $k = 0.50$ (primary an occultation and primary a transit). These solutions almost cover the whole range of k possible with the assumed eclipse depths and the restriction to partial eclipses. Later investigation showed that for other possible values outside this range (including complete eclipses), the size of one of the components

would exceed the size of its Roche lobe. Therefore these values of k cover the whole range of permitted solutions. Theoretical light curves were computed for the three values of k and compared with the rectified observations. The sums of the squares of the mean deviations for all three cases were nearly the same. Therefore the solution for these observations is indeterminate over the whole range of values of k. Previous solutions in the literature also mention this problem of indeterminacy. Eggen found a range of indeterminacy of k between the two values of 0.9, although all his solutions have one component that exceeds or nearly exceeds the size of its Roche lobe. Binnendijk found a "satisfactory" solution with k = 0.70 when he used 0.76 for the difference in magnitude between the eclipsing system and the brighter component of the visual binary. However, when he used 0.63 for this difference in magnitude, he found so large a range of possible k's that the solution was indeterminate. Since the light of the brighter component of the visual binary cannot be measured more accurately at this time, and, in fact, this light might even be slightly variable, it does not seem likely that further observations at this time will produce a better determined solution.

There are three solutions of photoelectric light curves of 44i Bootis B in the literature. Eggen's solution was made from the unfiltered photoelectric light curve

observed by Stebbins and Huffer in 1930. Binnendijk's light curve was observed with a yellow filter that does not correspond to a standard system. Catalano and Saittra observed the system in Hα light. These three light curves can be compared with the author's yellow light curve. The light curves, as illustrated in Figure 24 and Figure 25, for the four sets of observations show somewhat different shapes. It is difficult to make any direct comparisons of the light curves since some of the authors have included zero-point adjustments in their data. It is apparent, however, that differences in shape do occur in the various light curves. These zero-point adjustments, and the differing amounts of third light make direct comparisons of the various solutions somewhat meaningless. The best that can be said is that all the solutions suffer from the lack of precise knowledge of the two components of the visual binary system and from the poor determinacy of solutions when the stars are highly distorted and the geometrical depth is low.

The rectification coefficients and the light losses in the rectified minima differ in the various solutions. This is not surprising since both the rectification coefficients and the light losses in the rectified minima depend upon the shape of the light curve outside of eclipse and the amount of third light removed from the light curve. In the case of the author's yellow light curve, the changes in

the shapes of the light curve on the five nights the observations were made add greatly to the uncertainty of all the parameters. The light losses in the rectified minima are not well determined; however, this uncertainty in itself had little effect on the determinacy of the solution. The limb darkening coefficient for both components was chosen as x = 0.6 following the value determined for the sun which is of similar spectral type. All three previous solutions used a value of limb darkening x = 0.8. Changing the limb darkening to this value does not significantly affect the results of the solution. There are considerable differences in some of the orbital elements for the three solutions listed in Table XXXV. While the general problem of indeterminacy is typical of shallow minima or partial eclipses, the very large range of possible solutions may be attributed to the large amount of scatter in the observations. This large amount of scatter makes it virtually impossible to improve the determinacy of the solution.

Orbital elements were determined for these three possible solutions of the yellow light curve. The figures of the components were determined using the mass ratio $m_2/m_1 = 0.50$ taken from Popper's spectroscopic elements. These orbital elements are listed in Table XXXV. The sizes of the Roche lobes for the mass ratio $m_2/m_1 = 0.50$ are $y_1 = 0.441$, $z_1 = 0.414$, $y_2 = 0.313$, and $z_2 = 0.300$. (The

TABLE XXXV

Solutions and Orbital Elements with $x = 0.6$, $1 - \ell_o^{pr} = 0.23$, $1 - \ell_o^{sec} = 0.13$, $\Theta_e = 41°.0$, and $m_2/m_1 = 0.50$

	PRIMARY-OCCULTATION		PRIMARY-TRANSIT
k	.50	1.0	.50
p_0	-.4821	.0620	-.95
α_o^{oc}	.775	.3600	.9942
α_o^{tr}	.6917	.3600	.9798
a_1	.473	.358	.453
r_1	.444	.347	.428
b_1	.443	.347	.427
c_1	.416	.336	.404
a_2	.237	.358	.227
r_2	.230	.329	.221
b_2	.229	.322	.220
c_2	.224	.307	.216
$\cos i_r$	.35916	.38023	.23808
i_r	68°.9	67°.6	76°.2
L_1	.703	.639	.859
L_2	.297	.361	.131

b- and c- axes of the stars are in the y- and z- directions respectively.) Thus in the solution where k = 0.50 and the primary eclipse is an occultation, the size of the brighter star just exceeds the size of its Roche lobe. For the other case where k = 0.50, neither component exceeds the size of its Roche lobe. In the case where k = 1.0, the fainter component is larger in size than its Roche lobe. The Roche lobe is, in effect, the limiting surface for a dynamically stable star in a binary system where the two stars have distinct surfaces. If both components fill their lobes, which may often be the case for W Ursae Majoris systems, the components will share a common surface. The eclipsing system of 44i Bootis B is very likely near this limit of stability. Certainly the changes in the period and the light curve indicate that the system is not stable.

Since the solution of the yellow light curve was virtually indeterminate, no solution was made from the slightly poorer quality blue light curve. Further observations of the system of 44i Bootis for the purpose of determining orbital elements will probably not be productive until the two components of the visual binary can be observed separately. When this is possible, the problems caused by the uncertainty of the difference of magnitude of the two visual components and the possible variability of the brighter component should be resolvable. Then, it is possible that very accurate photoelectric observations might provide a better determined solution for the orbital elements. Even under the best circumstances, however, the

basic problem of indeterminacy in shallow minima of partial eclipses will remain. Until the time when the visual components can be observed separately, the combined system should be observed in order to determine the times of minimum light, and to detect from these times of minimum, any further period changes.

CHAPTER V

SUMMARY AND CONCLUSIONS

The light curves of three W Ursae Majoris sytems, two generated from theoretical astrophysical models and one which was observed, have been studied using the Russell-Merrill method of solution of light curves of eclipsing binaries. The observed system, 44i Bootis B, is, in many ways, typical of W Ursae Majoris systems. The light curve of the system changes with time in an apparently irregular manner. The period of the system also shows irregular variations, These variations, which are common in W Ursae Majoris systems may indicate that these systems are not dynamically stable. In addition 44i Bootis B is a member of a visual binary system.

Three major problems were encountered in the solution of the light curves. The light curves of 44i Bootis B and the first synthetic system had relatively shallow minima caused by partial eclipses. This led to a problem of indeterminacy in the solutions. The "observed" points in the shoulders of both synthetic light curves fell below the theoretical light curves predicted by the solutions. In all three light curves there was a problem with third light. In

the case of 44i Bootis B, there was a known visual companion whose light was included in the observations; however, the amount of this third light was not precisely known. The addition of third light in the solution of the two synthetic light curves somewhat improved the fit of the solutions to the light curves. There was, however, no sound basis for adding this third light. In addition to these problems, the orbital elements predicted by the solutions of the two synthetic light curves using the Russell-Merrill method were not at all close to the orbital elements that were used to generate these light curves from the theoretical astrophysical models. In both cases the Russell-Merrill solutions predicted that the stars were smaller and more detached than the actual stars used to generate the light curves.

The results summarized above led to the conclusion that the Russell model is not compatible with the theoretical astrophysical models used to generate the synthetic light curves. It is not possible to determine from this study which of the models more closely represents the actual conditions present in W Ursae Majoris systems. The solutions of the light curves of W Ursae Majoris systems which are in the literature should be regarded as crude approximations. Better solutions may be possible when the nature of the variations in the periods and light curves of these systems are determined. In this light, it is suggested that precise multicolor photoelectric observations of a few selected

systems, preferably those showing complete eclipses, carried out as continuously as possible and extending over a period of several years, would be more meaningful than observations of many systems solely for the purpose of deriving orbital elements. These observations, together with simultaneous spectroscopic observations, could add greatly to the knowledge of the nature of the W Ursae Majoris systems.

LIST OF REFERENCES

1. Binnendijk, L., "The Orbital Elements of W Ursae Majoris Systems," in Vistas in Astronomy 12 ed. by Arthur Beer (Pergamon Press, Oxford, 1970).

2. Russell, Henry Norris, and Merrill, John Ellsworth, "The Determination of the Elements of Elcipsing Binaries," Contributions from the Princeton University Observatory No. 26 (1952).

3. Lucy, L. B., "The Light Curves of W Ursae Majoris Stars," Astrophysical Journal 153, 877 (1968).

4. Merrill, John Ellsworth, "Tables for Solution of Light Curves of Eclipsing Binaries," Contributions from The Princeton University Observatory No. 23 (1953).

5. Merrill, John Ellsworth, "Nomographs for Solution of Light Curves of Eclipsing Binaries," Contributions from The Princeton University Observatory No. 24 (1953).

6. Rucinski, S. M., Private Communication.

7. Mochnacki, S. W., and Doughty, N. A., "A Model for the Totally Eclipsing W Ursae Majoris System AW UMa," Monthly Notices of the Royal Astronomical Society 156, 51 (1972).

8. Wilson, Robert E., and Devinney, Edward J., "Realization of Accurate Close-Binary Light Curves: Application to MR Cygni," Astrophysical Journal 166, 605 (1971).

9. Wilson, Robert E., Private Communcation.

10. Merrill, John E., "Rectification of Light Curves of W Ursae Majoris-Type Systems on the Russell Model," in Vistas in Astronomy 12 ed. by Arthur Beer (Pergamon Press, Oxford, 1970).

11. Kitamura, Masatoshi, Tables of the Characteristic Functions of the Eclipse and the Related Delta-Functions for Solution of Light Curves of Eclipsing Binary Systems (University of Tokyo, Tokyo, 1967).

12. Kopal, Zdenek, Close Binary Systems (John Wiley and Sons Inc., New York, 1959).

13. Gyldenkerne, Kjeld, and West,Richard M., ed., Mass Loss and Evolution in Close Binaries (Proceedings of the International Astronomical Union Colloquium No. 6, Copenhagen University Publications Fund, Copenhagen, 1970).

14. Wilson, Robert E., Private Communication.

15. Binnendijk, L., "The Orbital Elements of RZ Comae," Astronomical Journal 69, 154 (1964).

16. Bookmyer, Beverly B., "A Study of Photoelectric Observations of SW Lacertae," Astronomical Journal 70, 415 (1965).

17. Herschel, William, "Catalogue of Double Stars," Philosophical Transactions of the Royal Society of London, 72, 118 (1782).

18. Clerke, Agnes, "A Historical and Descriptive List of Some Double Stars Suspected to Vary in Light," Nature 39, 55 (1888).

19. Binnendijk, L., "The Light Variation and Orbital Elements of 44i Bootis," Astronomical Journal 60, 355 (1955).

20. Meeus, Jean, "Some Bright Visual Binary Stars-II," Sky and Telescope 41, 88 (1971).

21. Kurpinska, M., and Van't Veer, F., "Étude Photométrique en Huit Couleurs de la Binaire à Eclipse 44i Bootis," Astronomy and Astrophysics 4, 253 (1970).

22. Popper, Daniel M., "Five Spectroscopic Binaries," Astrophysical Journal 97, 394 (1943).

23. Batten, Alan H., "Sixth Catalogue of the Orbital Elements of Spectroscopic Binary Systems," Publications of the Dominion Astrophysical Observatory 13, 119 (1967).

24. Johnson, H. L., and Morgan, W. W., "Fundamental Stellar Photometry for Standards of Spectral Type on the Revised System of the Yerkes Spectral Atlas," Astrophysical Journal 117, 313 (1953).

25. Whitford, A. E., "Photoelectric Techniques," in Encyclopedia of Physics 54 ed.by S. Flügge (Springer-Verlag, Berlin, 1962).

26. Eggen, Olin J., "The System of 44i Bootis," Astrophysical Journal 108, 15 (1948).

27. Cannon, Annie J. and Pickering Edward C., "The Henry Draper Catalogue," Annals of the Astronomical Observatory of Harvard College 95-6 (1920-1).

28. Hardie, Robert H., "Photoelectric Reductions," in Astronomical Techniques ed. by W. A. Hiltner (University of Chicago Press, Chicago, 1962).

29. Johnson, Harold L., "A photometric System," Annales D'Astrophysique 18, 292 (1955).

30. Binnendijk, Leendert, Properties of Double Stars (University of Pennsylvania Press, Philadelphia, 1960).

31. Wood, Frank Bradshaw, "Observation of Eclipsing Variables," in Photoelectric Astronomy for Amateurs ed. by F. W. Wood (The Macmillan Company, New York, 1963).

32. Kwee, K. K., and Van Woerden, H., "A Method for Computing Accurately the Epoch of Minimum of Eclipsing Variable," Bulletin of the Astronomical Institutes of the Netherlands 12, 327 (1956).

33. Purgathofer, A., and Prochazka, F., "Periodenschwankungen Bei Kurzperiodischen Bedeckungsveränderlichen," Mitteilungen der Universitäts-Sternwarte Wien 13, 151 (1967).

34. Schneller, H., "Die Periode von i Bootis," Astronomische Nachrichten 288, 183 (1965).

35. Wehlau, William,and Leung, Kam-Ching, "Photoelectric Observations of i Bootis," Journal of the Royal Astronomical Society of Canada 56, 105 (1962).

36. Catalano, S., and Saitta, T., "Observazioni ed Elementi Orbitali del Sistema 44i Bootis B," Memorie Della Società Astronomica Italiana 35, 3 (1964).

37. Pohl, E., and Kizilirmak, A., "Beobachtungsergebnisse an Veränderlichen Sternen," Astronomische Nachrichten 288, 69 (1964).

38. Schneller, H., "i Bootis," Information Bulletin on Variable Stars 57 (1964).

39. Popovici, C., "Photoelectric Minima of Eclipsing Variables," Information Bulletin on Variable Stars 148 (1966).

40. Schneller, H., "44i Bootis," Information Bulletin on Variable Stars 144 (1966).

41. Kizilirmak, A., and Pohl, E., "Minima and New Light-Elements for Eclipsing Binaries," Astronomische Nachrichten 291, 111 (1969).

42. Brown, B. M. K., and Pinnington, E. H., "Photoelectric Observations of Three W Ursae Majoris Systems," Astronomical Journal 74, 538 (1969).

43. Johnston,Kenneth, Private Communication.

44. Popovici, C., "Photoelectric Minima of Eclipsing Variables," Information Bulletin on Variable Stars 322 (1968).

45. Pohl, E., and Kizilirmak, A., "Photoelectric Minima of Eclipsing Binaries," Information Bulletin on Variable Stars 456 (1970).

46. Bergeat, J., Lunel, M., Sibille, F., and Van't Veer, F., "Sudden Changes in the Period of the Eclipsing Contact Binary 44i Bootis," Astronomy and Astrophysics 17, 215 (1972).

47. Popovici, C.,"Photoelectric Minima of Eclipsing Variables," Information Bulletin on Variable Stars 419 (1970).

48. Scarfe, C. D., and Brimacombe, J., "Photoelectric Observations of Two W UMa Systems," Astronomical Journal 76, 50 (1971).

49. Kizilirmak, A., and Pohl, E., "Photoelectric Minima of Eclipsing Binaries," Information Bulletin on Variable Stars 530 (1971).

50. Popovici, C.,"Photoelectric Minima of Eclipsing Variables," Information Bulletin on Variable Stars 508 (1971).

51. Pohl, E., and Kizilirmak, A., "Photoelectric Minima of Eclipsing Binaries," Information Bulletin on Variable Stars 647 (1972).

52. Oosterhoff, P. Th., "Photographic Observations of Six Minima of 44i Bootis B," Bulletin of the Astronomical Institutes of the Netherlands 9, 11 (1939).

53. Plaut, L., "Photometric Observations of 44i Bootis," Bulletin of the Astronomical Institutes of the Netherlands 9, 1 (1939).

54. Schmidt, H., and Schrick, K. W., "Untersuchungen an W Ursae Majoris-Sternen, III. Lichtelektrische Beobachtungen von i Bootis," Zeitschrift Für Astrophysik, 43, 165 (1957).

55. Rekenthaler, Douglas A., Photoelectric Observations of the Eclipsing Variables VV Orionis, 44i Bootis, and Delta Librae (M. S. Thesis, University of Florida, 1965).

56. Chen, K-Y., and Rekenthaler, D. A., "Photoelectric Photometry of 44i Bootis," Quarterly Journal of the Florida Academy of Sciences 29, 1 (1966).

BIOGRAPHICAL SKETCH

Ian Stuart Rudnick was born October 30, 1942, in Chicago, Illinois. He attended primary schools in Chicago and St. Petersburg, Florida before moving to Coral Gables, Florida. He graduated from Coral Gables Senior High School in June,1960. He received his first three years of college at Massachusetts Institute of Technology after which he transfered to the University of Miami, from which he received the degree of Bachelor of Science cum laude with a major in physics in June, 1965. He then entered the graduate school of the same institution and received the degree of Master of Science with a major in physics in June, 1967. In September, 1968, he entered the graduate school of the University of Florida and began a study and research program leading to the degree of Doctor of Philosophy with a major in astronomy. During this period he held both graduate assistanships and a Graduate School Fellowship.

Ian Stuart Rudnick is married to the former Andrea Warshaw, and has one son. He is a member of Sigma Pi Sigma.

I certify that I have read this study and that in my opinion it conforms to acceptable standards of scholarly presentation and is fully adequate, in scope and quality, as a dissertation for the degree of Doctor of Philosophy.

Frank Bradshaw Wood

Frank Bradshaw Wood, Chairman
Professor of Astronomy

I certify that I have read this study and that in my opinion it conforms to acceptable standards of scholarly presentation and is fully adequate, in scope and quality, as a dissertation for the degree of Doctor of Philosophy.

K-Y. Chen

K-Y. Chen
Associate Professor of Astronomy

I certify that I have read this study and that in my opinion it conforms to acceptable standards of scholarly presentation and is fully adequate, in scope and quality, as a dissertation for the degree of Doctor of Philosophy.

Ralph C. Isler

Ralph C. Isler
Associate Professor of Physics

I certify that I have read this study and that in my opinion it conforms to acceptable standards of scholarly presentation and is fully adequate, in scope and quality, as a dissertation for the degree of Doctor of Philosophy.

Robert E. Wilson
Professor of Astronomy
University of South Florida

This dissertation was submitted to the Department of Physics and Astronomy in the College of Arts and Sciences and to the Graduate Council, and was accepted as partial fulfillment of the requirements for the degree of Doctor of Philosophy.

A. G. Smith
Dean, Graduate School

June, 1972